University of Alberta

Active Anti-Islanding Protection for Distributed Generators Using Impedance Measurements

By

Jacek Kliber

A thesis submitted to the Faculty of Graduate Studies and Research in partial fulfillment of the requirements for the degree of Master of Science

in

Power Engineering and Power Electronics

Department of Electrical and Computer Engineering

Edmonton, Alberta

Spring 2008

Library and
Archives Canada

Published Heritage
Branch

395 Wellington Street
Ottawa ON K1A 0N4
Canada

Bibliothèque et
Archives Canada

Direction du
Patrimoine de l'édition

395, rue Wellington
Ottawa ON K1A 0N4
Canada

Your file Votre référence
ISBN: 978-0-494-45834-1
Our file Notre référence
ISBN: 978-0-494-45834-1

NOTICE:
The author has granted a non-exclusive license allowing Library and Archives Canada to reproduce, publish, archive, preserve, conserve, communicate to the public by telecommunication or on the Internet, loan, distribute and sell theses worldwide, for commercial or non-commercial purposes, in microform, paper, electronic and/or any other formats.

The author retains copyright ownership and moral rights in this thesis. Neither the thesis nor substantial extracts from it may be printed or otherwise reproduced without the author's permission.

AVIS:
L'auteur a accordé une licence non exclusive permettant à la Bibliothèque et Archives Canada de reproduire, publier, archiver, sauvegarder, conserver, transmettre au public par télécommunication ou par l'Internet, prêter, distribuer et vendre des thèses partout dans le monde, à des fins commerciales ou autres, sur support microforme, papier, électronique et/ou autres formats.

L'auteur conserve la propriété du droit d'auteur et des droits moraux qui protège cette thèse. Ni la thèse ni des extraits substantiels de celle-ci ne doivent être imprimés ou autrement reproduits sans son autorisation.

In compliance with the Canadian Privacy Act some supporting forms may have been removed from this thesis.

While these forms may be included in the document page count, their removal does not represent any loss of content from the thesis.

Conformément à la loi canadienne sur la protection de la vie privée, quelques formulaires secondaires ont été enlevés de cette thèse.

Bien que ces formulaires aient inclus dans la pagination, il n'y aura aucun contenu manquant.

Canada

University of Alberta

Library Release Form

Name of Author: Jacek Kliber

Title of Thesis: Active Anti-Islanding Protection for Distributed Generators using Impedance Measurements

Degree: Master of Science

Year this Degree Granted: 2008

Permission is hereby granted to the University of Alberta Library to reproduce single copies of this thesis and to lend or sell such copies for private, scholarly or scientific research purposes only.

The author reserves all other publication and other rights in association with the copyright in the thesis, and except as herein before provided, neither the thesis nor any substantial portion thereof may be printed or otherwise reproduced in any material form whatsoever without the author's prior written permission.

_____

Signature

University of Alberta

Faculty of Graduate Studies and Research

The undersigned certify that they have read, and recommend to the Faculty of Graduate Studies and Research for acceptance, a thesis entitled **Active Anti-Islanding Protection for Distributed Generators Using Impedance Measurements** submitted by **Jacek Kliber** in partial fulfillment of the requirements for the degree of **Master of Science**.

_____

Dr. Wilsun Xu

Supervisor

_____

Dr. Ryan Li

_____

Dr. Amos Ben-Zvi

Date: _____

Abstract

Distributed generation is a growing business in electric power systems. Anti-islanding protection of distributed generators (DG) is a significant technical barrier in the industry. A DG while working in conjunction with the main electricity grid must disconnect if the main grid loses power, as it cannot control the voltage and frequency of the power island and poses a significant safety threat to utility workers.

The objective of this research is to investigate a new local active scheme to detect islanding conditions. The technique uses a thyristor controlled short-circuit to inject a disturbance to the power supply system. The supply system impedances are then extracted from the disturbances for determining the islanding condition. Experiments and computer simulations, along with analytical analysis of the proposed method were conducted to assess its effectiveness. The results showed that the method was effective and could be used as a reliable and cost-effective anti-islanding device.

Acknowledgements

I would like to thank my supervisor, Dr. Wilsun Xu, for providing me the opportunity to write this thesis and conduct my research with him and his team. Dr. Xu has been a terrific supervisor and most of all, mentor and teacher, to me. I have learned a great deal from him and will always be grateful for the guidance and direction I have received from him while I was at the University of Alberta. I would also like to thank Vivian Wang and Albert Terheide for their help and guidance. They have both shared their knowledge, experience and time with me through many late hours while running my experiments. Furthermore, I would like to thank the rest of the power team at the University for their help and friendship. You have all made my time here very pleasant and enjoyable.

I would also like to say a special "Thank You" to Wendy for her help, guidance and motivation. Thank you for always being there.

Last but not in the very least, I would like to thank my parents. They have always been there to encourage me and guide me, and through their support, this was all made possible. I am truly grateful and thank you deeply.

Table of Contents

CHAPTER 1 ..... **1**

INTRODUCTION **1**

1.1 THE ANTI-ISLANDING PROBLEM **3**

1.1.1 Power Quality Concerns *5*
1.1.2 Out-of-Phase Reclosing Concerns *5*
1.1.3 Protection Equipment Malfunctioning Concerns *6*
1.1.4 Safety Risks *7*

1.2 CURRENT METHODS FOR DETECTING ISLANDING CONDITIONS **9**

1.2.1 Passive Methods *9*
1.2.1.1 Under/Over Voltage Relay *10*
1.2.1.2 Frequency Based Relays *11*
1.2.1.3 Other Passive Schemes *12*
1.2.2 Active Methods *15*
1.2.2.1 Impedance Measurement Method *16*
1.2.2.2 Varying Generator Terminal Voltage Method *17*
1.2.2.3 Frequency and Phase Shift Method *18*
1.2.2.4 Voltage Shift Method *19*
1.2.3 Communication-Based Methods *21*

1.3 PROPOSED SOLUTION FOR ANTI-ISLANDING DETECTION **24**

1.4 OUTLINE OF THE THESIS **25**

CHAPTER 2 ..... **27**

A LOCAL ACTIVE ANTI-ISLANDING SCHEME BASED ON IMPEDANCE MEASUREMENTS **27**

2.1 POWER-LINE SIGNALING BASED SCHEME **28**

2.1.1 Signal Generator *30*
2.1.2 Signal Detector *31*
2.1.3 Disadvantages of this scheme *32*

2.2 THE PROPOSED SCHEME **32**

2.2.1 Signal Generator Operation *35*
2.2.2 Signal Extraction *38*
2.2.3 Signal Detection *39*
2.2.4 Advantages of the Proposed Scheme *42*

2.3 THEORY OF OPERATION **43**

2.3.1 Peak Current through a SCR Device *43*
2.3.2 Impedance Change *47*
2.3.3 Analytical Studies for Proposed Method *49*

2.4 HARDWARE **55**

2.5 ALGORITHM FOR DETECTING ISLANDING CONDITION **58**

2.5.1 Algorithm for Signal Generator *58*
2.5.2 Algorithm for Islanding Detection *61*

2.6 SUMMARY **66**

CHAPTER 3 ..... **68**

SIMULATION STUDIES **68**

3.1 SIMULATION SETUP **69**

3.2 SIMULATION RESULTS **70**

3.3 SENSITIVITY STUDY **79**

3.3.1 Branch Length *79*
3.3.2 Capacitor Size (MVARs Present in System) *80*
3.3.3 Size of Distributed Generator *81*
3.3.4 Utility Fault Level *83*
3.3.5 Feeder Length *84*
3.3.6 Firing Angle *85*
3.3.7 Load *87*

3.4 CONCLUSIONS ON SIMULATION RESULTS **89**

CHAPTER 4 ..... **90**

LABORATORY STUDIES **90**

4.1 LABORATORY SETUP **91**

4.2 LABORATORY TEST RESULTS **93**

4.3 SENSITIVITY STUDY **102**

4.3.1 Capacitor Size *102*
4.3.2 Firing Angle *104*

4.4 CONCLUSIONS ON LABORATORY TESTS **107**

CHAPTER 5 ..... **109**

CONCLUSIONS AND RECOMMENDATIONS **109**

BIBLIOGRAPHY **113**

APPENDIX A **120**

SIMULATION STUDY: DETAILED RESULTS **120**

APPENDIX B **135**

LABORATORY TEST DETAILED RESULTS **135**

List of Tables

Table 1: Peak of Thyristor Current on Different SG Channel 50

Table 2: Voltage Total Harmonic Distortion at the Point of Common Coupling 77

Table 3: Current Total Harmonic Distortion at the Point of Common Coupling 78

Table 4: Voltage Total Harmonic Distortion at the Point of Common Coupling 100

Table 5: Current Total Harmonic Distortion at the Point of Common Coupling 101

Table 6: Branch Length (DG to Load) – 1km to 10km 121

Table 7: Capacitor - 0 MVAR to 2 MVAR 122

Table 8: DG Level – 0.5 MVA to 50 MVA 125

Table 9: Fault Level – 40 MVA to 200 MVA 127

Table 10: Feeder Length – 1 km to 40 km 128

Table 11: Firing Angle – 5 Degrees to 30 Degrees 130

Table 12: Load – 0.5 MVA to 5 MVA 133

Table 13: Capacitor – 0 μF to 160 0 μF – 25 Degree Firing Angle 136

Table 14: Firing Angle – 25 to 30 Degrees (0 and 0.48 MVAR Capacitor) 139

List of Figures

Figure 1: Typical Distribution System 3

Figure 2: Distribution System with Power Islands 4

Figure 3: Non Detection Zone for Islanding Detection 14

Figure 4: Impedance Measurement Method 16

Figure 5: Transfer-Trip Scheme 21

Figure 6: Power Line Signaling Scheme 29

Figure 7: SG Connection 30

Figure 8: Voltage Waveforms at SG Site 31

Figure 9: Proposed Scheme 33

Figure 10: Representative System Showing Impedance Change 34

Figure 11: Signal Generator Connection 35

Figure 12: Waveforms of the Voltage at DG Terminal and the Thyristor Current 36

Figure 13: Voltage, Upstream Current and Thyristor Current Waveform 37

Figure 14: Upstream Current (Top), Theoretical Current Pulse (Middle), Actual (Bottom) . 38

Figure 15: Signal Extraction Process 39

Figure 16: Voltage, Upstream Current and Thyristor Current Waveform 40

Figure 17: Upstream Current Pulse 41

Figure 18: Circuit to be Analyzed to Find I_{PEAK} 44

Figure 19: Firing Angle δ 44

Figure 20: Circuit Including System Impedance 46

Figure 21: System Equivalent Circuit 47

Figure 22: Regular Operation 48

Figure 23: Islanded Condition 48

Figure 24: Uniform Circuit with Utility Connected or Disconnected 48

Figure 25 (a): Analysis of the Proposed Islanding Detection Scheme 49

Figure 26: Anti-Islanding Signal and Thyristor Current Waveforms 50

Figure 27: Voltage Deviation vs. Current Difference 52

Figure 28: Proposed SG/SD for Anti-Islanding Protection (One Phase Diagram) 55

Figure 29: Thyristor Firing 60

Figure 30: Signal Generator Algorithm 61

Figure 31: Threshold Setting for Laboratory Experiment 64

Figure 32: Flowchart for SD Algorithm 65

Figure 33: Simulation Setup - Typical Radial Distribution System 69

Figure 34: Simulation Waveforms for Voltage, Current and Extracted Signals 71

Figure 35: Harmonic Spectrum of the Extracted Signal (Normal and Islanded Operation) .. 72

Figure 36: Signal Generator's Thyristors Firing 72

Figure 37: Signal Pattern – Signal is Present in the Third Cycles 73

Figure 38: DG Voltage and Current Waveforms 74

Figure 39: Utility Voltage and Current on Utilized Phase 74

Figure 40: Thyristor Voltage and Current Waveforms 75

Figure 41: Load and Capacitor Voltage and Current Waveforms 75

Figure 42: Upstream Voltage and Current Extracted Signals 76

Figure 43: Vpcc During Normal Operation 76

Figure 44: Vpcc During Islanded Operation 77

Figure 45: Upstream Current During Normal Operation 78

Figure 46: Upstream Current During Islanded Operation 78
Figure 47: Detection Results with the Branch Line Length Varied 80
Figure 48: Detection Results with the Branch Line Length Varied (Thyristor Peak) 80
Figure 49: Detection Results with the Capacitor Size Varied 81
Figure 50: Detection Results with the Capacitor Size Varied (Thyristor Peak) 81
Figure 51: Detection Results with the Size of the DG Varied 82
Figure 52: Detection Results with the Size of the DG Varied (Thyristor Peak) 82
Figure 53: Detection Results with the Utility Fault Level Varied 83
Figure 54: Detection Results with the Utility Fault Level Varied (Thyristor Peak) 83
Figure 55: Detection Results with the Feeder Length Varied 84
Figure 56: Detection Results with the Feeder Length Varied (Thyristor Peak) 85
Figure 57: Detection Results with the Firing Angle Varied – 0 MVAR Capacitor Present ... 86
Figure 58: Detection Results with the Firing Angle Varied – 0 MVAR Capacitor Present 86
Figure 59: Detection Results with the Firing Angle Varied – 1 MVAR Capacitor Present 87
Figure 60: Detection Results with the Firing Angle Varied – 1 MVAR Capacitor Present 87
Figure 61: Detection Results with the Load Varied 88
Figure 62: Detection Results with the Load Varied (Thyristor Peak) 88
Figure 63: Laboratory Setup (Bottom) Derived from the 25kV System (Top) 91
Figure 64: Voltage, Current and Extracted Current Waveforms 94
Figure 65: Harmonic Spectrum of the Extracted Signal from Upstream Current 95
Figure 66: SG Thyristor Firing (Zoomed Image) 95
Figure 67: Voltage, Current, and Extracted Signal Waveforms for Full Signal Pattern 96
Figure 68: DG Voltage and Current Waveforms 97
Figure 69: Utility Voltage and Current Waveforms 97
Figure 70: Thyristor Current and Load Voltage Waveforms 98

Figure 71: Load and Capacitor Waveforms 98
Figure 72: Upstream Voltage and Current (Extracted Signals)..... 99
Figure 73: Vpcc Harmonic Spectrum during Normal Operation 100
Figure 74: Vpcc Harmonic Spectrum during Islanded Operation..... 100
Figure 75: Upstream Current Harmonic Spectrum During Normal Operation..... 101
Figure 76: Upstream Current Harmonic Spectrum During Islanded Operation..... 101
Figure 77: Detection Results with the Capacitor Size Varied..... 104
Figure 78: Detection Results with the Capacitor Size Varied (Thyristor Peak)..... 104
Figure 79: Detection Results with the Firing Angle Varied – 0 MVAR Capacitor Present. 105
Figure 80: Detection Results with the Firing Angle Varied (Thyristor Peak) – 0 MVAR.. 105
Figure 81: Detection Results with the Firing Angle Varied – 0.5 MVAR Capacitor 106
Figure 82: Detection Results with the Firing Angle Varied (Thyristor Peak) – 0.5 MVAR 107

List of Symbols

DG	Distributed Generator
DE	Distributed Energy
CO_2	Carbon Dioxide
AMR	Automatic Meter Reading
SCADA	Supervisory Control and Data Acquisition System
ROCOF	Rate of Change of Frequency
SG	Signal Generator
SD	Signal Detector
NDZ	Non-Detection Zone
RMS	Root-Mean-Square
p.u.	Per Unit
SCR	Silicon Controlled Rectifier
PCC	Point of Common Coupling
THD	Total Harmonic Distortion
W / kW	Watt / Kilo-Watt
MW	Mega-Watt
HV	High Voltage
MV	Medium Voltage
V / kV	Voltage - Volt / Kilo-volt (RMS)

v(t)	Voltage as a function of time
I / kA	Current – Amps / kilo-Amps (RMS)
i(t)	Current as a function of time
VAR / kVAR	Volt-Ampere (Reactive) / kilo Volt-Ampere (Reactive)
L	Inductance
C	Capacitance
R	Resistance
X	Reactance
Z	Impedance ($R + jX$)
t	Time (sec)
f	Frequency (Hz)
ω	System angular frequency ($2\pi f$) (rad/sec)

Chapter 1

Introduction

Distributed Generation (DG) refers to the scheme of generating power by a number of small generators (5kW to 80MW) interconnected at the substation, distribution feeder or customer load levels (120V to 44kV). Many distributed generator technologies use renewable resources such as wind, solar, small hydro, bio-mass, waste, etc., although internal combustion generators are also used.

There are many benefits of having DGs used in electric power systems. Some of the benefits to the power grid include [1, 2]:

- Reduced energy losses and upstream congestion in transmission lines
- Reduced or deferred infrastructure (line and substation) upgrades
- Improved grid reliability
- Higher energy conversion efficiencies than central generation
- Faster permitting than transmission line upgrades

They also serve to help improve a utility's ability to serve peak loads, and in the case of commercial/industrial users installing them, they can serve for reliability and peak shaving

applications and provide lower energy costs. DGs also have many environmental benefits associated with them. As mentioned before, many DGs use renewable power sources such as wind and solar, making them an environmentally friendly source of energy. Their use reduces the amount of carbon dioxide (CO_2) emissions (the main anthropogenic greenhouse gas emission) and as a result, many governments around the world are turning towards this source of power (it is estimated that 1000MW of installed renewable energy capacity reduces carbon dioxide emissions by a minimum of 1.2 million tonnes annually in Canada [3]) and thus, the DG industry has begun to play an increasing role in electric power systems.

Distributed generation has entered a period of expansion and commercialization and with the help of deregulation of the electric generation industry, this trend is expected to continue. A study by the Electric Power Research Institute (EPRI) indicates that in the United Kingdom, by the year 2010, 25% of new generation will be distributed [4], while the Energy Information Administration in the United States predicts an annual growth in the DG market of 5.9% a year between 2005 and 2030 [5]. In Canada, wind generation alone, accounted for 1,460 MW by the end of 2006, with provincial governments seeking to place a minimum of installed wind energy capacity of 10,000 MW by 2015 [3]. There are many benefits to having distributed generation in our electric power systems, and as this trend continues it is anticipated that it will lead to a competitive and environmentally-friendly electricity market. There are however, many barriers still in place for DGs. One of the largest technical problems is to make sure that the DGs operate in a safe environment, and that they disconnect from the electric grid if the power distribution system becomes isolated from the transmission system (known as islanding).

1.1 The Anti-Islanding Problem

An electric island is described as a section of the power distribution system that is isolated from the rest of the network and has generators providing power to customers in the section. To illustrate this, Figure 1 shows a typical radial distribution system. A substation, converts the transmission high voltage (HV – 69kV-500kV) to distribution medium voltage levels (MV< 44kV). The substation has several feeders coming out (only two are shown in detail). Each feeder has multiple loads, branches and DGs. Distribution networks typically have multiple layers of protective equipment such as relay/breakers, fuses, reclosers and sectionalizers (shown as boxes along the lines). In the case of Figure 1, the system is operating normally. The distributed loads along the feeders are drawing power from both the utility (substation) and the DGs.

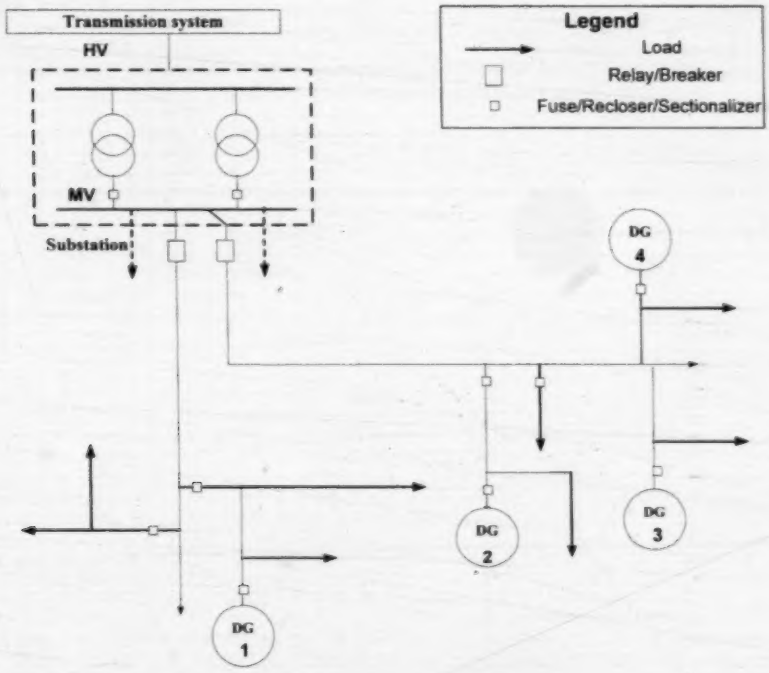

Figure 1: Typical Distribution System

Figure 2 demonstrates how an island in an electric system forms. Suppose that the breaker on third feeder from the left (labeled) opens. Island #1 is formed. This part of the distribution system is now isolated from the transmission system and is powered by DGs #2-4. It does not have to be an entire feeder as in the case of Island #1. In the figure, another islanding scenario is shown. Island #2 forms when an upstream fuse protecting the main feeder opens. This tap, if it includes a DG, becomes a small power island of its own, with only the DG (#1) supplying power to the nearby loads.

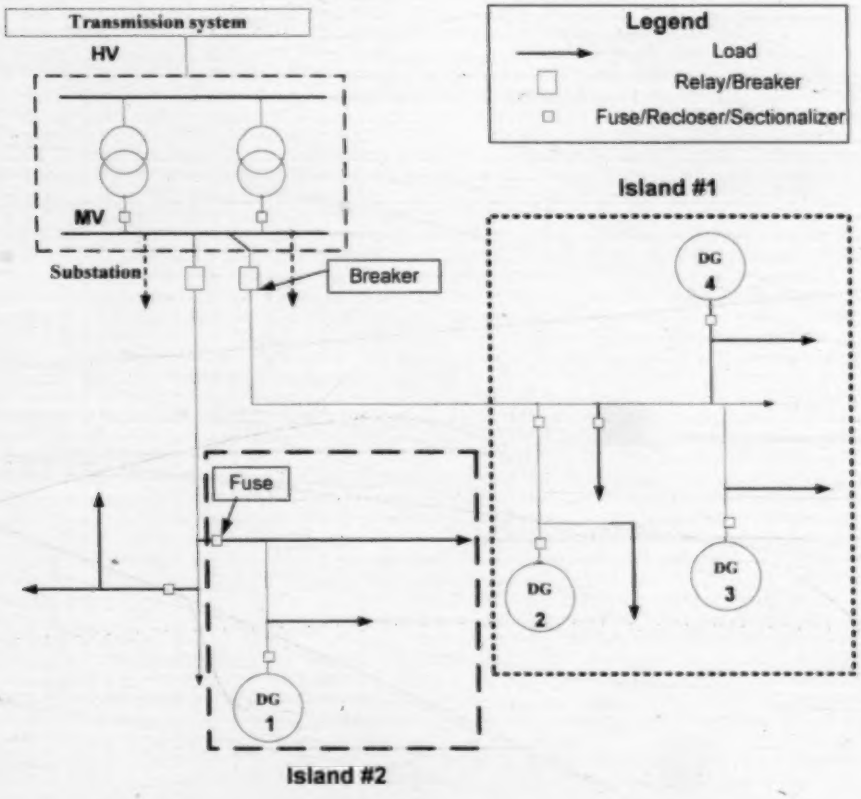

Figure 2: Distribution System with Power Islands

These islanded sections, due to the absence of a stiff power source can be very unstable, which may have very harmful effects on both system and customers.

It is very important not to allow power islands to occur so as to protect the DGs, distribution system equipment, neighbouring customers from electrical damage, and to ensure the public's and servicemen's (who operate the system) safety. The four main concerns can be classified as power quality, out-of-phase reclosing, protection equipment malfunctioning and safety. These are explained below in more detail.

1.1.1 Power Quality Concerns

A DG, working alone in an islanded system without the support of the utility's source, cannot regulate voltage and frequency properly and thus the resulting condition would be unpredictable and often would go beyond the operating limits of electrical equipment in the system. This power quality issue is of utmost concern, as even though utilities would have no control over the voltage and frequency that the DGs supply the customers with, they would still be responsible for any damages caused to the customer.

1.1.2 Out-of-Phase Reclosing Concerns

Another major concern of electric power islands is out-of-phase reclosing. Utilities utilize reclosers as a means to clear temporary faults, as they account for 50-90% of all faults [6]. A four year study was conducted and reported by EPRI which surveyed fifty distribution feeders belonging to thirteen different utilities, most of which were operating at 15kV. 93% of these feeders were overhead and the average length was 10.8 miles. The survey results showed that 85% of faults were temporary [7]. These can be caused by lightning, wind, frost, animals and others. Once a fault is detected, the recloser opens the line for a short time allowing for the fault to clear and then recloses back in, energizing the line once again. This helps improve reliability of the

distribution feeder greatly, but in the presence of a power island, can lead to equipment damage.

During the time that the recloser is open, a DG will most likely lose synchronism with the utility as it tries to adjust its power flow and serve neighbouring customers by itself. Reclosing to an island which is out of phase can lead to large mechanical torques and currents in rotating DGs and cause damage to the generator prime mover [8]. Out-of-phase reclosing can also cause unusually high inrush currents to transformers and motors (up to 6-10 times the rated full load current under transient conditions [9]). This simultaneous inrush to many devices can cause fuses and circuit breakers in the system to operate on both the utility and customer side. Large transients also occur, which can potentially damage all equipment along the line as they can be of several magnitudes higher than normal operating voltages.

Standard utility practices involve programming the reclose time interval to be within the range from 0.3 seconds to 5 seconds before the line is re-energized. Out-of-phase reclosing is a system issue, and thus appropriate measures need to be taken to ensure that a DG's islanding protection is coordinated with utility circuit reclosing practices, and therefore should trip the DG before reclosing takes place.

1.1.3 Protection Equipment Malfunctioning Concerns

Protection equipment would also malfunction and/or not coordinate in a DG powered electric island, as the short circuit current that is available from a distributed generator is very small due to the absence of the stronger utility source. This would increase the chances that a fault would be undetectable. Without protection equipment, equipment

failures can occur, and lines that have made contact with ground remain energized posing significant safety risks.

1.1.4 Safety Risks

An islanded DG would also pose serious health risks to the public, linemen and servicemen that maintain the distribution system, as it would keep the system energized and make it hazardous for them to make repairs or service the lines, especially when they believe that the line has been disconnected from the rest of the system and is de-energized. The public would be at risk also if the utility had no capability to de-energize fallen lines.

The most critical step to prevent such situations listed above is to equip every DG with the capability to detect an islanded condition, and once it occurs, to disconnect itself from the distribution system within a specified time. This is called an anti-islanding device. Typically, a distributed generator should disconnect within 100 to 300 ms after loss of main supply [10-12].

When selecting an anti-islanding scheme, it is important to consider its characteristics. Almost all DGs can be categorized into the following three types [13]:

Inverter-based generator: These types of DGs are relatively small in size (from a few hundred watts, to 1 MW). The DG can be PV (photovoltaic panels), fuel cells, small turbines, etc. Due to its small size, they are usually connected to secondary feeders. The inverter is the interface between the generator and the system and all inverter-based DGs have operating characteristics with respect to

the grid interaction. These are determined mostly by the inverter topology and controls. They are capable of sustaining an island and many inverter specific anti-islanding techniques have been proposed.

Induction Generators: These types of DGs can be fairly large in size, for example, up to 20MW, which is why they are typically connected to the primary feeder. They are usually not able to sustain a power island as they need reactive power support from the utility (there can be instances where there is enough reactive power support in the power island). Due to this, anti-islanding protection is usually not considered an issue.

Synchronous Generators: These DGs can be very large (as high as 30MW), and are usually also connected to the primary feeder. They are capable of sustaining an island and due to their large rating, there are limited options to control these generators for the purpose of islanding detection. These cause the greatest problem in this area and anti-islanding protection for them has emerged as one of the most difficult tasks for the industry.

1.2 Current Methods for Detecting Islanding Conditions

This section presents a review of the current methods for anti-islanding protection that have been developed and in use in today's distribution systems [13-21]. Islanding detection is a very important part of the overall protection scheme for distributed generators in distribution networks. As mentioned earlier, there is a growing interest in DGs and thus there has been extensive research done to overcome this major technical barrier. There are advantages and disadvantages to each method, and as will be shown, there is a great need to develop anti-islanding protection which is reliable and cost-effective. The common devices in use for this purpose can be categorized into two types, communication based, and local detection based which include both passive methods and active methods. They will be discussed in greater detail below.

1.2.1 Passive Methods

Most current anti-islanding devices work on passive methods which rely on the principle that in an electric power island, the mismatch between generation and load is great. This, in many cases is true, as the size of the DG is small and is used only to supplement the main power from the utility, but as will be shown further on, there are situations where this would not be the case. It would depend on the distribution system, size of DG, types and sizes of loads on the lines and the size of the power island. Passive methods use information available to them at the terminals of the DG, at the point of common coupling (PCC), such as voltage, current and frequency. They process that information to determine if an island has formed, and send a signal to the DG to trip if it has.

The most common devices used are modified versions of the under/over voltage relays, under/over frequency relays, and other frequency relays such as the Rate of Change of Frequency Relay (ROCOF) and Vector Surge Relays (VSR) [22, 23]. They work on the principle that the voltage will fluctuate once a system is islanded, a phase shift will occur, and frequency will drift due to the generation and load mismatch. These relays are often used together to improve the reliability of islanding detection, and as such, can drive the cost of an anti-islanding device high.

1.2.1.1 Under/Over Voltage Relay

The most common relay for islanding detection is the under/over voltage relay. This relay operates on the reactive power mismatch in an island principle. Excess reactive power will cause the voltage at the DG terminals to increase, while a shortage in reactive power will cause the voltage to decline. These relays can be used to measure the change or rate of change of voltage at the terminals of the DG to determine whether islanding has occurred.

They typically work faster than frequency based relays as voltage change can occur much sooner than a frequency change as there is no mechanical inertia associated with it. Distribution systems however, usually don't have a large reactive power mismatch due to the need for feeder loss reduction, and as a result, the reactive power mismatch and its associated voltage change in an islanded system can be small [13].

Under/over voltage relays can be used as a first line of defense for anti-islanding protection, as they are required to be installed for other protection in a DG, such as to prevent over-voltages to the DG unit, and thus require no extra cost.

1.2.1.2 Frequency Based Relays

There are three different types of frequency based relays:

Frequency Relay: This relay calculates the frequency of the terminal voltage waveform. It works on the under/over frequency principle, so if the frequency deviates from normal, say, lower than 59.5Hz or higher than 60.5Hz, it will send a signal to the DG to trip. The DG will have to be tripped within the time frame that is allowed.

ROCOF Relay: This relay also calculates the frequency of the terminal voltage waveform. Instead of using under/over frequency as a criterion to trip, it determines the rate that frequency is changing. The DG is tripped if the rate is higher than certain thresholds. Typical settings for ROCOF relays are between 0.1Hz/second and 1.2Hz/second [13].

VSR Relay: This relay measures the phase angle shift of the voltage waveform against a reference waveform. Although this is not a frequency measurement, it can be shown that the phase shift is an indirect measurement of the waveform frequency and thus this relay has similar performance characteristics as that of the frequency relay.

As was mentioned before, a large mismatch between generation and load will cause fast deviation of the frequency in a power island. Excess generation will drive up the frequency while deficit generation will result in a reduction in frequency. However, if the power imbalance is small, frequency will deviate slowly, and under these

conditions, these devices would fail as reliable anti-islanding protection because they would not operate in the time required.

1.2.1.3 Other Passive Schemes

There have been many other documented research works associated with anti-islanding protection:

Harmonic Change: This method is for inverter based DG applications. The inverter controller measures the total harmonic distortion (THD) of the terminal voltage, and if it is not within a specified range, it trips the DG. The distribution network, when operating normally, is a strong, stiff source (means that the impedance of the network is low). Thus the voltage THD at the inverter terminals is low. When an island forms, the impedance increases, as the impedance of the DG parallel to the rest of the islanded network is much higher than that of the utility. The voltage THD will increase, as the current harmonics will cause more of a voltage distortion due to the higher impedance. It is however, very difficult to set a proper voltage THD limit as the increase of non-linear loads in distribution systems causes a great deal of current harmonics.

Power Factor and Active and Reactive Power Output Methods: These schemes have been documented in [24, 25]. The active power output monitors the DGs active output power. This method will most likely be similar in effect as the frequency relay based method as the frequency change is a direct consequence of active power output [13]. The reactive power output method monitors the DG's reactive power output. It has the

possibility to be more effective than the voltage relays because it is a more sensitive index, however it would require the generator to be operating in voltage control mode, which is often prohibited [13]. The power factor method is based on both the reactive and active power output of the DG.

To summarize, voltage and frequency are controlled by the utility and are almost constant. The stronger source from the transmission and distribution networks is designed to work within certain tolerances so as not to cause any adverse effects or damage to customer loads. Once this power source is disconnected, the DGs could experience voltage sags or swells and the frequency can speed up or slow down. These anti-islanding devices count on these to happen. They compare the measured waveform values at the terminals of the DG with preset values and if they go beyond the programmed operating range, or they change faster than is expected, they trip the DG.

The problem with these anti-islanding protection methods occurs when generation and load are closely matched. The power mismatch level in an island can be affected in multiple ways. Different fuses, breakers, reclosers can operate creating different islands which can vary the amount of load connected. Feeder loads typically do not stay constant throughout the day but rather fluctuate, which also changes the power mismatch. An example of this is shown in Figure 3. This figure shows the load variation during the course of a day. Say that an 8MVA DG is present and an island forms by means of the feeder relay at the substation opening. It can be seen that there are a couple of times throughout the day that the power mismatch is small. It should be noted that this mismatch may become larger or smaller depending on which sections of the feeder become islanded, what loads were present, etc. During these times (shown with circles on Figure 3), if a power island was formed, voltage

and frequency may change only slightly or slowly, in which case the passive anti-islanding protection methods described will not operate in the required timeframe. This region is often called a Non-Detection Zone (NDZ). The example in Figure 3 shows a steady DG power output. This may not always be true, such as in the case of wind and solar generators. It is therefore often not possible to determine the mismatch level between the DG and islanded loads.

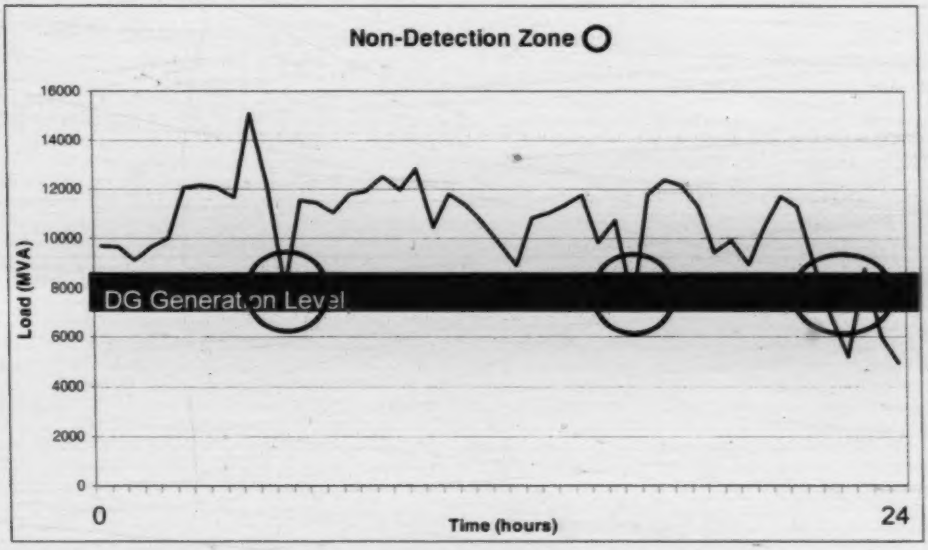

Figure 3: Non Detection Zone for Islanding Detection

The ROCOF relay is one of the most common used for anti-islanding protection as it has the best performance since its non-detection zone is the smallest [13]. However, due to this, it is more prone to nuisance tripping. Studies have revealed that a non-detection zone of 10% - 30% power mismatch exists for all relays [13]. To limit the size of the NDZ, the anti-islanding relays have to be set with tighter tolerances and while this creates a more effective islanding detection device, it also causes the DG to nuisance trip. The DG would trip even when a power island hasn't formed, but some of the parameters such as voltage or frequency suddenly changed for a brief moment. An example of this occurrence would be a large motor

starting across the line causing a momentary voltage sag. Thus, these devices have to compromise between detection reliability and nuisance tripping.

To summarize, the advantages and disadvantages of current passive methods are listed below:

Advantages:

- Have a lower cost and are simple
- Do not inject any disturbances and thus don't affect power quality

Disadvantages:

- Have a Non Detection Zone where they fail to operate (when generation and load mismatch is small)
- Often lead to nuisance tripping of the DG
- Utility has no control and cannot disconnect the DGs automatically

1.2.2 Active Methods

Active methods for anti-islanding protection have been developed [21, 26] in order to overcome the limitations of passive methods that were mentioned before. Active schemes inject disturbances into the distribution system and detect islanding conditions based on system responses with measurements taken locally. These methods are presented subsequently, with the first two being designed for synchronous DGs and the last two, for inverter-based DGs.

1.2.2.1 Impedance Measurement Method

An islanded system will have much higher impedance seen at the DG terminals than when operating in parallel with the utility. This is because the low impedance of the utility is disconnected and only the DG, loads and lines (with a larger impedance) in the island will contribute to the impedance seen at the terminals. Therefore, it is possible to detect an islanded condition by measuring system impedance on a continuous basis as shown in Figure 4.

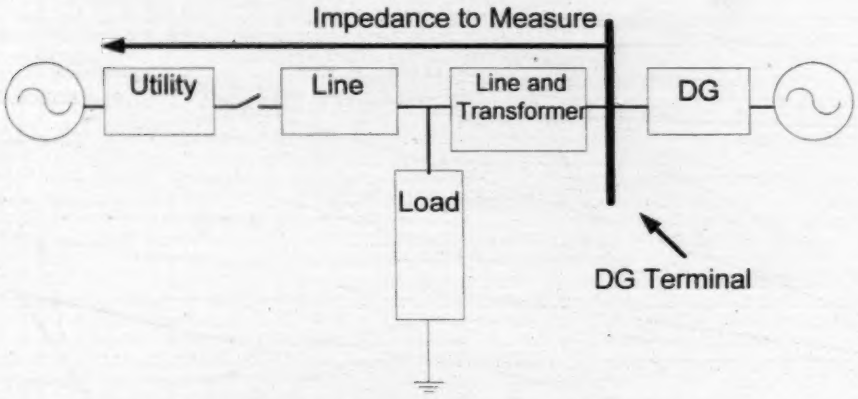

Figure 4: Impedance Measurement Method

Measuring system impedance is not an easy task however, and requires to inject disturbances into the system. In [21], a method is introduced that measures the system impedance by using thyristors to inject disturbances into the system. The response from the voltage and current is then used to determine the impedance. This measurement does not need to be very accurate as the impedance change will be drastic from a normal operating system to an islanded one.

Inverter-based DGs also use this active scheme. They inject a known signal into the output current and monitor the voltage response which is similar to the passive scheme mentioned before that uses harmonics to detect islanding, but has the advantage of being less sensitive to noise and distortions. Another method is to disturb the output current, which causes a change in the output power, and then monitor the change in output voltage that results [27].

Unlike the passive methods that were discussed earlier, these methods do not require that there be a large power mismatch for them to operate properly. They do however require a disturbance generator at each DG site which increases cost of the overall DG protection. Another downside is the fact that some loads may have a frequency response that prevents the injected disturbance from adequately impacting the parameters and therefore the ability to detect a power island. The main concern is one that is shared by all of the active schemes for anti-islanding protection. It is the interference of the injected disturbances when more than one DG is present. This interaction among DGs can make this scheme in-effective.

1.2.2.2 Varying Generator Terminal Voltage Method

Another active scheme that has been proposed [19], is measuring the change of reactive power flow when the voltage at the terminals of the DG is varied. This is a variation on the impedance measurement method, as the change of the DGs reactive power output can be quite different when there is a different impedance. When the system is working normally, with the DG and utility working in conjunction, the variation of reactive power flow will be small with a varying terminal voltage. Once

the DG is in an island, this change will be larger. This method requires to constantly vary the excitation system of the DG.

Another method [28] varies the terminal DG voltage which changes periodically with a frequency of 1 Hz to 5 Hz. Magnitude of the variation is about 1%. [28] shows that this voltage change will accelerate the change of frequency if the generator is operating in an island. Thus, this method is used to complement frequency based relay anti-islanding methods as it will allow them to detect islands with less difficulty, including when there is a small difference between generation and load. This technique is effective at reducing the frequency based relay methods non-detection zone.

Both these methods have the same problem as the impedance measurement method. There is potential for interference between DGs which are injecting similar disturbances into the system and may make it difficult or impossible to determine the generators response to them. They are much more complicated than passive methods, driving up the cost, and they deteriorate power quality, as well as introduce rotor vibrations.

1.2.2.3 Frequency and Phase Shift Method

When a power island forms and the distribution network is disconnected, an inverter's frequency will change to a new stable operating point which is determined by the resonant frequency of the load in the island. This may be within the operating frequency limits and thus frequency based relays will fail to operate. This technique applies positive feedback to control loops that control the inverter's phase, frequency,

or reactive power. This causes the inverter frequency to change quickly to the under/over frequency limits if the distribution network is absent and thus cannot maintain frequency.

This method is very successful in detecting islanding conditions and typically has a small non-detection zone. It does not require that there be a mismatch in power generation and load in an island and thus is a compliment to the frequency-based relays. Another important characteristic of this method is that interference among multiple DGs can be avoided if the gains in the feedback loop are chosen in a consistent manner [13]. This method is however not able to properly detect islanding conditions if the load quality factor is high [29, 30].

1.2.2.4 Voltage Shift Method

The voltage shift method is another active anti-islanding scheme that has been proposed [13]. It works on a similar principle as the frequency and phase shift technique as it also applies a positive feedback loop. This method, however, applies this loop to the current or active power regulation control loop to cause the inverter terminal voltage to increase or decrease rapidly towards the under/over voltage thresholds in the case of an island. This only occurs when the stiff distribution network is disconnected as it does not maintain the voltage at operating levels and reduce the effect of the positive feedback gain. Without this loop, the DG terminal voltage would change once an island is formed, but may still stay within permissible levels and thus the under/over voltage relays would not operate as the new stable operating point would be determined by the local load resistance. It introduces an instability that drives the voltage towards one of the limits.

This method also can be coordinated among multiple DGs in a distribution network so as not to encounter interference and reduce the effectiveness of the method.

To overcome the limitations of passive anti-islanding protection schemes, several active methods have been proposed. To summarize, the advantages and disadvantages of current active methods are listed below:

Advantages:

- Provide more reliable anti-islanding protection than passive methods (smaller NDZ)
- Can be used to increase the effectiveness of passive methods
- Inverter-based DG active anti-islanding schemes can provide relatively reliable islanding detection

Disadvantages:

- Injects disturbances into the system affecting power quality
- Interaction between multiple DGs that produce similar disturbances may affect reliability of methods
- Complex, and thus very expensive, especially for synchronous machines
- Some methods have not been tested (especially for synchronous machines)
- Utility has no control and cannot disconnect the DGs automatically

1.2.3 Communication-Based Methods

Communication anti-islanding methods detect islanding based on information collected at remote sites and sending a signal through communication methods to trip the DG if islanding has occurred. These methods are independent of the type of DG that is protected.

Transfer-trip schemes are used for anti-islanding protection and they work on the basis of monitoring all possible disconnect points that could island a distributed generator. The Control Centre receives status on all its breakers, reclosers and points of disconnect and using this information and running it through a central algorithm, it determines whether a DG power island has occurred. If it has, it then sends a trip signal to the DG which disconnects. A simple example of this is shown in Figure 5.

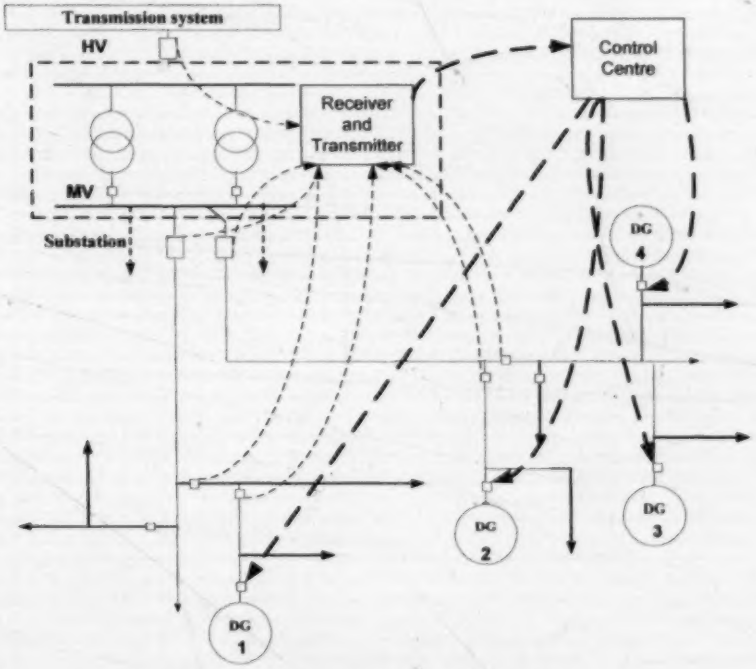

Figure 5: Transfer-Trip Scheme

In the case of a radial feed distribution system, a nearby recloser can send out a signal to the DG to trip if it operates or detects that an upstream protective device has operated.

This communication method is reliable at detecting islanded conditions but requires each DG to have a receiver and all reclosers, circuit breakers, sectionalizers, gang switches and any other upstream devices to have a transmitter. These devices would have to be SCADA equipped which drives up the cost, and also have telecom support in the area. There needs to be a control centre which would handle all the incoming data from the devices and send out a trip signal to the DGs once islanding has occurred. This may become a very complex task, especially if multiple feeds are possible towards the DG and switching takes place regularly, such as can be expected in a loop or mesh feeder topology. The DG may at one point be connected to one substation and at another time to another substation. This scheme is also very useful as it can be used to reconnect the DG once the main grid is re-energized.

Transfer-trip schemes can be very useful at detecting islanded DGs, but they require extensive communication infrastructure. Radio towers or telephone line can be used but if they are not present, as may be the case for many rural areas with low population, this scheme cannot be used or can be very expensive to set up. If telecom coverage is weak or non-existent, the cost of this scheme could easily kill a DG project.

There are other telecommunication methods in literature, but they are mostly variations to the method described here. A power line signaling scheme has also been proposed, which uses power lines in the distribution system as a carrier [31, 32]. This method has a signal generator placed at a substation. It then broadcasts a signal down the distribution lines and each DG has a receiver which checks for the continuity of the signal. If the receiver does not

detect the signal, it suggests that a break has occurred in the line and the DG is islanded. This method is described in more detail in Chapter 2.

To summarize, the advantages and disadvantages of telecommunication anti-islanding methods are listed below:

Advantages:

- Provide reliable anti-islanding protection for DGs
- Are in direct control of the utility
- Can be used to reconnect the DGs once normal service is restored
- Do not cause nuisance tripping

Disadvantages:

- Requires every disconnect device to have communication capabilities
- Is very expensive especially if telecom is not present and Distribution SCADA is not common
- Requires control center
- Can become very complex if feeder topology can vary

1.3 Proposed Solution for Anti-Islanding Detection

Anti-islanding protection for DG has become one of the more challenging technical barriers for DG interconnection. Many anti-islanding protection devices have been proposed, and some have been used. There is clearly a need however, for a device that will be simple, reliable and economical.

This thesis aims at presenting an active anti-islanding method that is based on impedance measurement. It requires a device that will disturb the voltage around the zero-crossing point of the waveform at the terminal of the DG. This creates minimal impact on the voltage waveform. The upstream current is then analyzed and a decision as to whether an island has formed is made based on the DC component of the current.

It is different than other proposed solutions as it is a simple device, thus a low cost alternative. It will be shown that this method is not only reliable, but it also overcomes the disadvantages of current anti-islanding methods. There is minimal impact to the voltage waveform, which reduces the effect of the device on power quality and also minimizes the possibility of multiple DGs with the same device to be interfering with each other.

The scope of this thesis is to review the theory behind the proposed anti-islanding method based on impedance measurements and develop an algorithm for islanding detection that is reliable, robust and responsive. The effectiveness of the algorithm and method will be demonstrated through many simulations and laboratory results using a scaled down model of a distribution system.

1.4 Outline of the Thesis

Current methods being used for anti-islanding protection have either a high price tag associated with them or reliability concerns. This thesis addresses these issues and proposes a new, reliable, and economic approach for anti-islanding protection. The following is an outline to the thesis.

Chapter 1 – is an introduction to distributed generators and the anti-islanding protection problem. It familiarizes the reader with the issues of islanding and the consequences associated with it. It also includes a summary of current anti-islanding devices used or proposed for DG protection. It explains each device briefly and illustrates the advantages and disadvantages of each and gives the reader some background to fully understand why a new method would be beneficial to the DG industry. It then briefly talks about the proposed solution that this thesis presents and finally concludes with a brief outline of the thesis.

Chapter 2 – is meant to introduce the reader to the proposed solution identified in this thesis. It starts off by discussing the power line signaling method for anti-islanding protection proposed by the Power Research Group at the University of Alberta. This research has been conducted for several years now and this thesis proposes a method which is an extension onto that one. Its purpose in this thesis is to explain how the signal generator works, as a modified version of it is required for the proposed solution.

An algorithm is presented in this section and the proposed method is then discussed and its advantages are explained. Theory and analytical studies are also presented. It then goes on to explain that this approach works well under many different operating parameters, such as distribution systems with or without capacitors.

Chapter 3 – presents simulation studies of the proposed method using PSCAD. The simulation setup is explained and results are provided. A sensitivity study is also conducted to demonstrate the robustness of the method. The results are then discussed.

Chapter 4 – Laboratory tests using a scaled down version of a typical distribution system are offered in this chapter. A small synchronous generator was used to simulate the DG and lines and loads were represented by resistors and inductors. These results corroborate the ones obtained during the simulation study in Chapter 3. The results are discussed and the limitations of such an experiment are explained.

Chapter 5 – Finally, in this chapter, conclusions on the proposed method are presented. The limitations of the algorithm are summarized, as well as any potential improvements. Future research related recommendations, are suggested.

Chapter 2

A Local Active Anti-Islanding Scheme Based on Impedance Measurements

This chapter contains the new proposed method for anti-islanding detection using impedance measurements. The first section introduces the reader to a power line signaling based method for islanding detection that was developed by the Power Group at the University of Alberta. This is required as it is this method that brought on the need for developing a local detection scheme and the equipment used for that scheme, modified slightly, will be implemented for this thesis' proposed method. The second section introduces the proposed local active anti-islanding protection scheme and provides an overview on how it is implemented. The third section presents analytical studies to support this scheme, including impedance change and detection. The forth section will discuss the hardware necessary to implement this scheme and the fifth section will discuss the algorithm for detecting islanded conditions. Two detection algorithms will be discussed, one that monitors the signal generator current, which can be used if the distribution system does not have capacitors present, and another that monitors the upstream current which will be shown in the analytical studies, simulations and experimental results to work for distribution systems with or without capacitors. The chapter will conclude with a summary on the proposed scheme and detection algorithms.

2.1 Power-line Signaling Based Scheme

A power line signaling based scheme for anti-islanding protection of distributed generators has been proposed by the Power Research Group at the University of Alberta [31, 33, 34]. This scheme is shown in Figure 6 and will be explained in greater detail in this section. This method of anti-islanding protection for DGs involves two pieces of equipment, a signal generator (SG), connected to the distribution bus at a substation, and a signal detector (SD), connected at the terminals of every DG that is connected to a feeder emanating from the substation. The signal generator broadcasts a signal to the distribution feeders continuously and with a preset protocol. The signal detector, present at each DG site, monitors the voltage waveform and checks for the presence of the signal. If it cannot detect the signal for a certain time, it means that a break in the distribution line has occurred and the DG is islanded. This can happen by having a protection device open between the DG and substation or if the substation loses power, which is also an island condition. All DGs that don't detect the signal will trip at that instant. The signal generator has auxiliary inputs which can be used to trip all downstream DGs if needed, such as when a transmission island occurs. In Figure 6, all 4 DGs would be protected by the one SG at the substation.

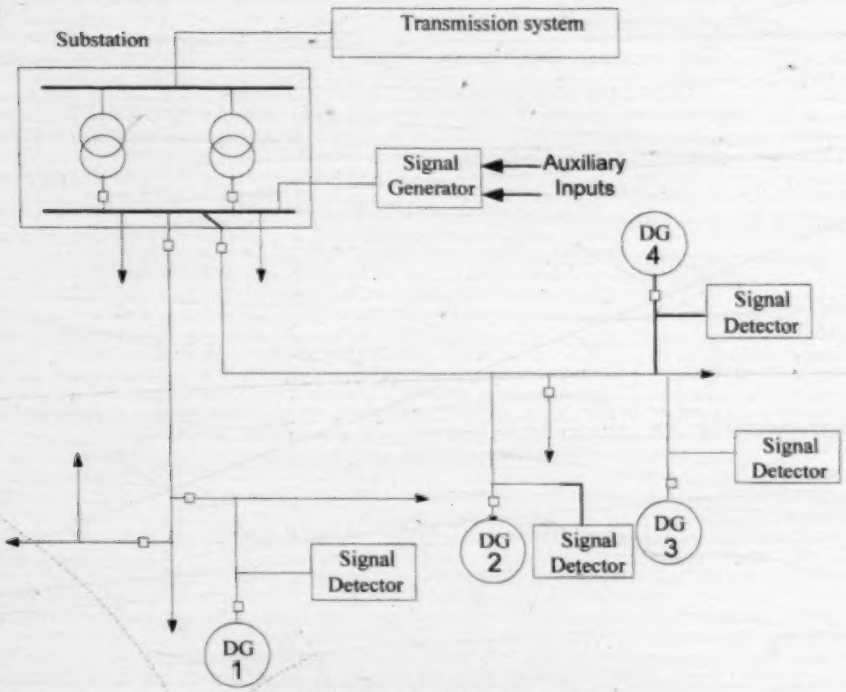

Figure 6: Power Line Signaling Scheme

This scheme works just like a transfer-trip scheme mentioned earlier, however it has many advantages. Since it works on the principle of signal continuity, it does not require all protective devices to have Supervisory Control and Data Acquisition System (SCADA) capability (communication ability) as an opening of these devices will disrupt the signal and the DG will trip. Another important characteristic of this device is that it is independent of network topology changes. It also has the advantage of being economical as there is a need for only one SG per substation to satisfy the needs of all downstream DGs and it can be tested without disrupting the distribution system, as the signal generator can be simply turned off and all signal detectors should then detect no signal.

2.1.1 Signal Generator

The signal generator is the device used in this method for communication with downstream DGs. There are many mature techniques available to send information over power lines, such as ripple control techniques, waveform shift techniques and waveform distortion techniques. Since this communication is needed for islanding detection, the signaling method that was chosen was the waveform distortions technique as it is reliable, low cost and has a fast response.

A step down transformer is used to reduce the main feeder voltage to a level that a thyristor can operate at. The thyristor turns on for several degrees before its voltage crosses zero, creating a momentary short circuit and then turns off when the current reverses its direction. This brief dip in the voltage (the distortion), around the zero crossing point of the waveform, is the signal that is propagated down all feeders. Figure 7 shows the SG connection at the substation's distribution bus.

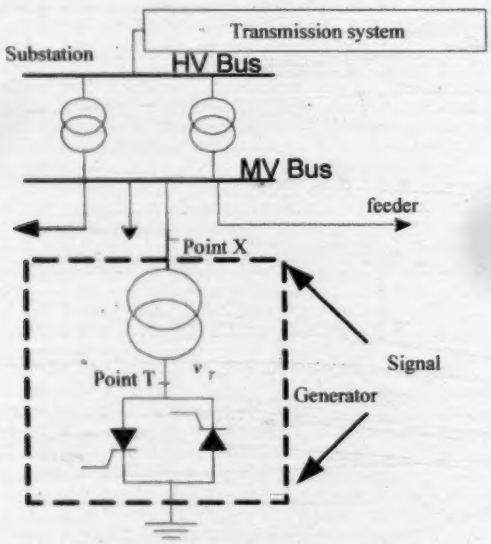

Figure 7: SG Connection

The signal detectors monitor the voltage waveform and use it to determine whether islanding has occurred. If the thyristor does not fire, then there is no voltage waveform distortion and thus no signal. Figure 8 shows the resulting voltage waveforms that occur when the thyristor is in operation. The waveforms in this figure are not to scale as the distortion is in reality very small.

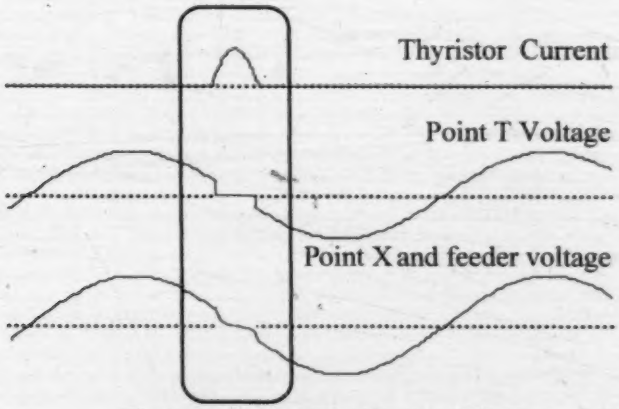

Figure 8: Voltage Waveforms at SG Site

This signaling technique has been very successful in AMR (Automatic Meter Reading systems) and as such, much data has been obtained through this method.

2.1.2 Signal Detector

The signal detector is installed at each DGs terminals and it examines the voltage waveform for the presence of the signal generated by the SG. Since anti-islanding protection has to operate usually within 100-300msec, the SG thyristors fire only every four cycles and therefore the signal is present once every four cycles. If the signal detector does not detect the signal within 4 of these periods (16 cycles), it sends a signal to the DG to trip. The detection algorithm is not discussed here in detail as it is beyond the scope of this thesis, and can be found in great detail in [31] and [33]. In short, the signal transmitted through the

distribution feeders has a typical frequency that is within 200-600 Hz. By monitoring the harmonics associated with those frequencies, the SD is able to determine whether the signal is present or islanding has occurred.

2.1.3 Disadvantages of this scheme

While this proposed anti-islanding protection scheme has many advantages and has been shown to work reliably and is much more economical than transfer-trip schemes using other forms of communication technologies, it has certain disadvantages. One disadvantage is that the SG has to be placed at the substation and as such, it requires access to the substation for any maintenance. Another is the effect on power quality and communication interference. Since this method works on voltage distortions introduced into the voltage waveform, it deteriorates the power quality for all customers and may interfere with existing communication technologies such as AMR's TWACS (Two-way Automatic Communication System) and any other power line signaling communications.

Because of these drawbacks, a new method that is a variation on this power-line based signaling method for anti-islanding protection of DGs has been proposed in this thesis.

2.2 The Proposed Scheme

In this thesis, a local active method is proposed for anti-islanding protection of distributed generators. This method is indirectly based on impedance measurements and is significantly different from published methods. It will be shown through analytical, simulation and

experimental studies to provide reliable islanding detection capability. This scheme utilizes a signal generator connected to the terminals of the DG similar to the one mentioned in the previous section. Since this method is suitable for protecting only one DG, there is no need to broadcast a voltage signal. The upstream current is monitored by the detection algorithm and once an islanding condition is detected, it sends a signal to the DG to trip. The benefit of this method is that it can serve only one DG without sending voltage signals down the rest of the feeder, thus not affecting power quality throughout the distribution system, and in the presence of other power line communications being present, it will reduce the chance of interfering with them. Since the voltage stays relatively constant and is minimally affected by the current pulse generated by the SG, the current becomes relatively proportional to the impedance and thus is used for the islanding detection criteria. Figure 9 illustrates this arrangement. As can be seen in this figure, all four DGs present will have a SG and a detector present at their terminals.

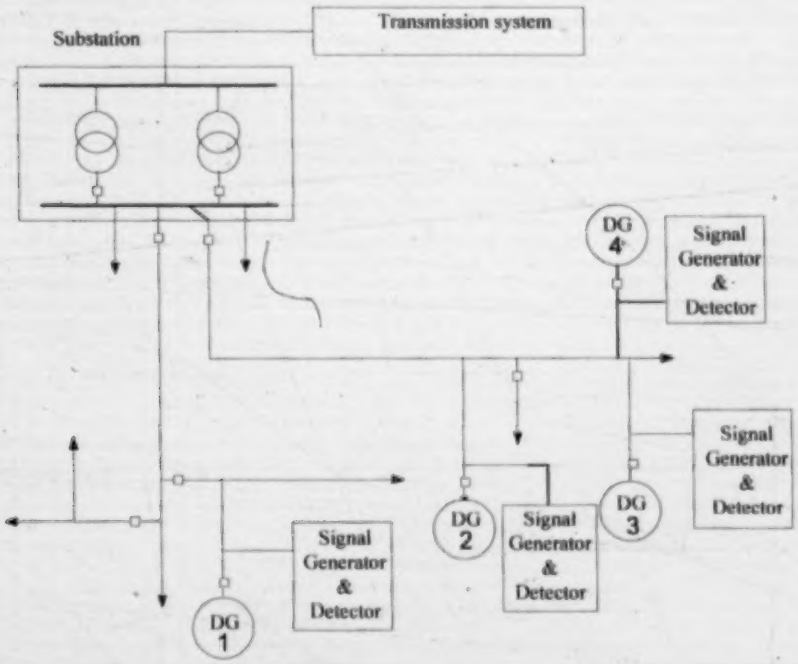

Figure 9: Proposed Scheme

Since the utility impedance is typically much smaller than the impedance of a distributed generator, the system impedance at a DG terminal is much larger when a power island is formed than that when the DG is connected to the power grid. This characteristic change is behind the proposed method and is the determining factor as to whether an island has formed or not. The change in system impedance seen at the DG terminal is shown in Figure 10. The impedance values are shown for illustrations sake and are selected to be a realistic representation of a system, but may vary. When the system is operating in normal synchronized mode with the breaker closed, the impedance at the DG terminal is approximately 0.187p.u., while when the switch opens, the system impedance at the DG terminal increases to 0.67pu

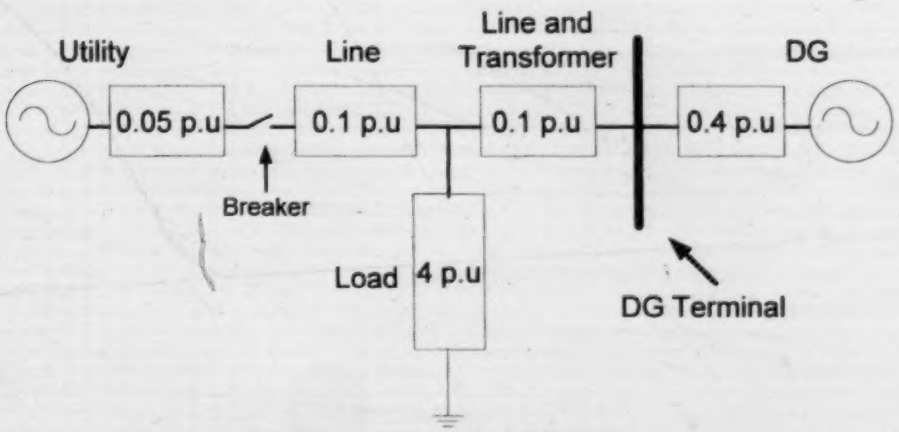

Figure 10: Representative System Showing Impedance Change

Any increase in system impedance seen at the DG terminals, to values much higher than those under normal operating conditions, is recognized to be an indicator of an island formation and the DG would be signaled to trip. This method would be immune to generator loading and would not cause nuisance tripping of the generator due to faults or transients. It overcomes the problems with current passive methods as it does not depend on a mismatch with the generation and load in an island and will be shown to be effective in detecting

islanding conditions with no apparent non-detection zone. It also has the benefit of being implemented fairly easily and economically as it requires minimal computational power.

Measuring network impedance can be a difficult task and is well documented [35-39]. However, since the difference in the impedance when the DG is connected to the grid and that when the DG is in a power island is considerably large, the impedance measurement need not be very accurate, which differentiates this proposed method from current practices while overcoming the difficult task of measuring network impedance precisely.

2.2.1 Signal Generator Operation

The proposed scheme utilizes a signal generator and detector at each DG's terminals. Figure 11 shows the SG connection to the terminals of the DG and the connection of the signal detector.

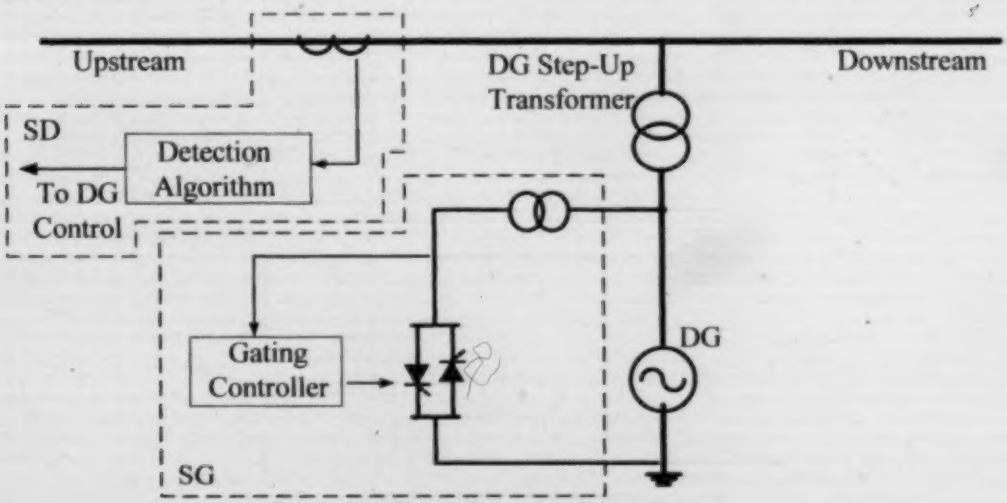

Figure 11: Signal Generator Connection

A thyristor in series with a current limiting transformer is connected at the DG terminal, before the DG step-up transformer. The DG step-up transformer converts distribution

voltages, say 24.9kV or 14.4kV to a level that the DG operates, say 480V – 5kV. The current limiting transformer is present between the thyristors and the DG step-up transformer and it converts the voltage to a level that the thyristors can operate in, say 480V. It also acts as an impedance to limit the current drawn by the thyristors and the distortion introduced to the system. The gate controller detects the rising or falling edge of the voltage waveform at the DG terminal, and fires the thyristor at a certain angle before the zero-crossing point of the voltage waveform. As shown in Figure 12, the firing angle δ is the angle from the zero crossing point of the voltage waveform. The thyristor draws a current pulse around the voltage zero crossing point, which has a duration of 2δ. When the thyristor conducts, the short-circuit introduces a dip in the primary voltage, near the zero-crossing point, which creates a distortion in the voltage and also draws a pulse current from the upstream current which is used for islanding detection. The voltage waveform is also shown for reference. With a fixed firing angle, the magnitude of the current pulse is determined by the system impedance at the DG terminal. The higher the impedance is, the lower (in magnitude) the current pulse will be. Two thyristors are shown, however, only one is used. Both are present to enable firing both on the falling and rising edge of the voltage waveform.

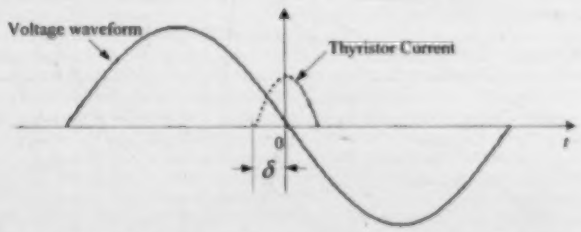

Figure 12: Waveforms of the Voltage at DG Terminal and the Thyristor Current (Not to Scale)

The firing angle is determined by considering both reliable detection and the requirement on power quality. It has been shown through simulations that a δ of 15° to 20° is sufficient for

islanding detection. Also, to further reduce the impact on power quality, the thyristor can be fired every 2 or 4 cycles, which will still be sufficient for detecting islanding conditions within the required time frame of 100-300ms. When multiple DGs implement the above method to detect islanding, a question arises as to whether they will interfere with each other and deteriorate detection reliability. In section 2.3, it is shown that the concern is unlikely to happen.

In Figure 13, the voltage at the DG terminal and the upstream current are shown for the SCR firing every two cycles. The distortions in both these waveforms are not drawn to scale for illustrative purposes. The current pulse drawn by the thyristor, for both DG normal and islanded operation is also shown and the difference in magnitude is made clear. An important consideration of this scheme is to obtain a large enough difference in the current pulse from when the DG is synchronized to when it is islanded, while minimizing the impact on the voltage waveform which will be discussed in Section 2.3.

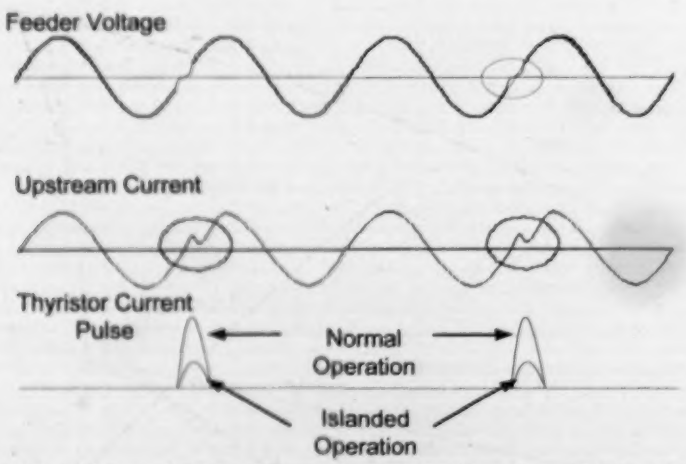

Figure 13: Voltage, Upstream Current and Thyristor Current Waveform

2.2.2 Signal Extraction

The current pulse drawn from the upstream current by the signal generator is used for anti-islanding detection. The extraction of this signal is of particular importance and the method proposed in this thesis allows for a small signal to be detected and be virtually immune from any waveform distortions. An example of the upstream current is shown in the top of Figure 14. Note, the distortion caused by the current pulse is not to scale and is shown in this way for illustrative purposes only. In this figure, we see the current pulse distortion occurring every 2 cycles, which corresponds to the signal generator firing every second cycle. If the fundamental component of the current waveform is removed, the current pulse should theoretically look as in the middle of Figure 14. However, a more realistic representation is shown in the bottom of the figure as the transient caused by the pulse will take some time to fade away. The key feature in this proposed method is that two consecutive cycles are subtracted from each other in order to give the current pulse. This method has been shown to be very effective for this application, and as mentioned before, it makes the extraction process immune to any background waveform distortions.

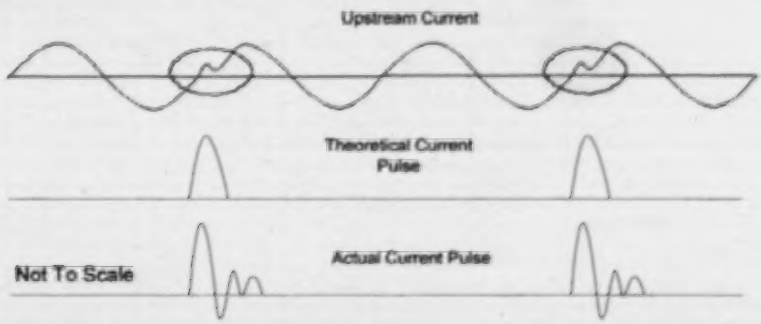

Figure 14: Upstream Current (Top), Theoretical Current Pulse (Middle) and Actual Current Pulse (Bottom)

Therefore, if the firing scheme mentioned before, once every 4 fundamental cycles as shown in Figure 15 is used, the signal would be extracted by subtracting Cycle 1 – Cycle 2 and Cycle 3 – Cycle 4, which would result in two cycles, only one of which would contain the signal.

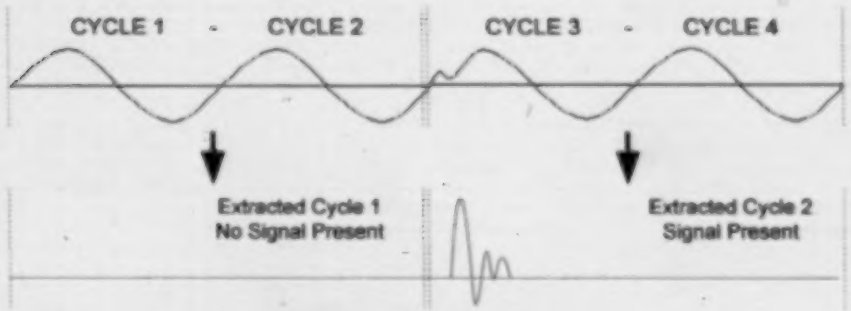

Figure 15: Signal Extraction Process

The decision on whether the DG has islanded would be based on whether the detected signal is lower than the expected value. If it falls short, then islanding is assumed and the DG is sent a signal to trip. Many features of the current pulse that could be used for detection were studied, such as the peak, duration, frequency spectrum and so forth and are presented next.

2.2.3 Signal Detection

While observing the waveforms in Figure 16, the first conclusion that can be drawn is to monitor the SG SCR (silicon controlled rectifier – thyristor) peak current. It is evident from this figure that it is highly dependent on the system impedance and would drop in value when the DG is islanded as there is a considerable increase in system impedance. Therefore, if the peak is below a certain level, it would suggest that an island has formed. The detection process would therefore not need to be very accurate as the change would be large. This can

be used as a detection criterion, but the problem arises when large capacitors or power factor correction equipment are present in the system. These capacitors would be supplying current to the thyristors and may cause the system impedance to appear lower, even in islanded situations, and thus, monitoring the peak of the SCR current, may be unreliable in such cases because there may be very little difference in the peak of the current pulse. Due to this problem, a solution was achieved by monitoring the upstream current instead of the SCR current through a current transducer.

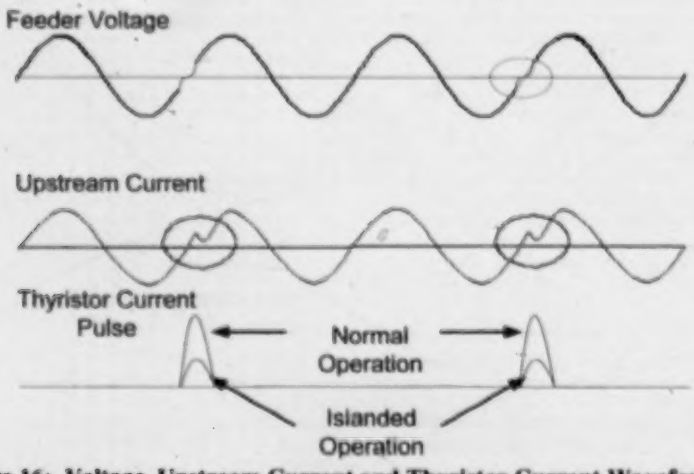

Figure 16: Voltage, Upstream Current and Thyristor Current Waveform

The current pulse drawn by the thyristor appears in the upstream current as the utility supplies most of it due to its lower impedance. By extracting this pulse from the upstream current, which was discussed in the previous section, we can see that it has similar characteristics as with the SCR current. If no capacitors are present, the peak of this extracted signal is much larger when the DG is synchronized with the main grid than when it is islanded. As reactive power is increased throughout the distribution system, this peak difference becomes smaller; however, the characteristic shape of the extracted current pulse becomes different as shown in Figure 17. When the system is working under normal operation, the extracted signal appears

as shown on the left side of the figure, and has a similar shape to the current pulse drawn by the thyristor, while when it is islanded it appears as shown on the right side of the figure and has a more sinusoidal shape and a longer duration transient associated with it. By observing these two waveforms, we can see that the DC component difference of the two extracted signals will be large, even though the peak may be similar as the pulse of the islanded system has a more sinusoidal shape and dips much further below zero. This criterion will be used to detect islanding conditions and will be shown through numerous simulations and experimental tests to work reliably, independent of system parameters.

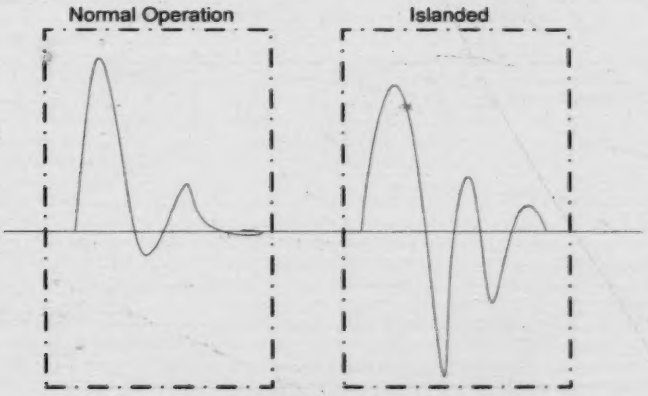

Figure 17: Upstream Current Pulse

The measurement of the DC component does not need to be extremely accurate as the difference will be considerably large and instead of having a fixed value, a percentage can be chosen as the threshold. For instance, if the signal has a DC component less than 50% than normal for a period of 12 cycles, then the signal detector sends a signal to the DG control telling it to trip. This method is also very immune to any noise as it does monitor only the DC component of the spectrum. Algorithms for islanding detection will be presented in Section 2.5 for systems with and without capacitors.

2.2.4 Advantages of the Proposed Scheme

This thesis proposes a very simple, yet effective approach to anti-islanding protection. The main advantages to this method can be summarized as follows:

- The scheme works reliably and has been determined to detect islanding conditions within the required time. There is no non-detection zone present which means it will reliably detect islanding conditions within all operating conditions.
- This method can be implemented easily and inexpensively
- Very little computational power is needed since accuracy is not of paramount importance as the difference in impedance between operating in normal and islanded conditions is large.
- The disturbance injected into the system has a minimal impact on the voltage, thus not affecting power quality significantly.
- Will work for both synchronous and induction distributed generators

2.3 Theory of Operation

This section contains analytical studies to support the scheme of anti-islanding protection based on measurement of system impedance. It will start with the derivations of current through a simple SCR circuit and then move on to show how this will apply at the DG terminals and the difference in current drawn by the SCR during normal and islanded operation. It will conclude by showing the minimal voltage distortion caused by such a device and how it is unlikely to disrupt existing power line communications that may be present on the system and other DGs using this method of anti-islanding protection.

2.3.1 Peak Current through a SCR Device

The following is a derivation of the peak current through the SCR module. A simple system shown in Figure 18 is first used and then expanded upon. Resistance and capacitance are ignored for simplicity.

Assuming the simple circuit shown below where:

AC source: $e(t) = \sqrt{2}E\sin(wt + \theta)$

V(t) : = e(t)

Inductor: = L

Thyristor: firing angle is δ (defined in Figure 19)

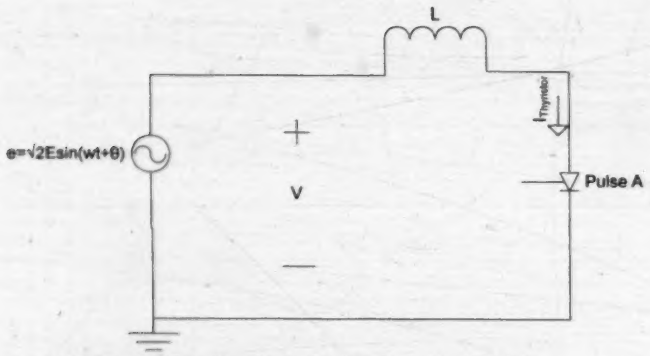

Figure 18: Circuit to be Analyzed to Find I_{PEAK}

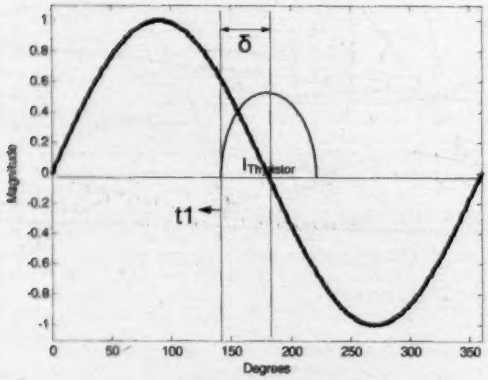

Figure 19: Firing Angle δ

For this circuit we define:

$$\omega t + \theta = (2k+1)\pi \tag{1}$$

$$\omega t_1 + \theta = (2k+1)\pi - \partial \tag{2}$$

To find the equation for $i_{Thyristor}(t)$, the following steps are taken:

$$v(t) = L\frac{\partial i_{Thyristor}}{dt} \tag{3}$$

$$i_{Thyristor}(t) = \frac{\sqrt{2}E}{\omega L}\int_{t_1}^{t}[\sin(\omega\tau + \theta)d(\omega\tau)] \tag{4}$$

$$i_{Thyristor}(t) = \frac{\sqrt{2}E}{\omega L}[\cos(\omega t_1 + \theta) - \cos(\omega t + \theta)] \quad (5)$$

$$i_{Thyristor}(t) = \frac{\sqrt{2}E}{\omega L}[\cos((2k+1)\pi - \partial) - \cos(\omega t + \theta)] \quad (6)$$

$$i_{Thyristor}(t) = \frac{\sqrt{2}E}{\omega L}[-\cos(\partial) - \cos(\omega t + \theta)] \quad (7)$$

The peak current occurs when the voltage passes the zero crossing point. This happens at $t_1+\delta$ (at the zero crossing point as shown in Figure 19). The following is a derivation for $I_{Thyristor\text{-}Peak}$:

$$I^{Peak} = \frac{\sqrt{2}E}{\omega L}\int_{t_1}^{t_1+\frac{\partial}{\omega}}[\sin(\omega t + \theta)d(\omega t)] \quad (8)$$

$$I^{Peak} = \frac{\sqrt{2}E}{\omega L}[\cos(\omega t_1 + \theta) - \cos(\omega t_1 + \theta + \partial)] \quad (9)$$

$$I^{Peak} = \frac{\sqrt{2}E}{\omega L}[\cos[(2k+1)\pi - \partial] - \cos[(2k+1)\pi]] \quad (10)$$

$$I^{Peak} = \frac{\sqrt{2}E}{\omega L}[1 - \cos(\partial)] \quad (11)$$

For our purpose, anti-islanding protection, the SG is connected to a system, so there is another impedance source in series as seen in Figure 20.

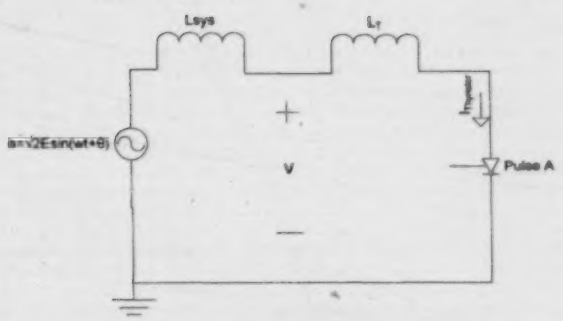

Figure 20: Circuit Including System Impedance

For this system:

$$i_{Thyristor}(t) = \frac{\sqrt{2}E}{(X_{SYS} + X_T)}[-\cos(\partial) - \cos(\omega t + \theta)] \quad (12)$$

$$I^{Peak} = \frac{\sqrt{2}E}{(X_{SYS} + X_T)}[1 - \cos(\partial)] \quad (13)$$

Where X_{SYS} and X_T are the positive sequence system impedances of the system and transformer respectively.

If the SG is firing between phases and not phase to ground, the above equations would have to be modified by replacing $\sqrt{(2)}E$ in (13) by $\sqrt{(2/3)}U_N$, where U_N is the system rated line to line voltage:

$$I^{Peak} = \frac{\sqrt{\left(\frac{2}{3}\right)}U_N}{(X_{SYS} + X_T)}[1 - \cos(\partial)] \quad (14)$$

As seen from equation 13, when the firing angle $\delta=0$, $I_{Peak}=0$. I_{PEAK} is largest when the thyristor is on for the whole half cycle:

When δ=180, $I^{Peak} = 2\left[\frac{\sqrt{2}E}{(X_{SYS} + X_T)}\right]$ (15)

2.3.2 Impedance Change

This section explains the theory of system impedance change that occurs when a DG is islanded. This method works on the simple principle that the system impedance is much lower than the DG impedance and thus when an electrical island occurs, the impedance seen by the SG increases and current through the SCR decreases (most notably the peak if power factor correction equipment is not present). The following circuit can be used to analyze the system:

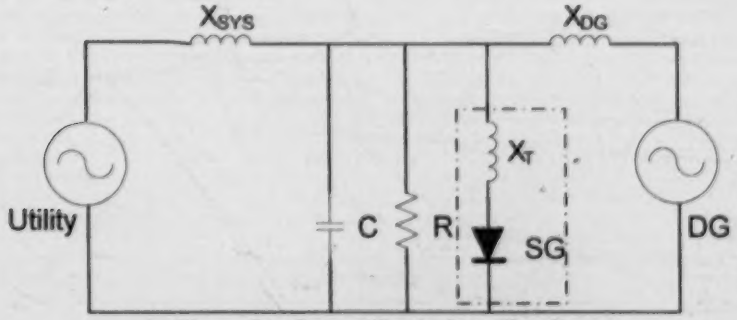

Figure 21: System Equivalent Circuit

This system can be further divided into two; one circuit for regular operating conditions and another for islanded conditions. The circuit in Figure 22 represents the system when regular operating conditions are present, where X_{SYS} is the positive sequence system impedance. The DG is removed from the circuit because its impedance is much larger than that of the utility and therefore the simplification can be made. The circuit in Figure 23 represents the system during islanding conditions.

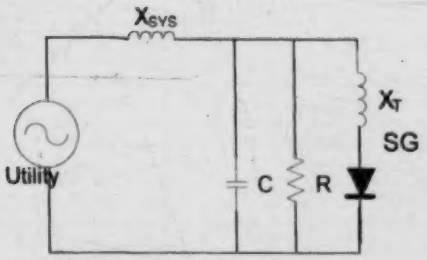

Figure 22: Regular Operation

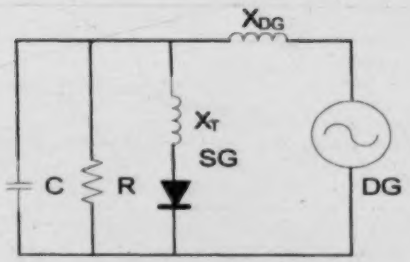

Figure 23: Islanded Condition

The circuit is further simplified and the load resistance and capacitance is neglected. The impedance of the load would be much larger than X_T and therefore will not impact the overall system performance and analysis. It is clear that in both cases, utility connected or disconnected, the circuits have a similar structure and can be represented by one circuit shown below in Figure 24, where $X_S = X_{DG}$ when utility is disconnected and $X_S = X_{SYS}$ when the DG is synchronized with the Utility. The current through the SG SCR is $i_{thyristor}(t)$.

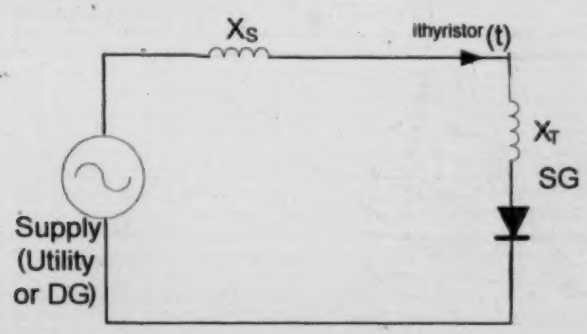

Figure 24: Uniform Circuit with Utility Connected or Disconnected

2.3.3 Analytical Studies for Proposed Method

This section introduces analytical studies of the proposed method; the current drawn by the SCR and the voltage distortion introduced. The analysis is done for the case of the SG connected between two phases at the DG terminal. Similar results can be obtained if the SG was connected between phase and ground. This case is shown in Figure 25(a). Denote the steady state sinusoidal voltage between the two phases when the thyristor does not fire as:

$$v_{PP}(t) = -\sqrt{2}V_N \sin \omega t \qquad (16)$$

where V_N is the rated phase-to-phase voltage at the secondary side of the transformer in series with the thyristor. The detection process is analyzed with a circuit energized by $-v_{PP}(t)$ as shown in Figure 25(b), where X_s and X_{DG} are the positive sequence inductances of the utility system and DG respectively, and X_{TDG} and X_{TSG} are the inductances of DG step-down transformer and SG step-down transformer respectively.

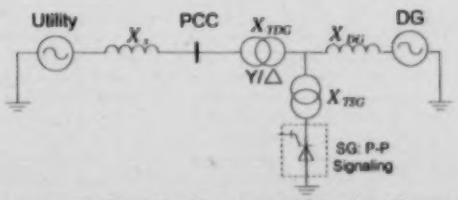

Figure 25 (a): Analysis of the Proposed Islanding Detection Scheme

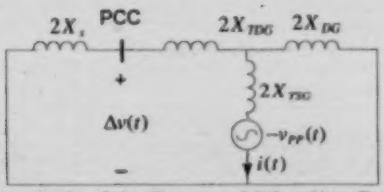

Figure 25 (b): Analysis of the Proposed Islanding Detection Scheme

Supposing the thyristor firing angle equals δ, the thyristor angle will be equal to 2δ. The obtained current pulse when the utility is connected (i.e. in normal condition) is:

$$i_1(t) = \frac{\sqrt{2}V_N}{X_s + X_{TDG} + X_{TSG}}(\cos\omega t - \cos\delta) \qquad \omega t \in [-\delta, \delta] \qquad (17)$$

The current pulse when the DG is islanded is shown below:

$$i_2(t) = \frac{\sqrt{2}V_N}{X_{DG} + X_{TSG}}(\cos\omega t - \cos\delta), \quad \omega t \in [-\delta, \delta] \qquad (18)$$

Since $X_s + X_{TDG}$ is typically much smaller than X_{DG}, the current pulse when DG is connected to utility, i.e., in normal condition, is much higher than that when DG is islanded. This feature is used for islanding detection. The difference between the peaks of the above two currents is:

$$\Delta I = \sqrt{2}V_N(1-\cos\delta)[(X_s + X_{TDG} + X_{TSG})^{-1} - (X_{DG} + X_{TSG})^{-1}] \qquad (19)$$

$$\Delta I = I_{max1} - I_{max2} \qquad (20)$$

This difference is plotted in Figure 26 and a summary of peak current formulas is presented in Table 1, where V_N is the rated phase to phase voltage and V is the rated phase to ground voltage.

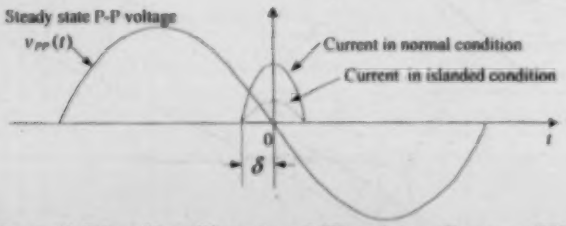

Figure 26: Anti-Islanding Signal and Thyristor Current Waveforms

Table 1: Peak of Thyristor Current on Different SG Channel

SG Channel	Peak of Thyristor Current
A-G	$I^{Peak} = \frac{\sqrt{2/3}V}{(X_{SYS} + X_{DG} + X_T)}[1 - \cos(\partial)]$ (21)
A-B	$I^{Peak} = \frac{\sqrt{2}V_N}{(X_{SYS} + X_{DG} + X_T)}[1 - \cos(\partial)]$ (22)

When multiple DGs implement the above method to detect islanding, a question arises as to whether they will interfere with each other and deteriorate the detection. In the following, it is shown that the concern is unlikely to happen. When one DG fires, it may affect firing of other DGs by drawing a current pulse through system impedance X_s, which is a mutual path. This current pulse causes a voltage deviation at the DG terminal, which can be used to quantify the impact of one DG firing to the distribution system. In normal condition, the deviation is:

$$\Delta v_1(t) = \frac{X_s \sqrt{2} V_N \sin \omega t}{X_s + X_{TDG} + X_{TSG}} \quad \text{(Normal)} \tag{23}$$

The peak of voltage deviation equals:

$$\Delta V_{max} = \sqrt{2} V_N \frac{X_s}{X_s + X_{TDG} + X_{TSG}} \sin \delta \quad \text{(Normal)} \tag{24}$$

Assume that if $\Delta V_{max} \leq 1\%$, the impact of SG firing to the system power quality is negligible, which also implies the interference between multiple DGs adopting the proposed schemes is negligible. Suppose that to achieve reliable islanding detection, there should be $\Delta I \geq 5$A (current value is at the distribution level of, say, 25kV or 12.5kV).

In Figure 27, a case is studied with the components in Figure 25 assuming their typical values. The utility three-phase-to-ground fault level is 300MVA. The DG is 5MVA with impedance of 25%. The DG transformer is 6MVA with impedance of 5%. The SG transformer is 300kVA with impedance of 3%. Therefore, X_s, X_{DG}, X_{TDG}, and X_{TSG} equal to 6, 31.3, 5.2 and 62.5 ohm respectively. As the firing angle increases from 5° to 30°, a curve of $\Delta V_{max} \sim \Delta I$ (curve 1) is plotted. When this curve is within the range limited by $\Delta V_{max} < 1\%$ and $\Delta I > 5$A, which is

denoted as a "operable region", both the requirement on signal strength and that on power quality are satisfied. It is seen in Figure 27 that the proposed scheme can operate in a large region. Sensitivity studies were performed for utility fault level being reduced from 300 to 100 and 50MVA. The region becomes narrower for the new $\Delta V_{max} \sim \Delta I$ curves. However, a larger SG transformer of 500kVA can help to enlarge the operational region when the fault level is 50MVA (curve 4).

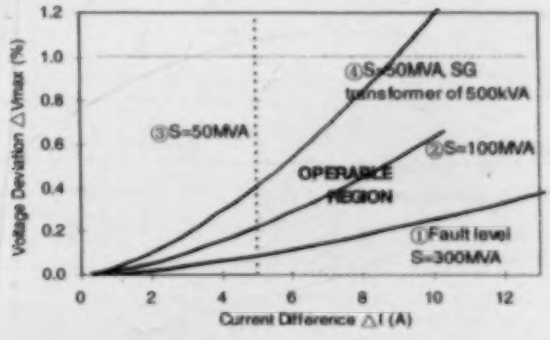

Figure 27: Voltage Deviation vs. Current Difference

Figure 27 shows that the proposed method for anti-islanding detection will work very well, and have a small power quality impact on the system. The larger the current difference is from normal to islanded condition, the more reliable the anti-islanding device will be. As the difference gets larger, we see an increase in the voltage deviation, but this increase is very small and thus a large area of the above graph can be used for operation. This is for a system without the presence of large capacitors. As was mentioned before, capacitors may make the current difference smaller (in terms of peak), but this still applies as this thesis proposes to monitor the upstream currents DC component which changes drastically with or without capacitors when islanding occurs.

The characteristic change in the waveform shape of the upstream current pulse is explained in [40] and shown below for reference. A frequency domain analysis is conducted to explain the difference in the harmonic spectrum of the upstream current from when the system is operating in normal condition and when it is islanded. The main supply inductance L_{SYS}, DG inductance L_{DG}, load resistance R_L and capacitance C compose a parallel current-dividing circuit. The different components have different frequency responses which determine how the harmonic currents are distributed between them.

The resonant frequency of the system can be represented by the following equation:

$$\nu = \frac{1}{\sqrt{L_{EQ}C}} \qquad (25)$$

Where $L_{EQ} = L_{SYS} // L_{DG} // L_{SG}$ when the system is working under normal conditions and $L_{EQ} = L_{DG} // L_{SG}$ when the system is islanded.

During normal operating conditions $L_{EQ} \approx L_{SYS}$ since its impedance is much smaller. The system shown in Figure 21 is resonant at around the 15th harmonic (component values can be found in Section 3.1). The main harmonic components (DC to approximately the 7th harmonic) are divided among the low pass filters of L_{SYS}, L_{DG}, and L_{SG}. The upstream current signal is the current flowing through L_{SYS}. Once the system is islanded however, $L_{SYS} = +\infty$ and $L_{EQ} \approx L_{DG}$. The system is resonant around the 5th harmonic and the large currents around the 5th harmonic flow through L_{DG} and C. The low frequency components of the current (DC component), flow through L_{DG} and L_{SG}. Since they do not flow through R_L or C, the upstream

current does not contain the low frequency components of the current and thus the large difference in the DC component between normal and islanded operation.

This study is important to determine how large the firing angle and SG transformer need to be for reliable anti-islanding detection.

2.4 Hardware

This section describes the necessary hardware to implement this scheme for anti-islanding protection of distributed generators. The proposed anti-islanding device is a modified version of the one discussed in Section 2.1. The main difference is the presence of a signal detector along with a signal generator, as this scheme is a local one. It is proposed to use a thyristor to short-circuit the voltage at the point of the SG connection (at the terminals of the DG) to generate the current signals required to detect islanding. The short-circuit occurs through a transformer impedance and a thyristor as shown in Figure 28. When the thyristor conducts, the short circuit introduces a dip in the primary voltage which creates a voltage distortion but also draws a pulse current (Current peak is derived in Section 2.3) from the upstream current. This will be used to indicate whether the device has been disconnected from the main supply and an island has formed.

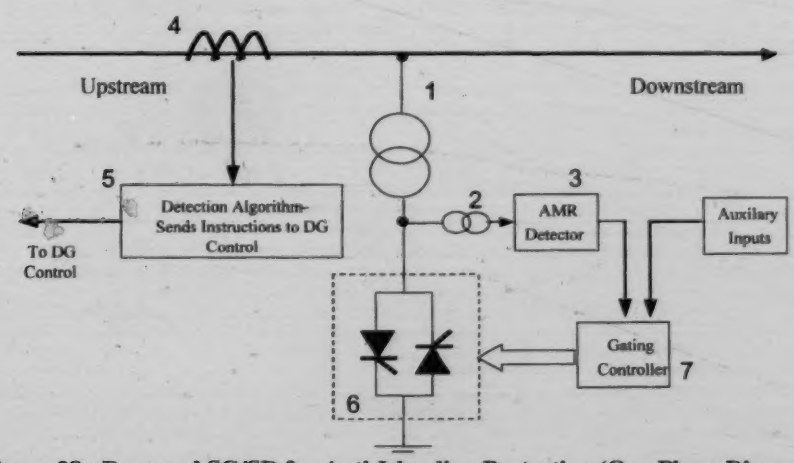

Figure 28: Proposed SG/SD for Anti-Islanding Protection (One Phase Diagram)

The architecture of the signal generator is shown on the previous page. The components are not selected specifically (actual ratings, size, etc) as that will vary depending on the location, size of DG, etc. The components are explained in greater detail below:

1. **Step-Down Transformer**: transforms the primary voltage (Feeder voltage, for example 25kV or 14.4kV) to a voltage that the thyristor can operate in since power electronic devices cannot operate at such high voltages (for example 480V). It also provides an impedance which limits the current drawn by the thyristor and the distortion introduced into the system. This can also be placed before the step-up transformer of the DG.
2. **Voltage Transducer**: is used to provide reference information for the gating operation (allows to activate thyristors accurately depending on the set firing angle) and to send information to the Power Line Communication Detector (#3) which determines the presence of other power-line communications
3. **Power Line Communication Detector**: analyzes the voltage to determine the presence of other communications along the line, such as AMR. It uses that information to determine the channel the anti-islanding protection device will use (current pulse can be created by firing in 6 different combinations: A-G, B-G, C-G, A-B, A-C, and B-C) in order to minimize the chance of interfering with the existing power line communications.
4. **Current Transducer:** is used to measure the upstream current drawn by the signal generator. This current is used for detection purposes.
5. **Detection Algorithm**: will capture the current from the current transducer, extract the current pulse signal by means of subtraction as mentioned in Section 2.2.2, and then analyze the spectrum of the signal and calculate the DC component. It will then

compare that value to its programmed value (can be a set number or a percentage – will be explained in the next Section 2.5) and based on this it will determine whether islanding has occurred. If it has, it will send a signal to the DG to trip. This device can be implemented via a DSP or even a microprocessor which is much less expensive and capable of the task as minimal computational power is required.

6. **SCR Module:** consists of a pair of thyristor, and they act as a switch between the step-down transformer and ground (or phase to phase depending on the firing channel), leading to the momentary short-circuit of the secondary side of the transformer. The current drawn by these thyristor is used to determine whether the SG has been disconnected from the main supply and is working in an island. The anti-parallel thyristor is used so that the short circuit can occur on both the voltage rising edge and falling edge. This would be chosen depending if there are AMR signals present (for example, if there are AMR signals present on the voltage rising edge, then the signal generator would use the voltage falling edge).
7. **SCR Gating Control:** establishes the pattern of the signal that is broadcast (such as fire every 2, 3 or 4 cycles) and it triggers the thyristor to conduct at δ degrees. It also decides which channel to broadcast on from the information given by (3).

This section describes the hardware necessary to facilitate this anti-islanding protection scheme. The algorithms associated with the detection module are described next.

2.5 Algorithm for Detecting Islanding Condition

There are many algorithms that would work with this method for islanding detection. To produce a viable low-cost product for anti-islanding protection, the algorithm has to be simple and implemented using inexpensive components. For this to happen, the computations have to be kept simple enough to allow for a cheap microprocessor or a digital signal processor to handle. The following will list a pseudo algorithm for implementation in this proposed anti-islanding protection device. It will show two alternatives, the first can be used in a system where there are no shunt capacitors (power factor correction capacitors) present, while the second can be used in any distribution system, with or without capacitors present. The following is divided into two sections, one for the algorithm used to control the signal generator (thyristor gate control), and the other section to control the signal detector (algorithm to detect islanding condition).

2.5.1 Algorithm for Signal Generator

This section contains a brief outline of the algorithm used for generating the signal that is used for islanding detection.

1. Algorithm Initializes
2. It will determine the channel that will be used to send the signal and the polarity by determining the presence, if any, of existing power line signaling schemes present in the system. This will determine which channel (A-B, A-C, B-C, A-Ground, B-Ground, C-Ground) that the thyristors will fire, and this information is stored for the signal detection algorithm. This information is obtained by either user control, or by

utilizing the Signal Detector algorithm to scan the different channels until it finds one that does not appear to have any signals present. Step 3-6 in the SD algorithm can be run for a duration of time, say a couple of seconds. If no signal is detected then that channel can be used.

3. Channel is selected. This information is passed on to the Signal Detection Algorithm.
4. User (through the user auxiliary inputs), or factory settings will determine and program the firing angle, α, that will be used. Through extensive simulations and lab test results shown in the next sections, 20° firing angel provides excellent islanding detection, but this angle can be changed depending on the situation.
5. User (through the user auxiliary inputs), or factory settings will determine and program the broadcast pattern of the thyristor. A signal sent every four cycles can be used and will be sufficient to detect islanding in required time and minimize the power quality impact.
6. Capture the upstream voltage waveform by using a sampling rate of 256 samples/cycle (sampling rate can be reduced to 128 or 64 samples/cycle).
7. Send a signal to the thyristor to fire at a specific time and every 4^{th} (if 4 is chosen in step 3) cycle by using the zero-crossing point from the voltage waveform that was captured and adding a specific time (in Figure 29, the time interval 't1')

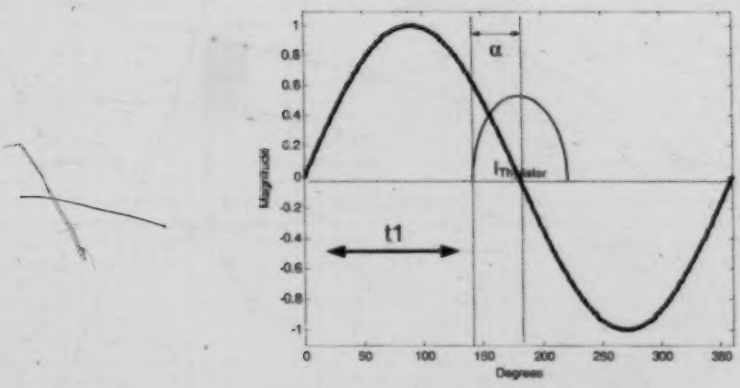

Figure 29: Thyristor Firing

8. Repeat step 6

Figure 30 shows a flowchart of the signal generator algorithm. The signal detector algorithm is presented next.

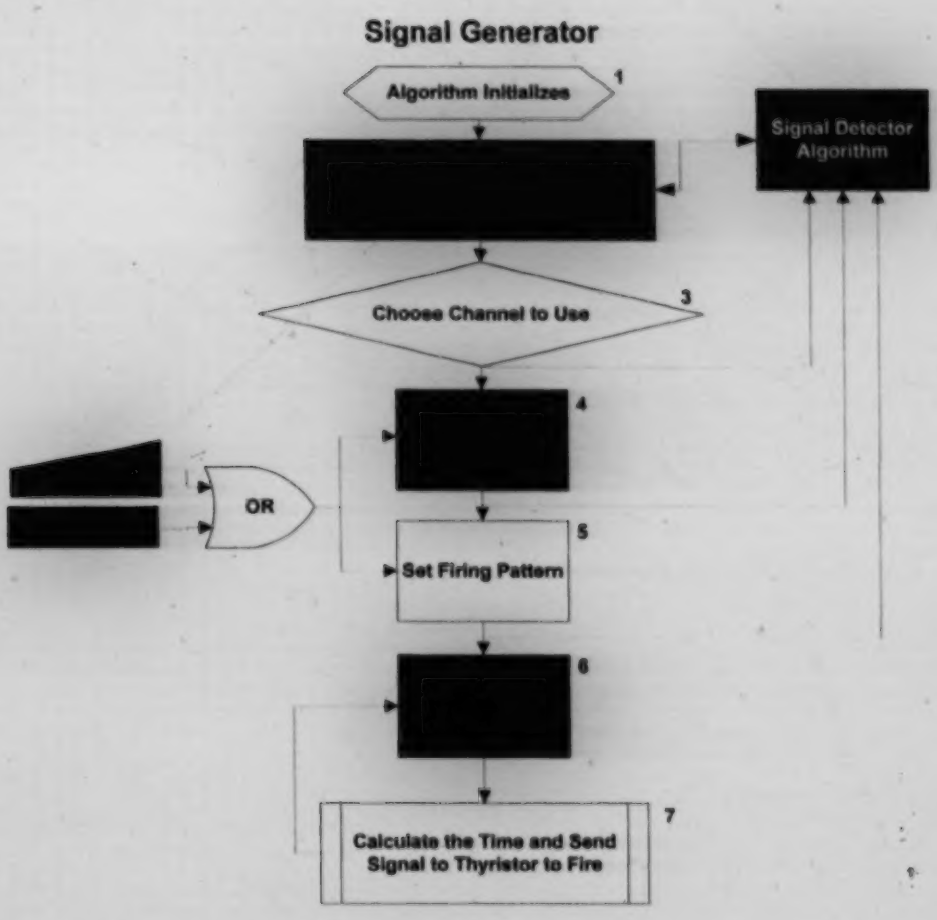

Figure 30: Signal Generator Algorithm

2.5.2 Algorithm for Islanding Detection

This section contains a brief outline of the algorithm used for analyzing the signal generated by the signal generator and determining whether an island has occurred.

1. Initialize – Use the data from the signal generator algorithm (firing angle, signaling pattern) and the threshold, which will be determined by the

firing angle and can be either a set threshold or a percentage. The channel chosen by the signal generator will determine which current the signal detection algorithm will monitor.

2. A counter is initialized, labeled here as 'Status'. 'Status' will be used to count how many cycles have passed since the last detected signal. A counter 'n' is initialized. This is used by step #5. 'Max Time' is used to determine when the DG is told to trip and is determined at this step. If the signaling pattern is one signal per 4 cycles, the Max Time will be 4 Signal Cycles as this will be equivalent to 16 cycles.
3. The current is sampled at a rate of 256 samples/cycle (can be 128 or 64 samples/cycle if sampling rate is a factor) and recorded.
4. Two consecutive cycles are subtracted from each other and the result is recorded (will be referred to as extracted cycle #n).
5. If (Signaling Pattern)/2 = n, Set 'n' = 0 and jump to Step #6, otherwise set 'n' = 'n' + 1 and loop back to step #3. For example, if the sampling period is one signal per 4 cycles, then the next two consecutive cycles are subtracted and recorded (referred to as extracted cycle #2).
6. Both extracted cycles are analyzed for the presence of the signal. The DC value is determined for both cycles. The simplest way to do this is to just add all the points of the extracted cycle together and store it. If no capacitors are present, the peak of the two extracted signals can be used. To improve reliability of the signal detection process, both the DC component of the extracted signals and the peak can be found and stored in memory for the next step (only for systems without power factor correction capacitors).

7. The DC component (and/or thyristor current peak) is compared to a set threshold which can be determined when the DG is installed.
    - If the DC value is above the set threshold for one of the 'extracted cycles' for the duration of the signaling period, it suggests that the signal is present and islanding has not occurred. The 'status' counter is reset and the program loops back to step #3.
    - If the DC value is lower than this threshold by a certain value or percentage for every 'extracted cycle' suggesting that no signal (or weak signal due to an increase in impedance) is present, the program proceeds to step #8.
8. The 'status' counter is incremented. If 'Status' < 'Max Time' then the program loops back to Step #3. If 'Status' = 'Max Time', the program jumps to step #9.
9. Algorithm determines that islanding has occurred and the DG is sent a signal to trip.

As was mentioned earlier, the method that uses the DC component for detection will work reliably with or without capacitors being present in the system and thus from this point forward, only this method will be discussed.

The figure on the following page shows an example of where the threshold would be set. It has been set arbitrarily at 0.04A as this lies in the middle of the two curves. It should be set at the midpoint because this will allow for fluctuations in the DC component of the extracted upstream current to not interfere with the reliability of the device and also to not cause any nuisance tripping of the DG.

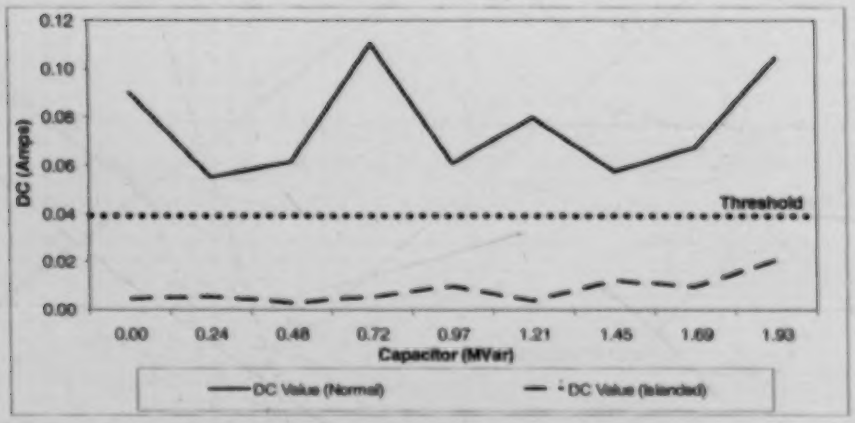

Figure 31: Threshold Setting for Laboratory Experiment

Anything below this threshold would be an indication of islanding, regardless of the amount of VARs present in the system.

This algorithm is very easy to implement using non-expensive equipment such as a microprocessor, FPGA or DSP. This is because the calculations are simple and the sampling frequencies are relatively low. It is also very reliable as the threshold can be set to a value that will not result in nuisance tripping and also provide great detection reliability since the change in the DC component (or peak) will be large as the impedance change in an islanded condition will be large. It has been tested extensively using computer simulations and experimental laboratory setups. Results of these studies are presented in Chapter 3 and Chapter 4 respectively. A flowchart of the signal detection algorithm is presented on the following page.

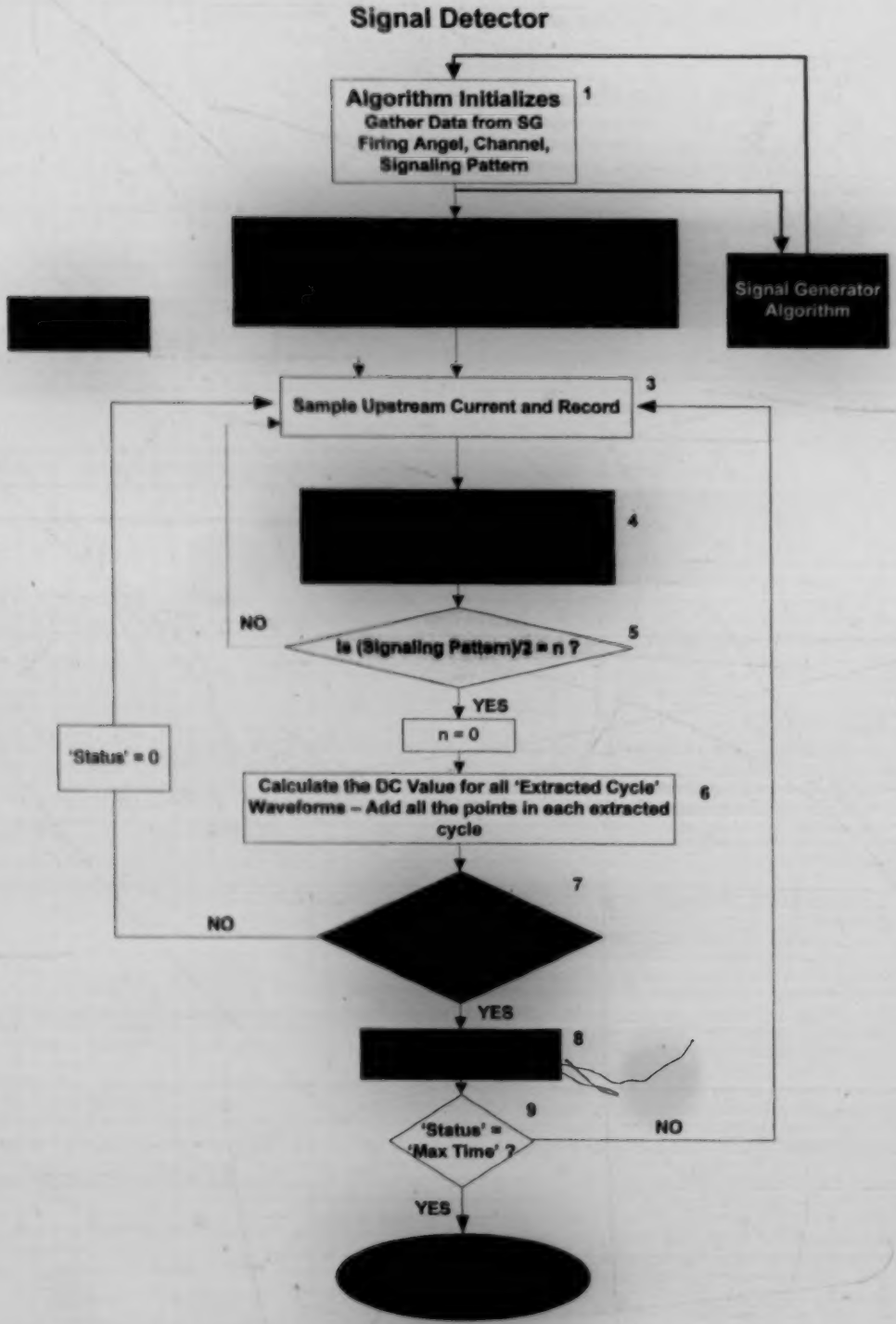

Figure 32: Flowchart for SD Algorithm

2.6 Summary

This thesis proposes a very simple, yet effective algorithm to be used in this method of anti-islanding protection. The scheme is based on an active method which injects a disturbance via a thyristor based device. The upstream current is monitored and each two consecutive cycles are subtracted from each other. This allows for this method to be very immune from any background noise. These extracted cycles are then analyzed. The peak of the thyristor current can be used as a detection criterion if no capacitors are present in the system. However, if large capacitors are present, the difference in peak will be small from normal to islanded operation. Due to this, this thesis proposes a detection algorithm which utilizes the upstream current. Two consecutive cycles are subtracted and the presence of the signal is determined by the DC component of the extracted cycles. It is then compared to a set threshold. If the DC value is greater than the threshold, it means that the impedance is still within normal operating parameters, while if it falls below the threshold, it would suggest that the impedance has increased beyond expectation and that an island has formed. If the signal is generated every 4 cycles, then if the DC value is lower than the threshold for greater than 3 or 4 signaling cycles, which corresponds to 12 and 16 cycles of the fundamental current waveform respectively, the DG is sent a signal to trip. This way, if by some anomaly the impedance looks larger in one cycle, it will not cause a nuisance trip of the DG.

The threshold is selected to the lowest value that would be possible under normal operating conditions and since the difference in impedance is large between normal and islanded operation, the threshold can be set in a way that would allow for very reliable anti-islanding detection.

Through analytical studies, and later on in this thesis, through numerous simulations and experiments, this method is validated and shown to be very reliable at detecting islanded conditions, while introducing a disturbance that is very small and thus not affecting the voltage waveform greatly, making this an attractive new approach to this problem. It is shown to work reliably and detect islanded conditions within the required time with no apparent non-detection zone. It has a minimal impact on power quality. It can also be implemented easily and inexpensively, as very little computational power is required, and it can work with both induction and synchronous generators.

Chapter 3

Simulation Studies

This chapter contains simulation results of the proposed method working in conjunction with a typical distribution system. Simulations were conducted using PSCAD, an EMTP (Electromagnetic Transients Program) program. The first section will describe the simulation setup (distribution system that was modeled) and the values of the components that were chosen. The second section will show results of the simulations for a typical system using the algorithms introduced in Section 2.5, programmed in MATLAB. The third section will present a sensitivity study on the proposed scheme. Each variable in the distribution system is varied one by one, with everything else kept constant. The results are presented with more detail in Appendix A. This study will show that the proposed method is very robust and dependable under many different system conditions. The chapter will then conclude with a discussion on the results obtained with simulations.

3.1 Simulation Setup

To validate the proposed anti-islanding protection scheme, digital simulations were conducted using PSCAD with a model of a realistic distribution system as shown in Figure 33:

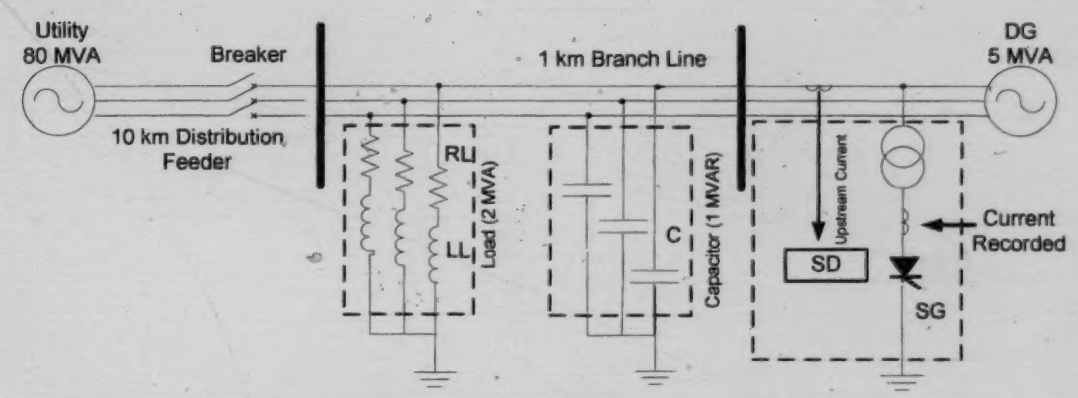

Figure 33: Simulation Setup - Typical Radial Distribution System

- The utility was chosen to be a voltage source behind an impedance (Fault Level of 80 MVA) at line to line voltage of 25kV, 60Hz
- DG is a 5MVA, 25kV generator with X''_{DG}=25%, R_{DG}=0.1X''_{DG}
- DG transformer was chosen to be a 6 MVA with % IZ = 6%
- A 10km distribution feeder (from substation to load) was modeled using a π model. The feeder length between the DG and the load is also modeled with a π model and the length is chosen to be 1km. The parameters of the line, R_1, X_1, R_0, X_0 are 0.2138, 0.3928, 0.3875, 1.8801 ohm/km respectively, and B_1, B_0 are 4.2315 and 1.6058 Microsiemens/km respectively.

- The load was varied during the simulations but was later set to be a 2 MVA load with a power factor of 0.9. The load terminal voltage was not allowed to go below 0.95 p.u.
- The capacitor was chosen to be 1 MVAR under the criterion that the terminal voltage will be no higher than 1.05p.u. after compensation.
- The transformer in series with the signal generator was a 150 kVA, 25kV/480V Y/Y transformer with a positive sequence leakage reactance of 0.05p.u.
- Thyristor is fired between phase A and ground at an angle of 30 degrees before the zero crossing point of the voltage waveform every four cycles.
- Sampling rate was chosen to be 256 samples/cycle
- The breaker was set to open and island the DG half way through the simulation.

3.2 Simulation Results

This section presents the results from the simulations conducted using PSCAD and the distribution system model presented in Section 3.1. The data collected from PSCAD was exported to a spreadsheet and then into MATLAB, where it was run through the algorithm explained in Section 2.5.2. The waveforms for voltage, upstream current and extracted current waveform (two consecutive cycles subtracted from each other) on the phase that the signal generator was firing (V_a) are shown in Figure 34 for both normal and islanded conditions. As can be seen from these results, the extracted signal has very different characteristics when the distribution system is operating normally and when a power island forms. It is very easy to see from this figure that the DC component will be very different in the two cases and thus will be used for islanding detection. When working in normal operation the extracted upstream current pulse is mostly positive, and in islanded operation

the pulse has a sinusoidal shape and fluctuates from positive to negative and thus has a smaller DC component. Since the power generated by the DG is larger than the load that is present, we can see a drop in the upstream current magnitude (in the figure the magnitude of the current is 10x the scale on the right axis) when an island forms and a slight drop in the voltage is present too, as expected since the stronger utility source is not present.

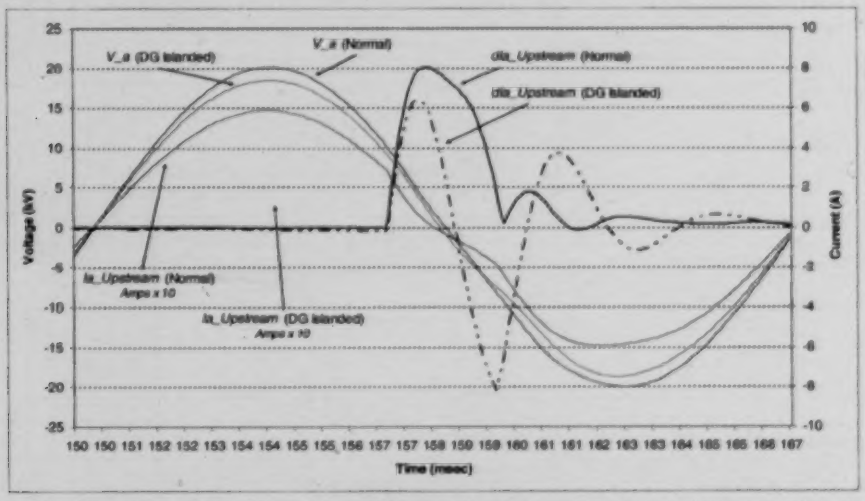

Figure 34: Simulation Waveforms for Voltage, Current and Extracted Signals (Normal and Islanded Operation)

Figure 35 shows the harmonic spectrum of the extracted signal for both normal and islanded operation. It is evident that when an island forms, the spectrum of the signal generated by the thyristor shifts to higher frequencies. As mentioned in Section 2.5, many different methods can be chosen to detect an island condition, but it will be shown that by monitoring only the DC component, we can get reliable detection with a very simple algorithm.

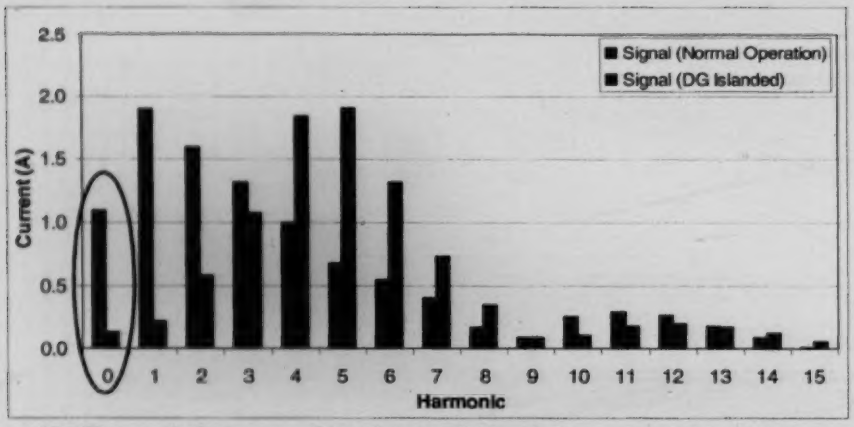

Figure 35: Harmonic Spectrum of the Extracted Signal (Normal and Islanded Operation)

Figure 36 is a blown up version of Figure 34 at around the point that the signal generator fires. It is presented here to show the difference of the extracted signals when the distribution system is working normally, and when it is islanded from the utility, in greater detail.

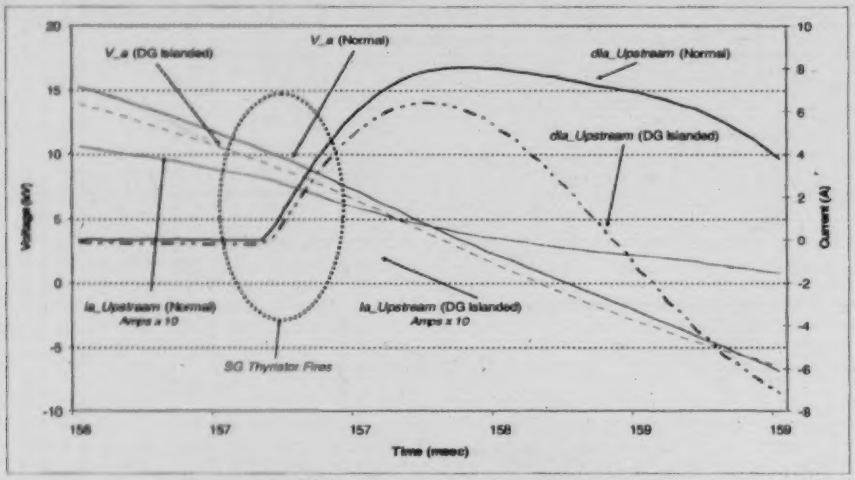

Figure 36: Signal Generator's Thyristors Firing

Figure 37 is presented on the following page. It shows a full signal cycle. Since the SG fires every 4 cycles of the fundamental voltage waveform, four cycles are shown. The signal generator's thyristor fires on the third cycle and thus is present only then. The graph shows four cycles of the voltage and upstream current and the two cycles of the extracted current (stretched out over the 4 cycles for clarity).

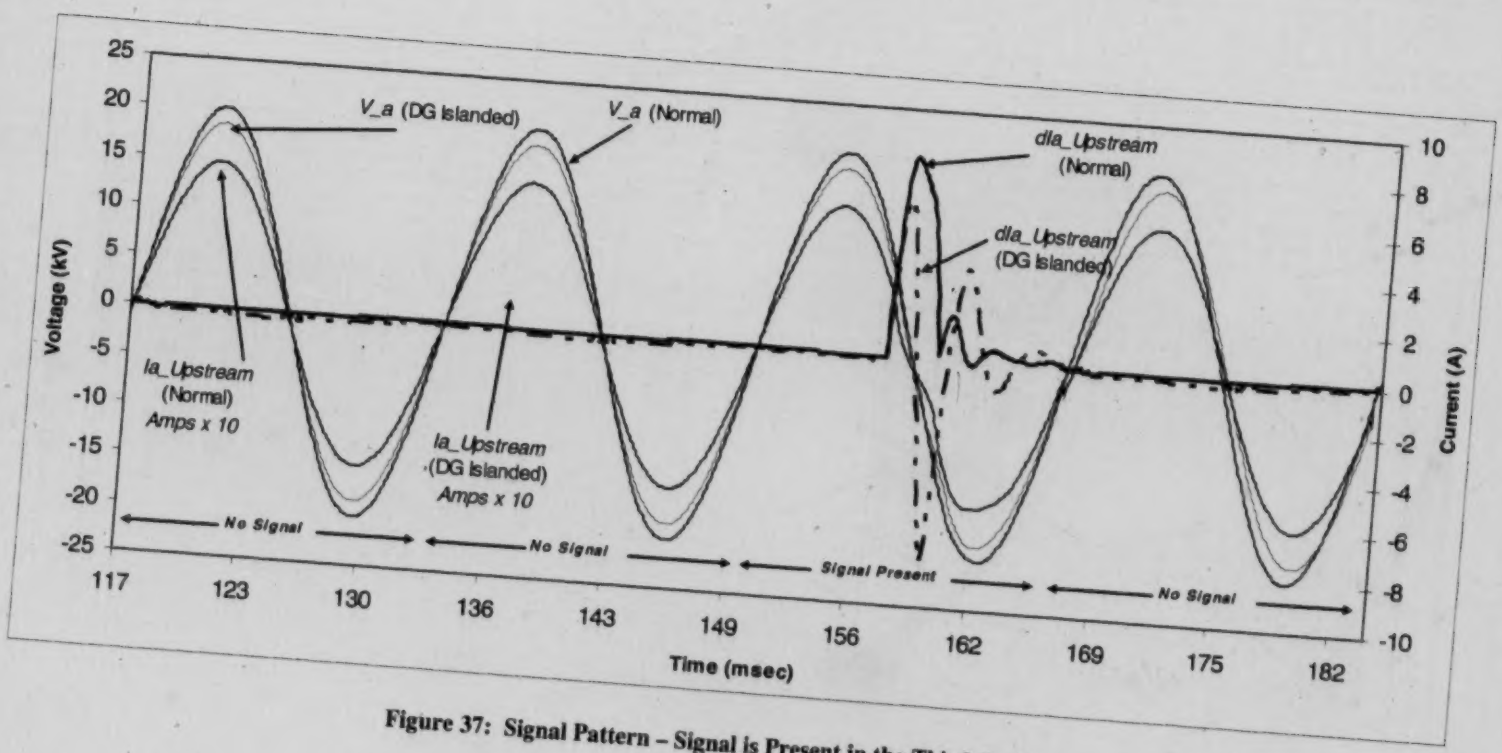

Figure 37: Signal Pattern – Signal is Present in the Third Cycles

Figure 38 shows the voltage and current waveforms of the DG for both normal and islanded operations. Only phase A (the phase that the thyristor fires on) for the current is shown along with the voltage for all three phases. The distortion created by the signal is clearly seen in the current but is very minimal on the voltage.

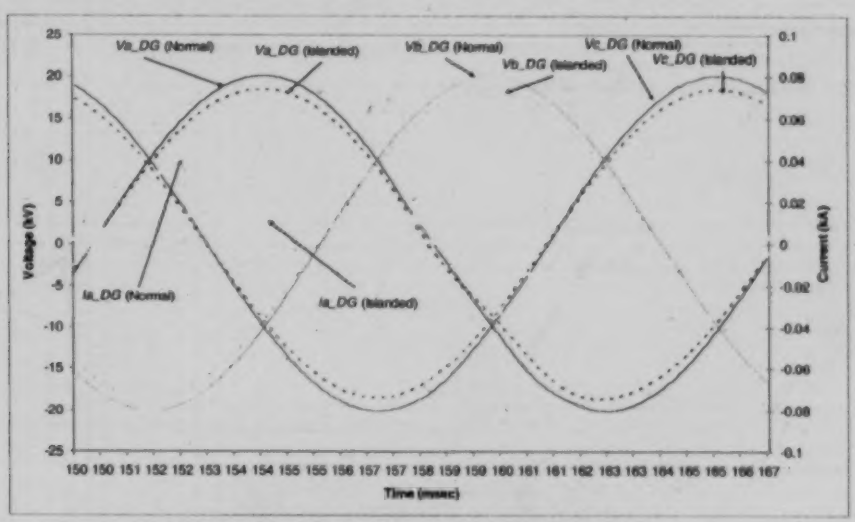

Figure 38: DG Voltage and Current Waveforms

Figure 39 shows the voltage and current waveform of the utility for both normal and islanded operations on the phase that the SG is using. Figures 38 and 39 are shown here to demonstrate the minimal impact on the voltage waveform caused by the signal injected.

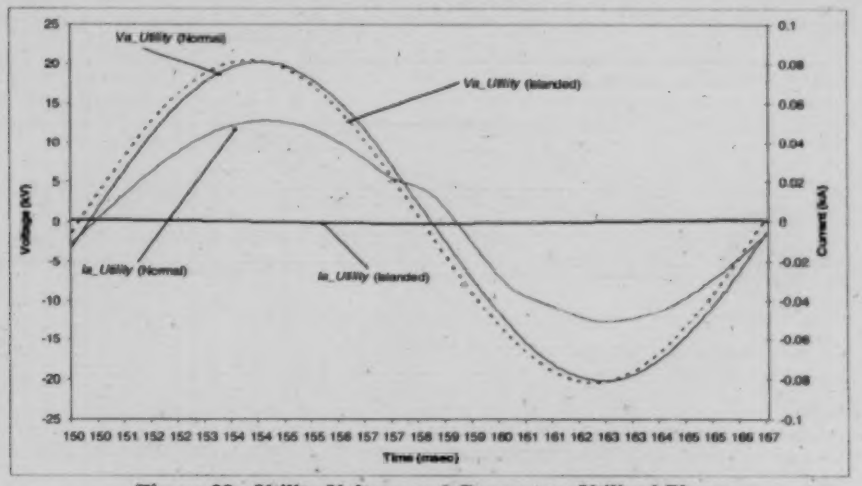

Figure 39: Utility Voltage and Current on Utilized Phase

Below, in Figure 40, the thyristor voltage and current are presented while in Figure 41, the load and capacitor voltage and current waveforms are shown along with the difference of these waveforms for normal and islanded operation. We can see that there is a difference in magnitude of the thyristor current pulse. This difference is not static though. As the capacitance of the system increases, this difference diminishes and will be shown in the sensitivity studies in the next section. The load voltage is shown not to be affected by the signal generated.

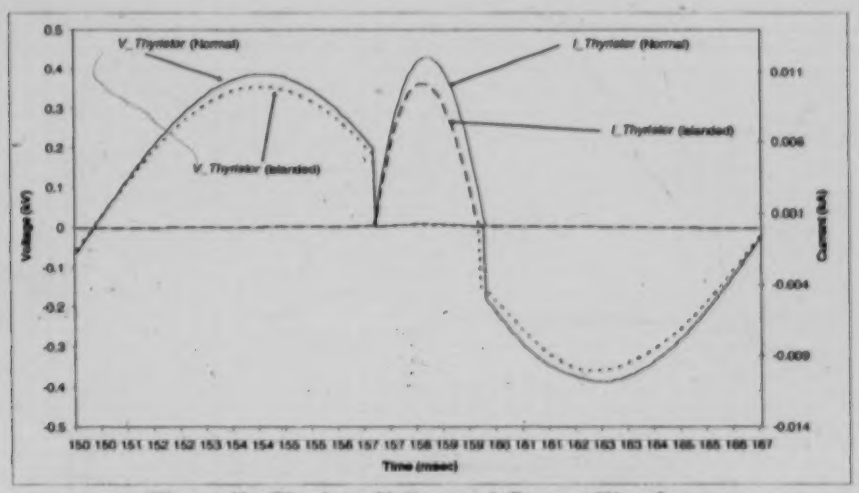

Figure 40: Thyristor Voltage and Current Waveforms

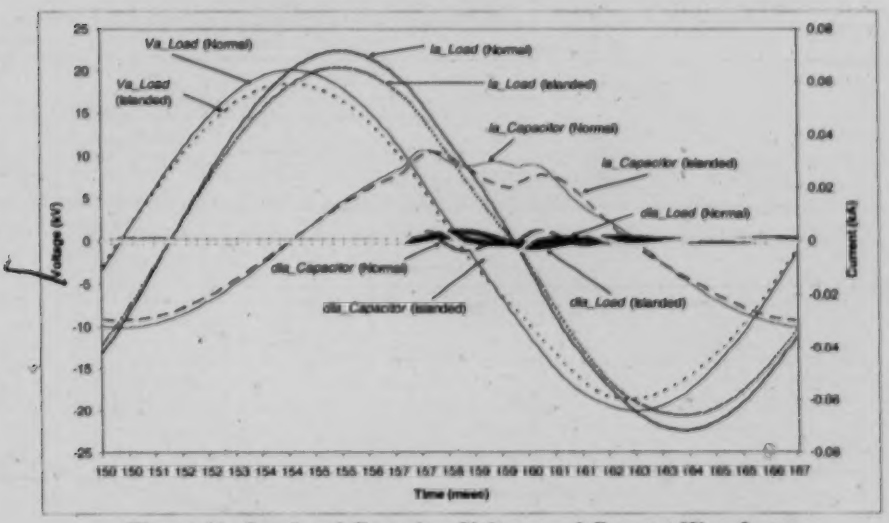

Figure 41: Load and Capacitor Voltage and Current Waveforms

Figure 42 illustrates the signal that was extracted from the upstream voltage and current waveforms by subtracting two consecutive cycles on both waveforms.

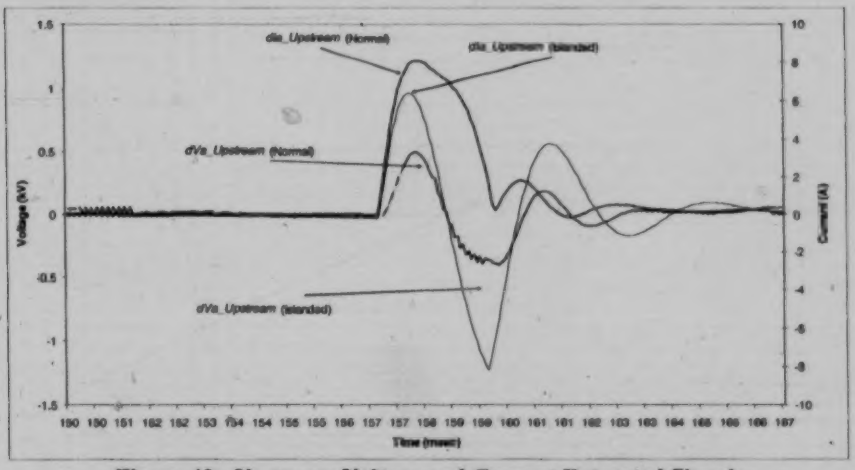

Figure 42: Upstream Voltage and Current Extracted Signals

To demonstrate how minimal the impact on power quality is when the signal generator fires, Figures 43 and 44 show the harmonic spectrum of the voltage at the point of common coupling (Vpcc) when the system is working normally and when an island forms respectively. Since this is a simulation, and no sources of noise or non-linear devices are included, when the signal is not present, only the fundamental frequency contains content for both scenarios, normal and islanded.

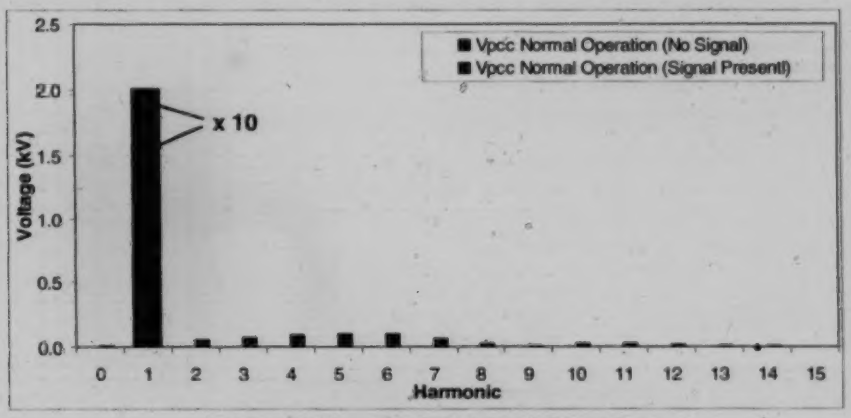

Figure 43: Vpcc During Normal Operation

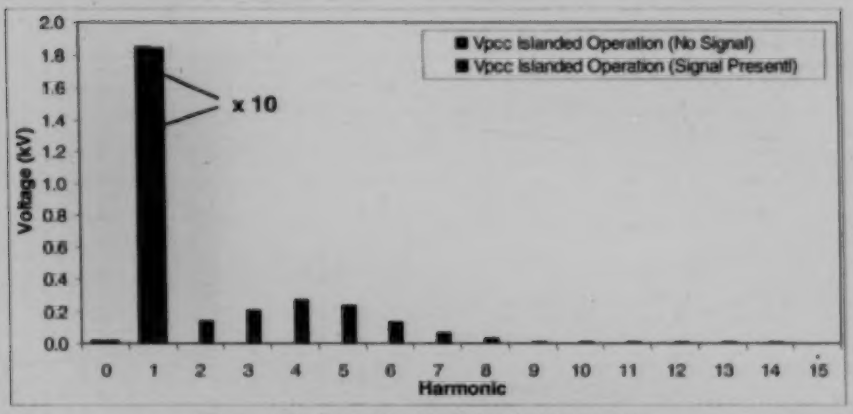

Figure 44: Vpcc During Islanded Operation

Table 2 presents the results for both operations; the THD of the voltage waveform is around 1% for normal and 2.47% for islanded operation. Since only the normal operation is of concern, as the islanded scenario should not last for more than 100-300msec, we can assume that the distortion is minimal.

Table 2: Voltage Total Harmonic Distortion at the Point of Common Coupling

V_{pcc}	Normal Operation		Islanded Operation	
	Signal Not Present (%)	Signal Present (%)	Signal Not Present (%)	Signal Present (%)
V_{thd}	0.00000	1.03655	0.00000	2.47880

A similar study was conducted on the upstream current. Figures 45 and 46 show the harmonic spectrum of the upstream current when the system is working normally and when an island forms respectively. Again, since this is a simulation and no sources of noises or non-linear devices are included, only the fundamental frequency contains content when the signal is not present. Table 3 presents the results and as can be easily seen, the THD of the upstream current has the same characteristics as the voltage.

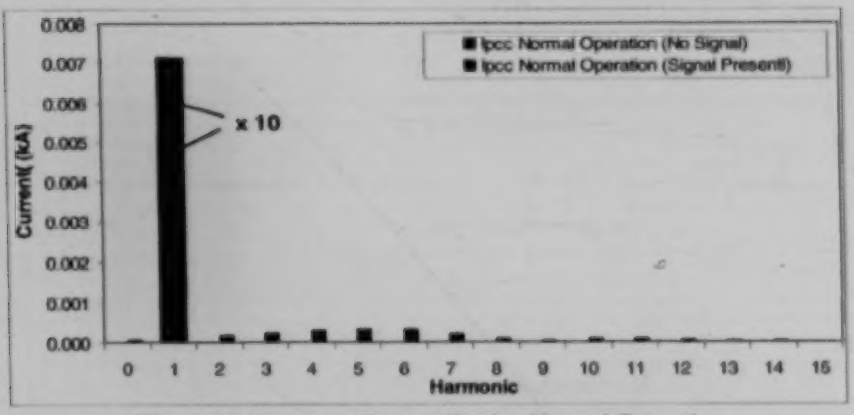

Figure 45: Upstream Current During Normal Operation

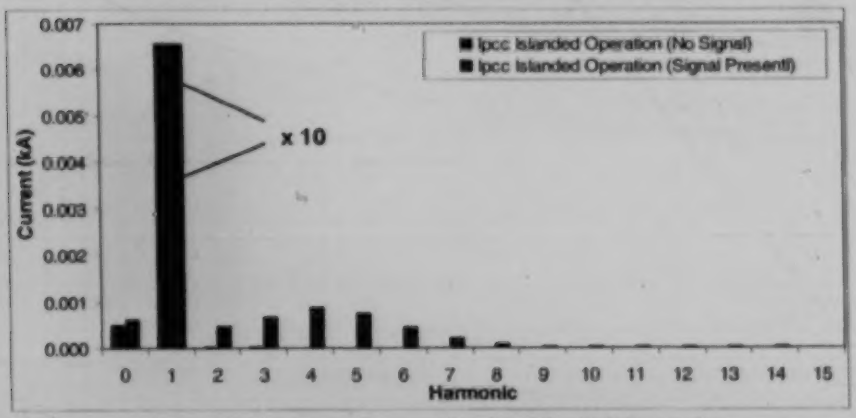

Figure 46: Upstream Current During Islanded Operation

Table 3: Current Total Harmonic Distortion at the Point of Common Coupling

Upstream Current	Normal Operation		Islanded Operation	
	Signal Not Present (%)	Signal Present (%)	Signal Not Present (%)	Signal Present (%)
I_{thd}	0.00000	0.94085	0.00000	2.25342

3.3 Sensitivity Study

To determine whether the proposed anti-islanding protection method will be robust and reliable, a sensitivity study is required which is presented in this section. One variable of the distribution system is varied at a time, with everything else kept constant. The same system and values as explained in Section 3.1 were used. The results of these simulations are then run through MATLAB, on the same algorithm from the previous section. The difference in the DC component of the extracted upstream current is shown, along with the thyristor peak current and extracted upstream peak current to illustrate the effectiveness of using the DC component as a detection technique. Branch length, capacitor size, size of distributed generator, utility fault level, feeder length, firing angle (for system with no capacitors and also for system with a 1MVAR capacitor bank), and load are varied and presented in the following pages.

3.3.1 Branch Length

The branch length was varied between 1 and 10 km. In Figure 47 we can see that the separation between the normal and islanded operation for the DC component is stable and is not affected by the difference in branch length. The thyristor current peak, shown in Figure 48, is also not affected by the branch length as there is clearly a steady difference between normal and islanded operation. Thus, branch length will not affect the detection capabilities of these two criteria. The same cannot be said for the upstream extracted signal peak seen in Figure 47.

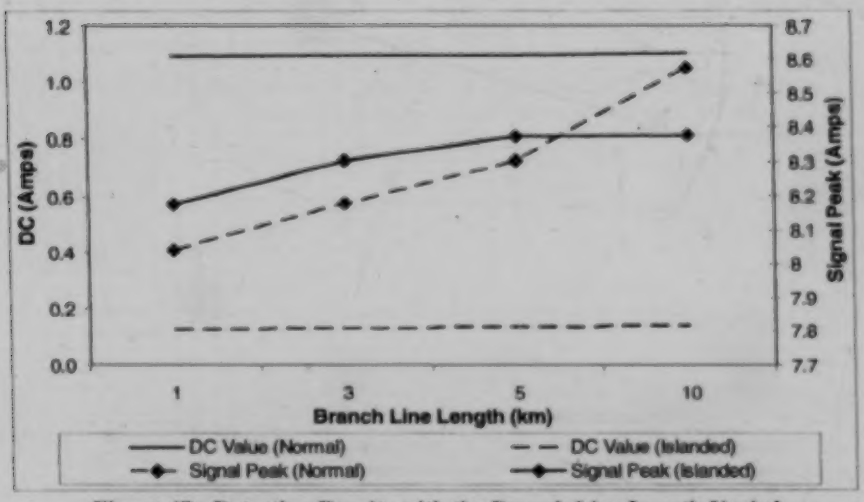

Figure 47: Detection Results with the Branch Line Length Varied

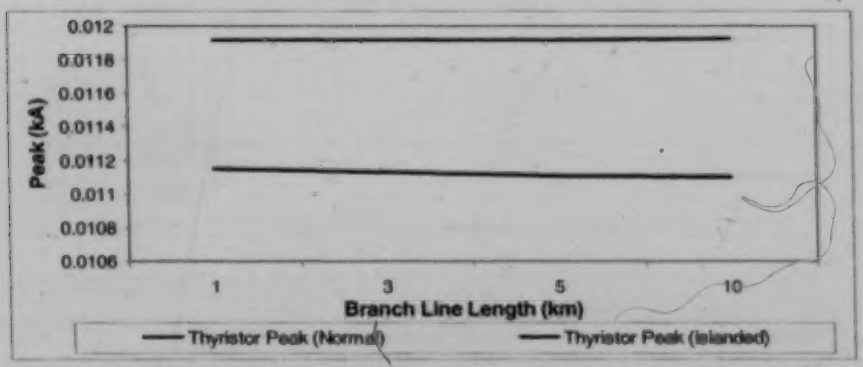

Figure 48: Detection Results with the Branch Line Length Varied (Thyristor Peak)

3.3.2 Capacitor Size (MVARs Present in System)

In this section, the size of the capacitor bank was varied between 0 and 2 MVAR with 0.25 MVAR increments. In Figure 49, the separation between the normal and islanded operation for the DC component of the extracted upstream current signal is shown. It is stable and is not affected by the amount of VARS present in the system and therefore does not affect its detection capabilities. The upstream extracted signal peak seen on the same figure and the thyristor current peak shown in Figure 50, however, cannot be used

as for islanding detection as it is evident that their difference between normal and islanded operation gets smaller and actually intersects as the size of the capacitor increases.

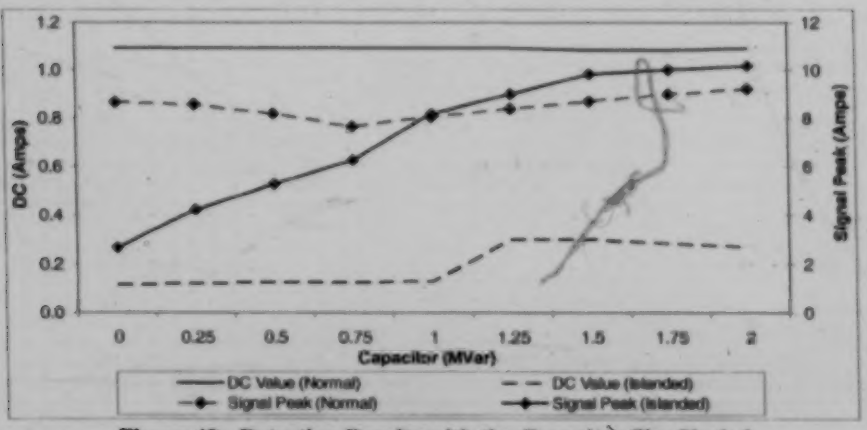

Figure 49: Detection Results with the Capacitor Size Varied

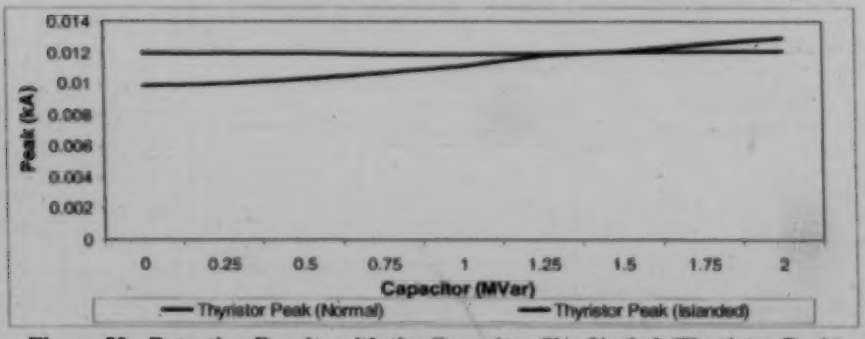

Figure 50: Detection Results with the Capacitor Size Varied (Thyristor Peak)

3.3.3 Size of Distributed Generator

The size of the distributed generator was varied between 0.5 and 50 MVA. An additional simulation was conducted with the load changed to 0.5MVA for the 0.5MVA DG case. In Figure 51 we can see that the separation between the normal and islanded operation for the DC component is large, and gets smaller as the DG's size is increased significantly. However, even when a large DG is present, a threshold that will be used to determine

whether islanding has occurred can be chosen that will still provide reliable islanding detection. For the case of a 50MVA DG, the threshold would be chosen at 0.3A. If the DC component was found to be lower than the threshold for a specified time, islanding would be assumed and the DG signaled to trip.

The upstream extracted signal peak and the thyristor current peak are shown in Figure 51 and 52 respectively. These signals are clearly sensitive to the size of the DG and would not be suitable for islanding detection.

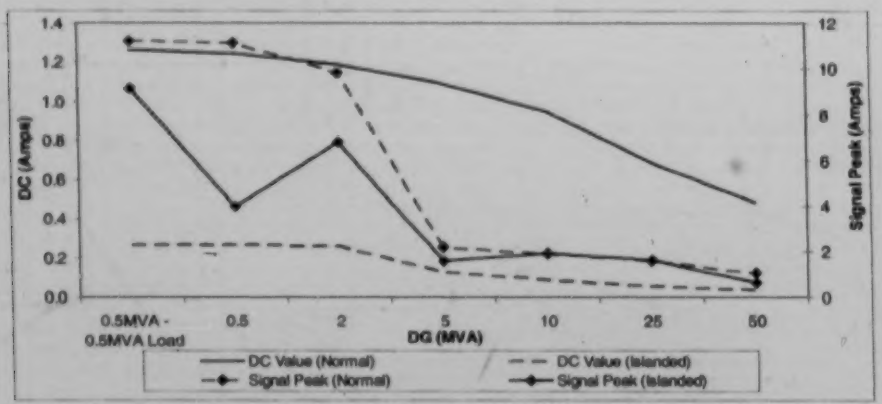

Figure 51: Detection Results with the Size of the DG Varied

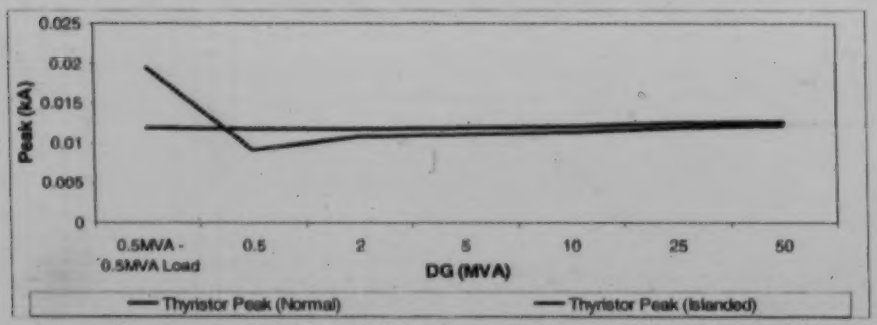

Figure 52: Detection Results with the Size of the DG Varied (Thyristor Peak)

3.3.4 Utility Fault Level

For the next sensitivity study, the utility fault level was varied. Simulations were conducted for fault levels of 40, 80, 150, and 200 MVA. In Figure 53, we can see that the separation between the normal and islanded operation for the DC component is large and the difference in thyristor peaks in Figure 54 stays steady also. This suggests that the utility fault level does not affect either of these method's ability to be used for islanding detection. The upstream extracted signal peak, however, would not be appropriate for islanding detection as the difference is small and erratic, as is clear from Figure 53.

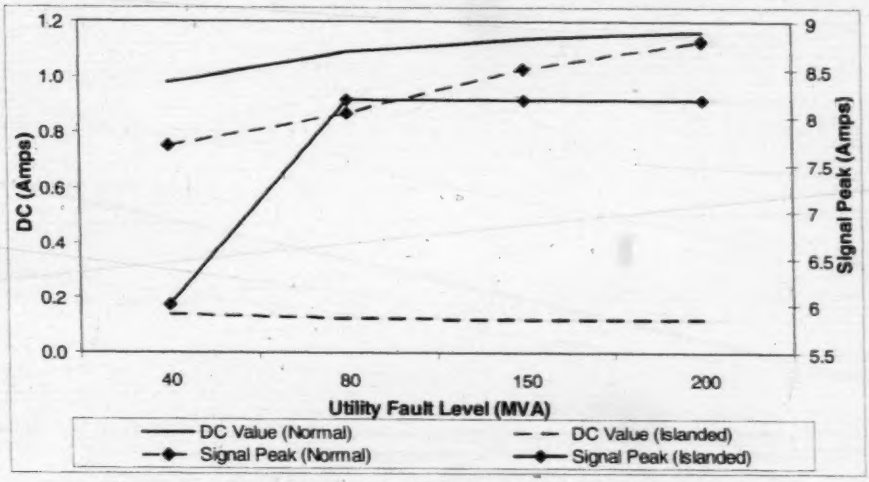

Figure 53: Detection Results with the Utility Fault Level Varied

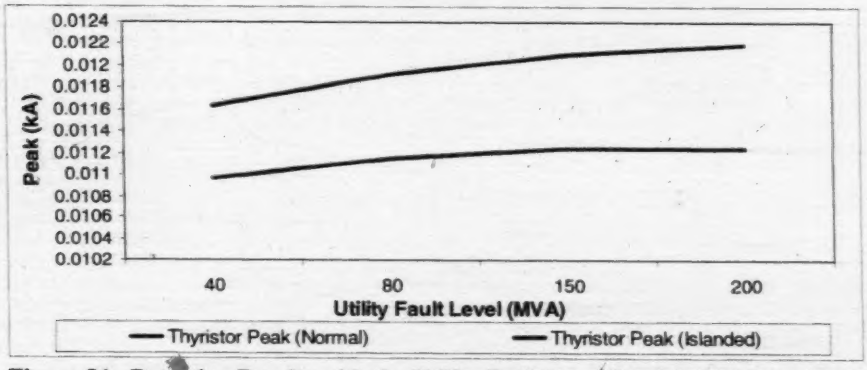

Figure 54: Detection Results with the Utility Fault Level Varied (Thyristor Peak)

3.3.5 Feeder Length

Figures 55 and 56 show the results for the feeder lengths impact on the DC component of the upstream signal, the extracted upstream signal peak and the thyristor peak. Feeder length was varied between 1 and 40 km for this study. The DC components difference for normal and islanded operation is large and gets slightly smaller for longer feeder lengths, which is expected as the fault level at the DG site is smaller. Even with this declining difference, the DC component would still be able to be used to reliably detect islanding conditions on long feeders as the difference in the DC component is large enough to set a detection threshold between the two curves. If the algorithm detects the DC component to be less than the threshold for a specified period of time, islanding would be assumed. The thyristor peak exhibits the same characteristics while the upstream extracted signal peak would not be useful (the difference is small and intersects) as is clear from the graph below.

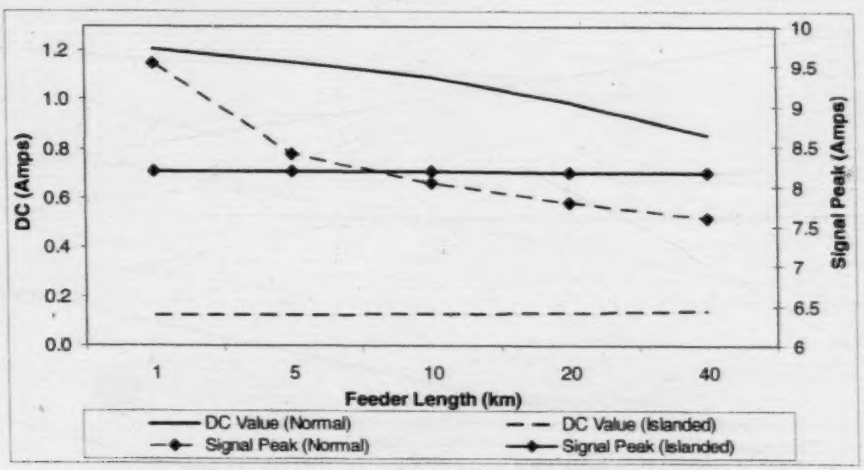

Figure 55: Detection Results with the Feeder Length Varied

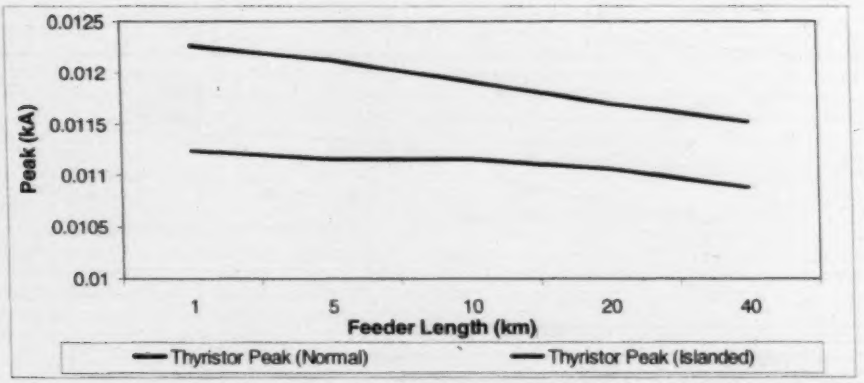

Figure 56: Detection Results with the Feeder Length Varied (Thyristor Peak)

3.3.6 Firing Angle

To determine the firing angles effect on the detection, simulations were conducted for firing angles of 5° through to 30° (before the zero crossing point of the voltage waveform) at 5° intervals. These studies were conducted for the system explained in Section 3.1 and also for the same system without a capacitor bank. Figures 57 and 58 show the results for the firing angle impact on the DC component of the upstream signal, the extracted upstream signal peak and the thyristor peak for the distribution system without capacitors. From the figures, it is clear that as the firing angle is increased, the difference for all three curves gets larger. A firing angle of 20° to 25° is sufficient to have a large enough margin to provide reliable detection. As the firing angle increases, the detection capability of all three methods improves.

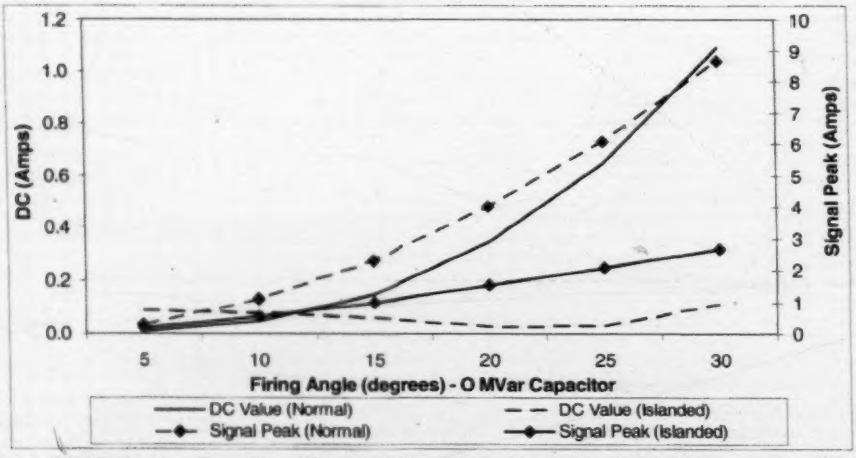

Figure 57: Detection Results with the Firing Angle Varied – 0 MVAR Capacitor Present

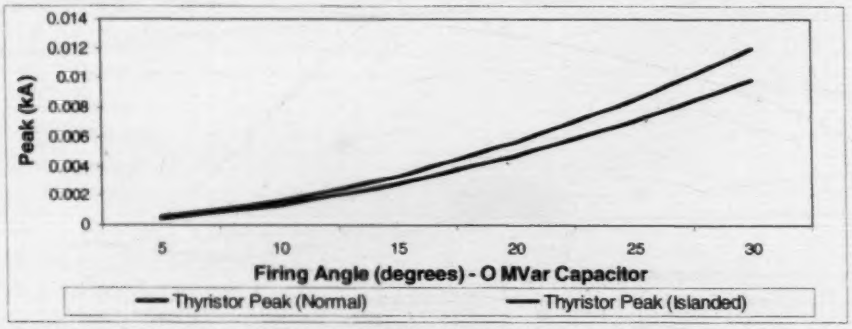

Figure 58: Detection Results with the Firing Angle Varied – 0 MVAR Capacitor Present (Thyristor Peak)

When capacitors are present, the results change significantly as can be seen in the following two figures. While the DC component's difference between normal and islanded operation stays large, the thyristor peak and upstream extracted signal peak converge quickly and have a very small difference, making them useless for islanding detection. As in the case of no capacitors present, a firing angle of 20° to 25° is sufficient to have a large enough margin to provide reliable detection if using the DC component. With the presence of capacitors in the distribution system, only the DC component can be used for islanding detection.

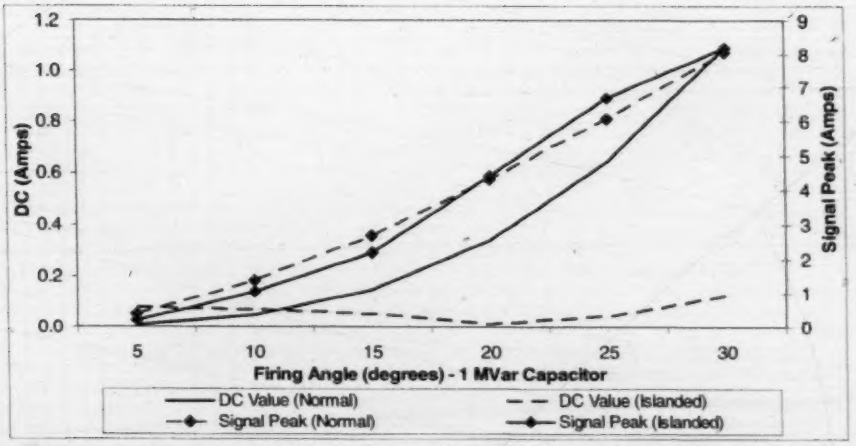

Figure 59: Detection Results with the Firing Angle Varied – 1 MVAR Capacitor Present

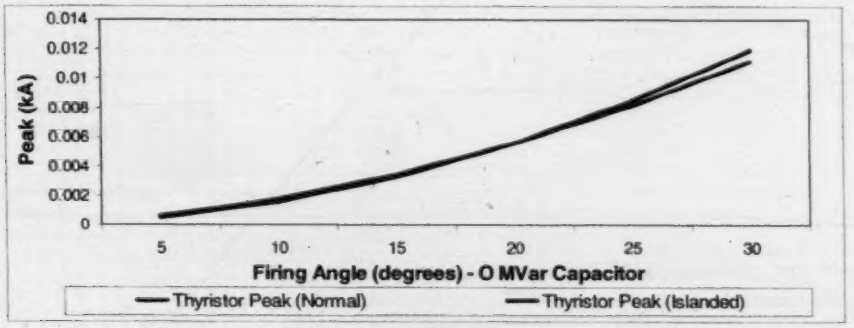

Figure 60: Detection Results with the Firing Angle Varied – 1 MVAR Capacitor Present (Thyristor Peak)

3.3.7 Load

Figures 61 shows the results of the load impact on the DC component of the extracted upstream signal and the extracted upstream signal peak, while Figure 62 shows the impact on the thyristor current peak. The load was varied between 0.5 MVA and 5 MVA. The DC components difference for normal and islanded operation is relatively steady and large enough for reliable detection with the threshold set in between the two lines. The thyristor current peak and the upstream extracted signal peak would provide

unreliable detection, as the difference in the peaks is small or nil in some cases, from when the system is in normal and islanded operation, as seen from the graphs.

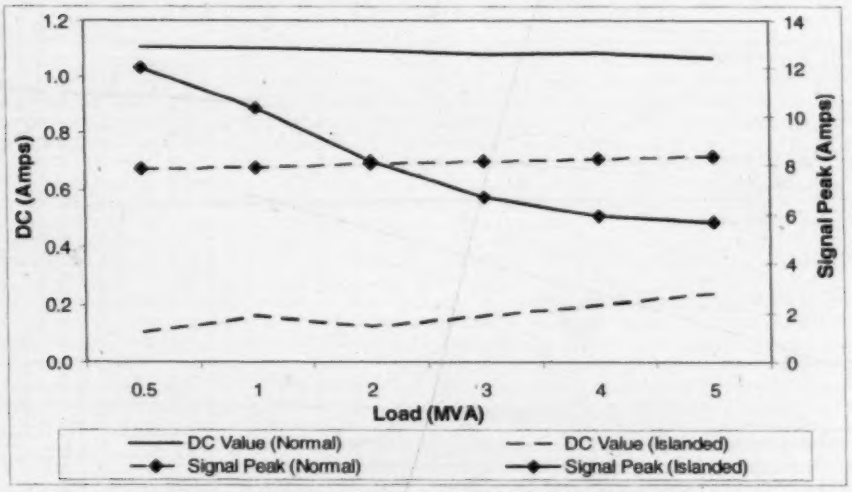

Figure 61: Detection Results with the Load Varied

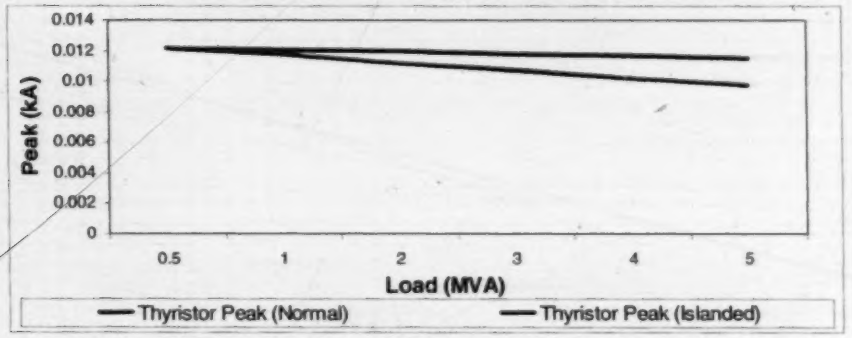

Figure 62: Detection Results with the Load Varied (Thyristor Peak)

3.4 Conclusions on Simulation Results

In this chapter, simulations were conducted to determine the validity of the proposed method. A distribution system was modeled in PSCAD and simulated. The results of the simulations were run through the algorithm explained in Section 2.5, programmed in MATLAB and the results were presented.

The proposed method using the DC component of the extracted upstream current (two consecutive cycles subtracted from each other) as the condition to determine whether islanding has occurred is shown to work extremely well with a large difference in the DC between normal and islanded operations. A threshold can easily be set with enough margin to eliminate nuisance tripping of the DG and have no NDZ.

Sensitivity studies were conducted by varying the major components of the distribution system and signal generator one by one, and analyzing the effects on the detection ability of the proposed method. The simulations have shown that the proposed method using the DC component of the extracted upstream current to detect islanding is very robust and can work reliably under different system conditions.

In order to further demonstrate the proposed method of anti-islanding protection's ability to perform effectively, lab experiments were carried out and are presented in the next chapter.

Chapter 4

Laboratory Studies

This chapter contains laboratory results of the proposed method working in conjunction with a typical distribution system. The system was scaled to a one phase, 120V system. A 7 hp synchronous machine was used to represent the DG. All components of the distribution system were built using power resistors, capacitors and inductors. The first section will describe the laboratory setup (scaled down distribution system that was built) and the values of the components that were chosen. The second section will show results of the laboratory tests using the algorithms explained in Section 2.5, programmed in MATLAB (same as used in Chapter 3). The third section will present the effects of the capacitor on detection reliability as well as the firing angle. More detailed results of the laboratory tests are presented in Appendix B. This study will corroborate the simulation results obtained in the previous chapter. It will then conclude with a discussion on the results obtained.

4.1 Laboratory Setup

To further validate the proposed method, laboratory experiments were conducted and the results were analyzed. This section will explain the laboratory setup. Figure 63 and the information following explain the scaled down system. On the top of the figure, there is a 25kV 3ϕ system and the bottom represents the 120V 1ϕ system that was built for this study.

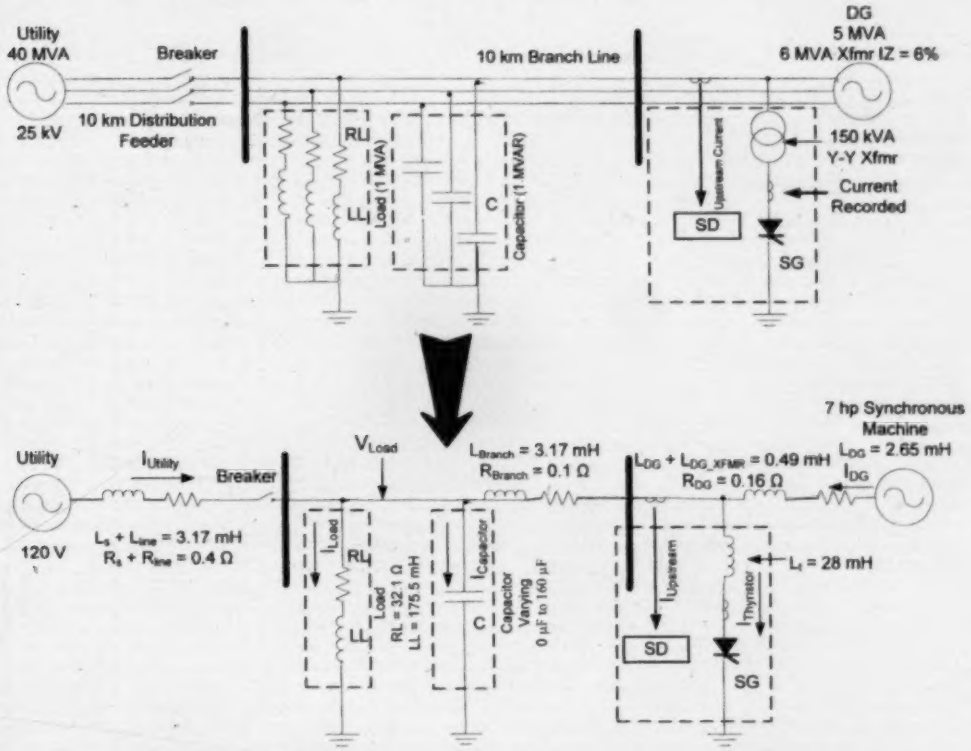

Figure 63: Laboratory Setup (Bottom) Derived from the 25kV System (Top)

- The utility was chosen to be a 1 phase, 120V voltage source (receptacle in the lab).
- To model the utility impedance and feeder impedance, an inductor of 3.17mH and a 0.4Ω resistor was placed in series with the utility.

- A 120V, 20A Breaker was used as a means of utility disconnect.
- The load was modeled using an inductor with 175.5mH impedance and a 32.1Ω resistor.
- An 80 μF capacitor was chosen (capacitance was varied in the experiments).
- The branch was modeled using a 3.17 mH inductor and a 0.1Ω resistor.
- The 7 hp synchronous machine was used to model the DG. The inductance of this machine was determined to be 2.65 mH.
- The impedance of the DG (excluding existing inductance mentioned above) and the DG transformer was modeled using a 0.49 mH inductor and a 0.16Ω resistor.
- The SG transformer was modeled using a 28 mH inductor.
- The Signal Generator was built by the Power Group at the University of Alberta previously (hardware is explained in Section 2.4) and was utilized for this experiment. It was connected between the phase that was used for this experiment and ground.
- The SG was programmed to fire every 4 cycles at an angle of 25° before the zero crossing point of the falling voltage waveform.
- Software was written in LABVIEW and a National Instruments data acquisition device was used for saving the data from the experiment. Sampling rate was chosen to be 256 samples/cycle.
- The data was later imported into MATLAB and run through the algorithm explained in Section 2.5 and used for the simulation tests in Chapter 3.

4.2 Laboratory Test Results

This section presents the results from the laboratory experiments conducted using the components mentioned in the previous section. The data was gathered using a data acquisition device and exported to a spreadsheet and then into MATLAB, where it was run through the algorithm explained in Section 2.5.2.

An important point to keep in mind while reading through the rest of this chapter, is that the signal generator was not functioning to specifications during these tests. This was probably due to the low signal level and lots of noise and distortion present in the system. The SG had trouble pinpointing the exact zero crossing point of the voltage waveform and even though the firing angle was set to 25°, it was found to be actually firing between 23.2° and 27.4°. This will be seen further on in the chapter especially when viewing the thyristor current peak. It is larger in some cases for islanded operation, even though no capacitors are present. However, this does not lead to dismissing the results because even though the firing angle was not constant, the difference in the DC component of the extracted upstream current between normal and islanded operation stayed large, even when the firing angle was larger during islanded operation. Thus, the results can be used with confidence. The SG also had trouble initializing for firing angles lower than 20°, and therefore only results for angles larger than this are presented in the following sections.

The waveforms for voltage, upstream current and extracted current (two consecutive cycles from the upstream current waveform subtracted from each other) are shown in Figure 64 for both normal and islanded conditions. As can be seen from these results, they are very similar

to the simulations in Chapter 3. The extracted signal has very different characteristics when the distribution system is operating normally and when a power island forms. It is very easy to see that the DC component will be very different in the two cases which allows it to be used for islanding detection purposes.

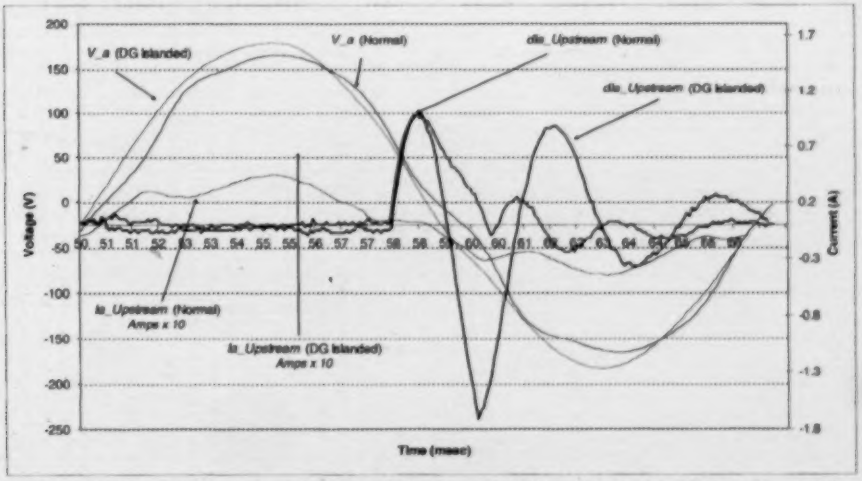

Figure 64: Voltage, Current and Extracted Current Waveforms for Normal and Islanded Operation

In the next figure, Figure 65, the harmonic spectrum of the extracted signal for both normal and islanded operation is presented. It is evident that when an island forms, the spectrum of the signal generated by the thyristor shifts to higher frequencies as in the simulations. It will be shown that by monitoring only the DC component, we can get reliable detection with a very simple algorithm.

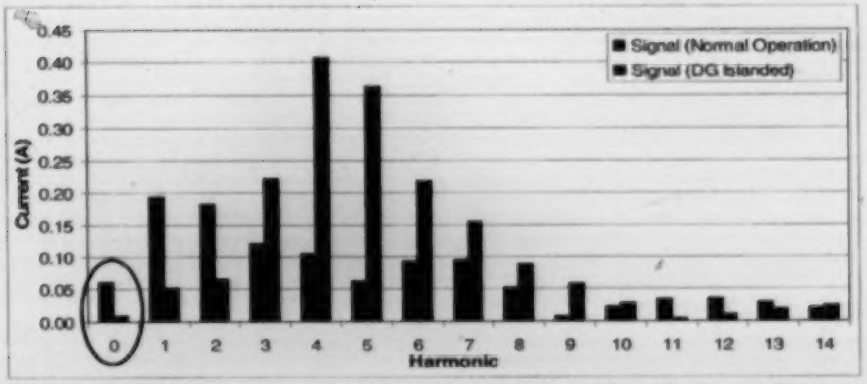

Figure 65: Harmonic Spectrum of the Extracted Signal from Upstream Current

Figure 66 is a blown up version of Figure 64 at around the point that the signal generator fires. It is presented here to show the difference of the extracted signals when the distribution system is working normally and when it is islanded from the utility in greater detail.

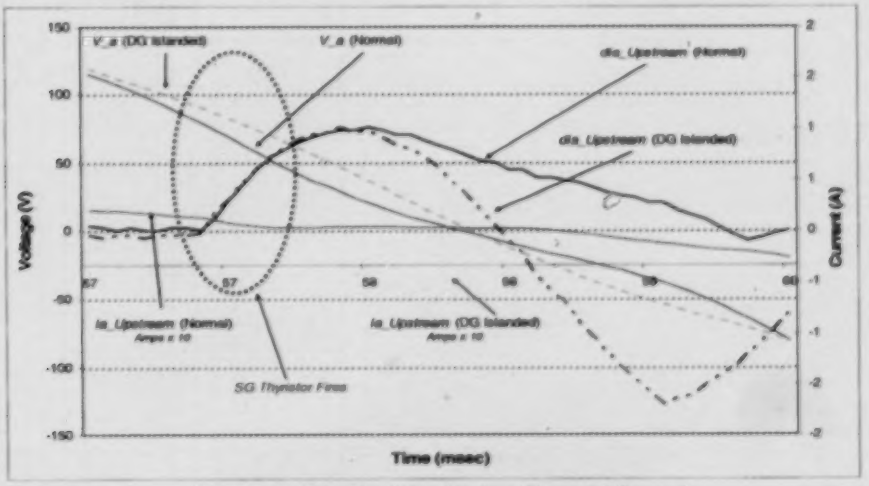

Figure 66: SG Thyristor Firing (Zoomed Image)

Figure 67, showing a full signal pattern is presented on the following page. Since the SG fires every 4 cycles of the fundamental voltage waveform, four cycles are shown. The signal generator's thyristor fires on the third cycle and thus is present only then. The graph shows four cycles of the voltage and upstream current and the two cycles of the extracted current (stretched out over the 4 cycles for clarity).

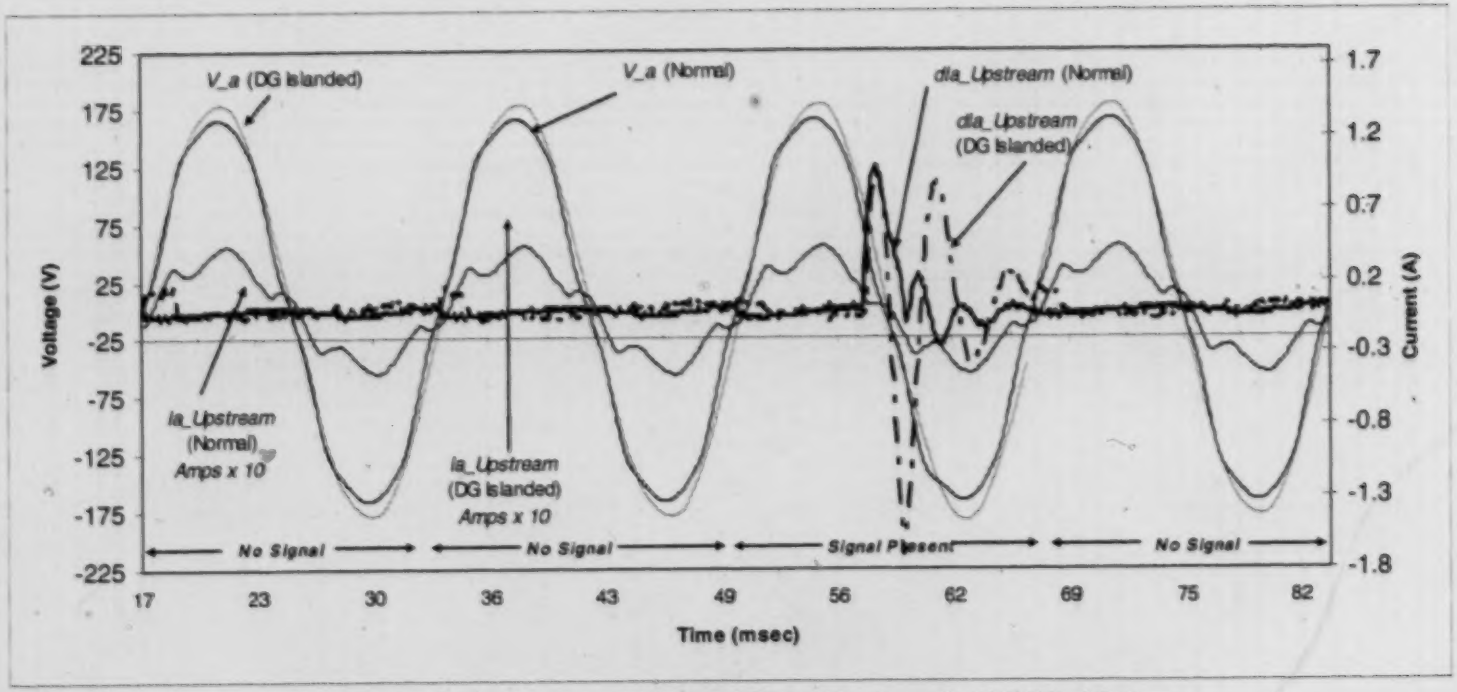

Figure 67: Voltage, Current, and Extracted Signal Waveforms for Full Signal Pattern

Figure 68 shows the voltage and current waveforms of the DG for both normal and islanded operations. The distortion created by the signal is not clearly seen in the current or the voltage because of the high distortion present.

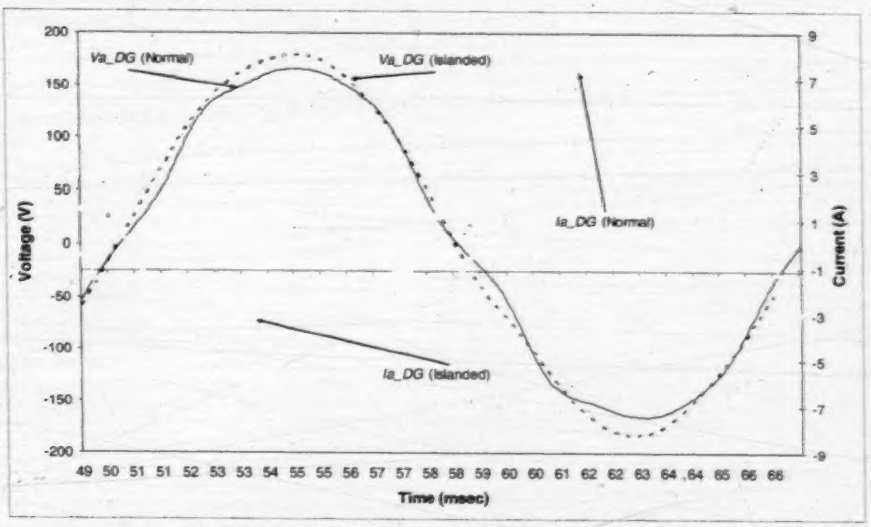

Figure 68: DG Voltage and Current Waveforms

The voltage and current waveforms of the utility for both normal and islanded operations are shown in Figure 69.

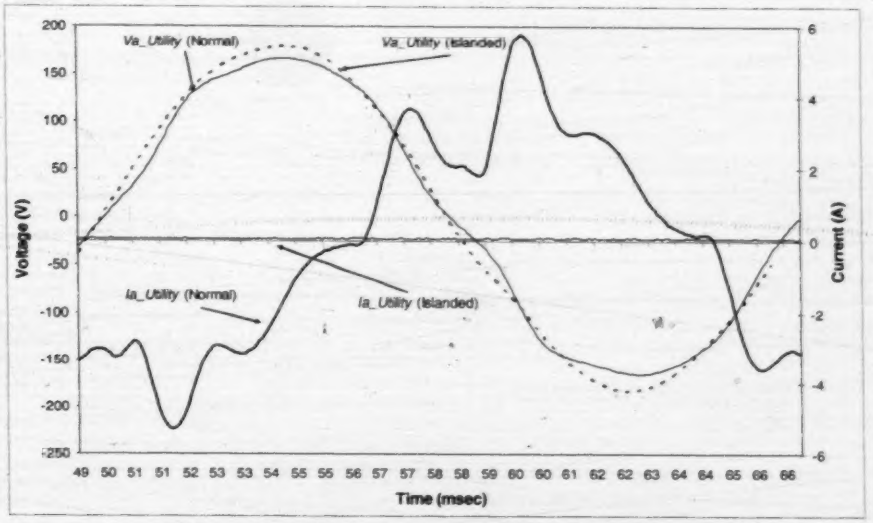

Figure 69: Utility Voltage and Current Waveforms

Below, in Figure 70, the thyristor current is presented, along with the load voltage for reference only, because the thyristor voltage was not acquired due to the limitations of the data acquisition device (only able to measure six channels at the specified sampling rate). In Figure 71, the load and capacitor voltage and current waveforms are shown along with the difference of these waveforms for normal and islanded operation. We can see that there is very little difference in magnitude of the thyristor current pulse. The load voltage is shown not to be affected by the signal generated.

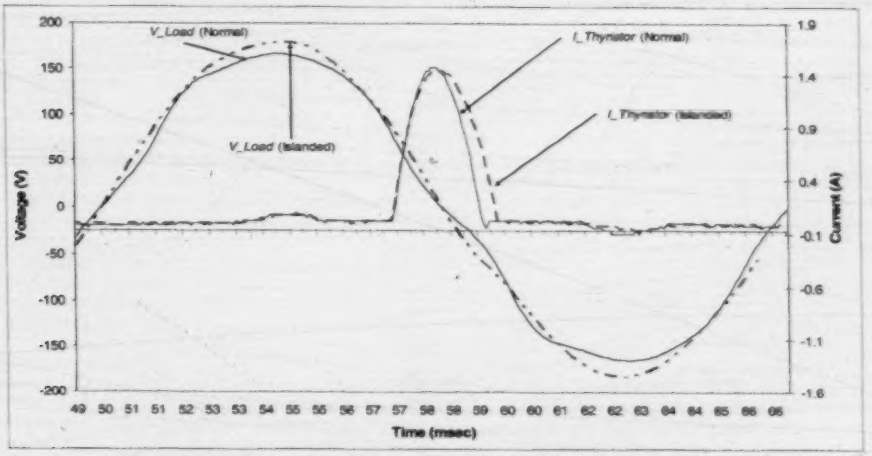

Figure 70: Thyristor Current and Load Voltage Waveforms

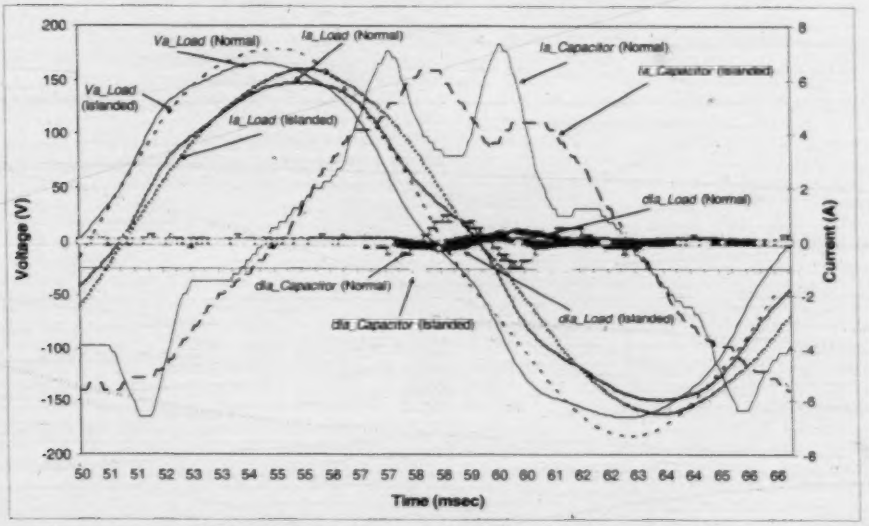

Figure 71: Load and Capacitor Waveforms

Figure 72 illustrates the signal that was extracted from the upstream voltage and current waveforms.

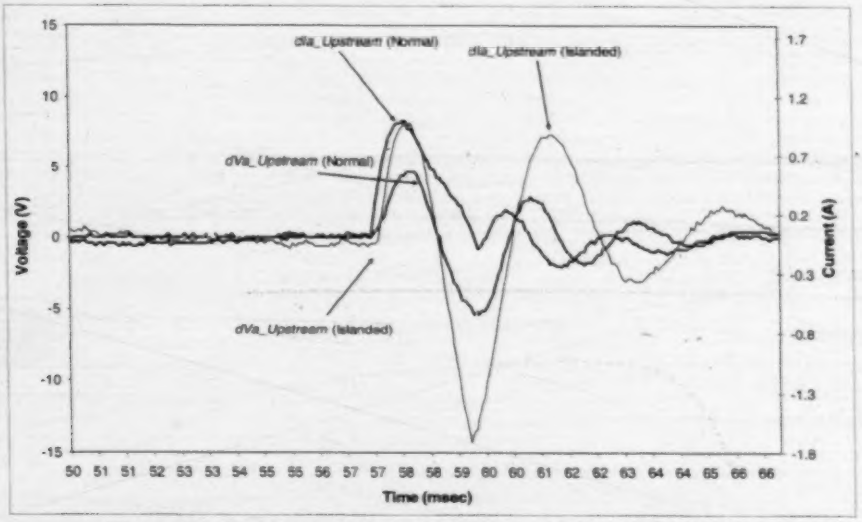

Figure 72: Upstream Voltage and Current (Extracted Signals)

As with the simulations in Chapter 3, in order to demonstrate how minimal the impact on power quality is when the signal generator fires a pulse to be used for islanding detection, Figures 73 and 74 show the harmonic spectrum of the voltage at the point of common coupling (Vpcc) when the system is working normally and when an island forms respectively.

Table 4 presents the results for both operations; the THD of the voltage waveform deteriorates by less than 1% for normal and just over 1% for islanded operation with the signal being present. The results thus confirm the simulations conducted in Chapter 3.

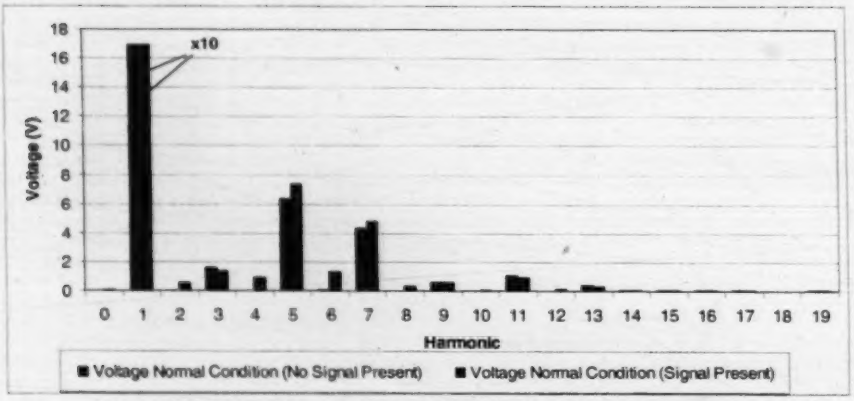

Figure 73: Vpcc Harmonic Spectrum during Normal Operation

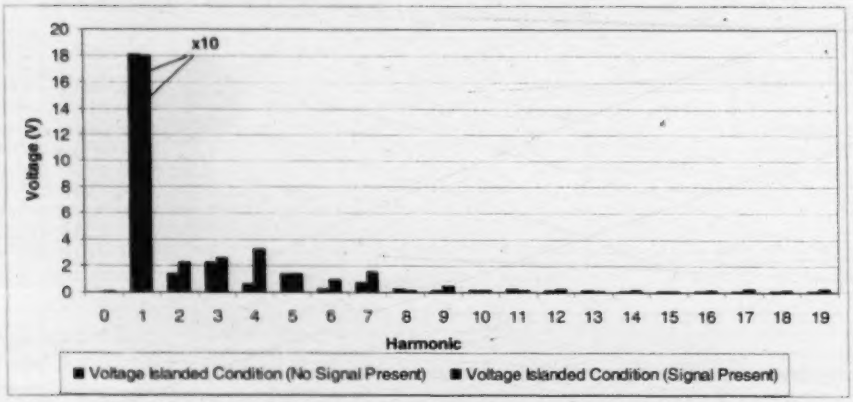

Figure 74: Vpcc Harmonic Spectrum during Islanded Operation

Table 4: Voltage Total Harmonic Distortion at the Point of Common Coupling

V_{pcc}	Normal Operation		Islanded Operation	
	Signal Not Present (%)	Signal Present (%)	Signal Not Present (%)	Signal Present (%)
V_{thd}	4.685	5.403	1.738	2.928

A similar study was conducted on the upstream current. Figures 75 and 76 show the harmonic spectrum of the upstream current when the system is working normally and when an island forms respectively. Table 5 presents the results. The THD of the upstream

current increases by less than 1% during normal operation and just over 1% during islanded operation.

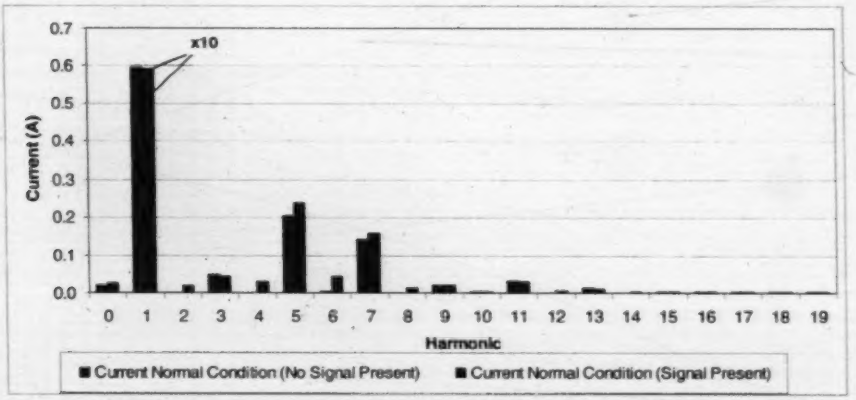

Figure 75: Upstream Current Harmonic Spectrum During Normal Operation

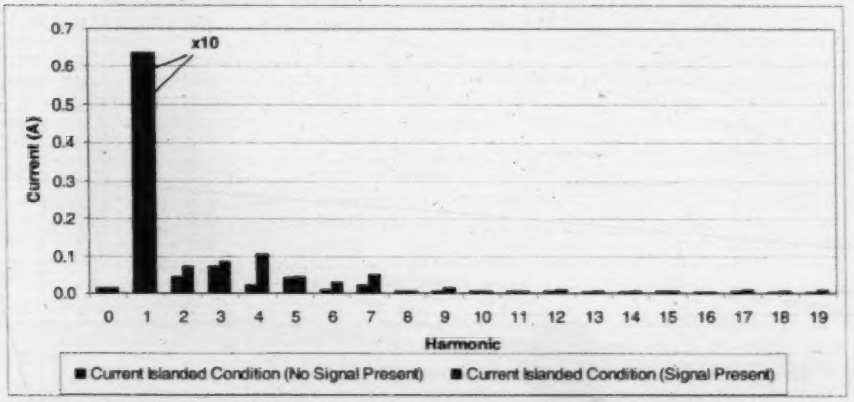

Figure 76: Upstream Current Harmonic Spectrum During Islanded Operation

Table 5: Current Total Harmonic Distortion at the Point of Common Coupling

Upstream Current	Normal Operation		Islanded Operation	
	Signal Not Present (%)	Signal Present (%)	Signal Not Present (%)	Signal Present (%)
I_{thd}	4.294	4.978	1.592	2.696

4.3 Sensitivity Study

Simulations have shown the proposed method and algorithm to be reliable and robust. To verify these results, a sensitivity study was conducted using the laboratory equipment. Unlike in the simulations, where every variable was varied, only the capacitor size and firing angle sensitivity studies have been completed. These are important variables that have a larger effect on detection as was demonstrated in Chapter 3 in the sensitivity study. The firing angle has a very large impact on the signal strength and magnitude, while the capacitor size has an impact on overall system impedance and thus affects the characteristics of the current pulse drawn by the SG.

The same system and values were used as explained in Section 4.1, with only the capacitor and firing angle being varied, one at a time. The results of these tests are then run through MATLAB, on the same algorithm from the previous section. The difference in DC component of the extracted upstream signal is shown below, along with the thyristor peak current and upstream current signal peak to illustrate the effectiveness of using the DC component for islanding detection purposes.

4.3.1 Capacitor Size

In this section, the size of the capacitor bank was varied between 0 and 160 μF (0 to 2 MVAR on a 25kV base). In Figure 77, it is shown that the separation between the normal and islanded operation for the DC component of the extracted upstream current is large, albeit not very stable. Unlike in the simulations, the resulting curves are not as

smooth, however, even though the DC component fluctuates, there is still a large separation between normal and islanded operation. A threshold can easily be set which would work reliably and not cause nuisance tripping. Only the results are shown here and greater details from each individual test can be found in Appendix B. It is clear that the DC element is not affected by the amount of VARS present in the system. The upstream extracted signal peak seen on the same figure and the thyristor peak shown in Figure 78, however, cannot be used as for islanding detection as it is evident that their difference between normal and islanded operation is small and intersects. The thyristor peak shows some unexpected results, as the peak through the thyristor should be higher during normal than in islanded operation for small or no capacitors present. This can be attributed to the problem mentioned previously in Section 4.2. The SG was having difficulties detecting the zero-crossing point of the voltage waveform and the firing angle was varying slightly. In this case, it is clear that the firing angle was larger during islanded operation. This provides us with pessimistic results as the difference in the DC component of the extracted upstream current would be smaller than expected. However, it can be seen in Figure 77 that this method's islanding detection capability is able to accommodate such small fluctuations by virtue of the large interval resulting from the difference produced between the DC component curves during normal and islanded operations and thus, even under those circumstances, it can still be used for reliable islanding detection.

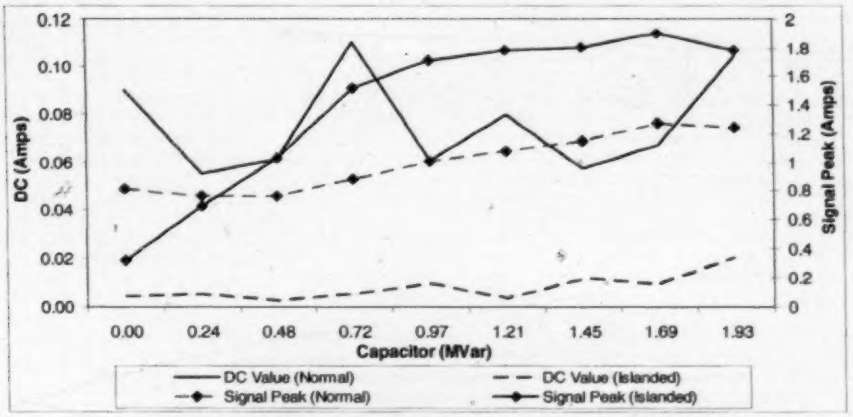

Figure 77: Detection Results with the Capacitor Size Varied

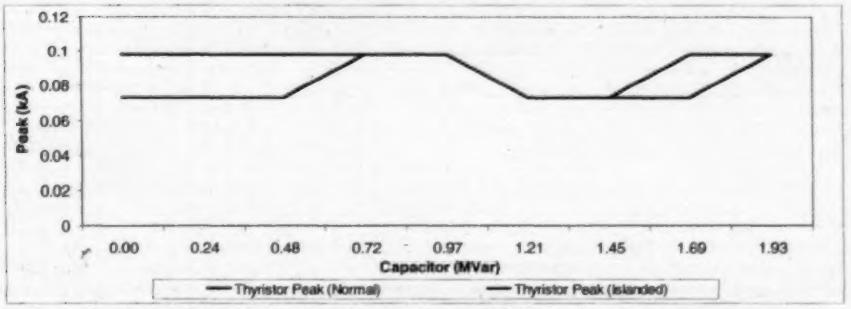

Figure 78: Detection Results with the Capacitor Size Varied (Thyristor Peak)

4.3.2 Firing Angle

To determine the firing angles effect on the detection, laboratory tests were conducted for firing angles of 25° and 30° (before the zero crossing point of the voltage waveform). These studies were conducted for the system explained in Section 4.1 and also for the same system without a capacitor bank. Figures 79 and 80 show the results of the firing angle impact on the DC component of the upstream current extracted signal, the extracted upstream signal peak and the thyristor peak for the distribution system without capacitors. From the first figure, it is clear that as the firing angle is increased, the difference for both the DC component and the extracted signal from the upstream current

curves gets larger. A firing angle of 25° is sufficient to have a large enough margin to provide reliable detection. The thyristor peak for this laboratory experiment is actually larger for the islanded condition and the reason and justification of using these results is presented in Section 4.3.1.

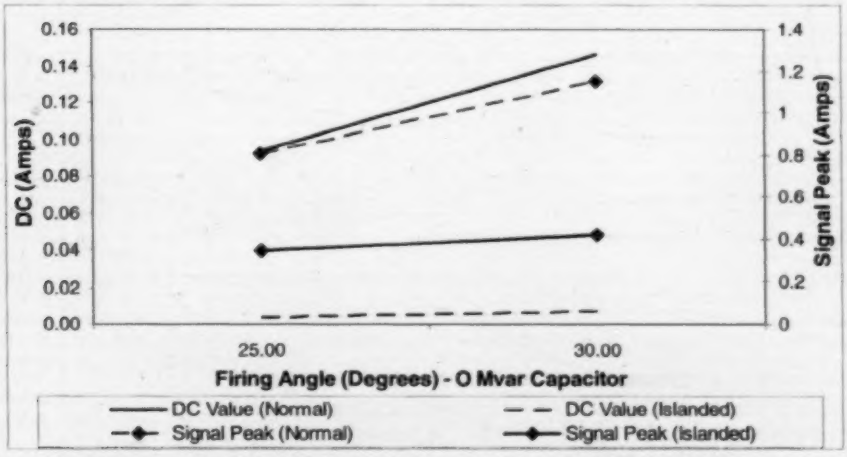

Figure 79: Detection Results with the Firing Angle Varied – 0 MVAR Capacitor Present

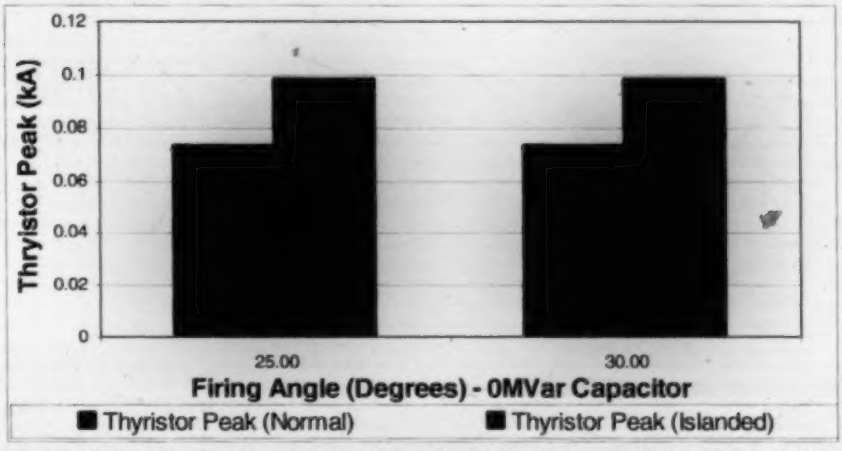

Figure 80: Detection Results with the Firing Angle Varied (Thyristor Peak) – 0 MVAR Capacitor Present

When capacitors are present, the results change significantly as can be seen in the following two figures. While the DC component's difference between normal and

islanded operation stays large (and increases as the firing angle increases), the upstream current extracted signal peak's difference between normal and islanded operation is much smaller. The thyristor current peak would also not be useful for islanding detection as its difference between normal and islanded operation is small. This corroborates the findings in Section 3.3.2 for this amount of capacitors present in the system, however the results may also have been influenced by the problems the SG had in firing at a precise angle (discussion in Section 4.3.1). As in the case of no capacitors present, a firing angle of 25° is sufficient to have a large enough margin to provide reliable islanding detection if using the DC component.

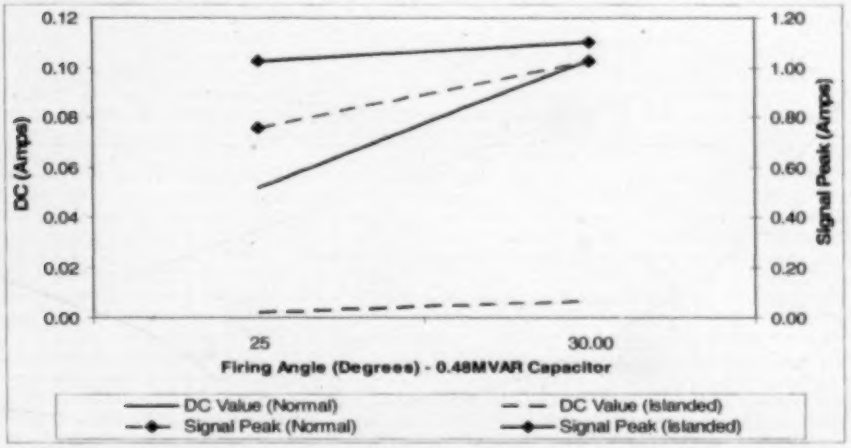

Figure 81: Detection Results with the Firing Angle Varied – 0.5 MVAR Capacitor Present

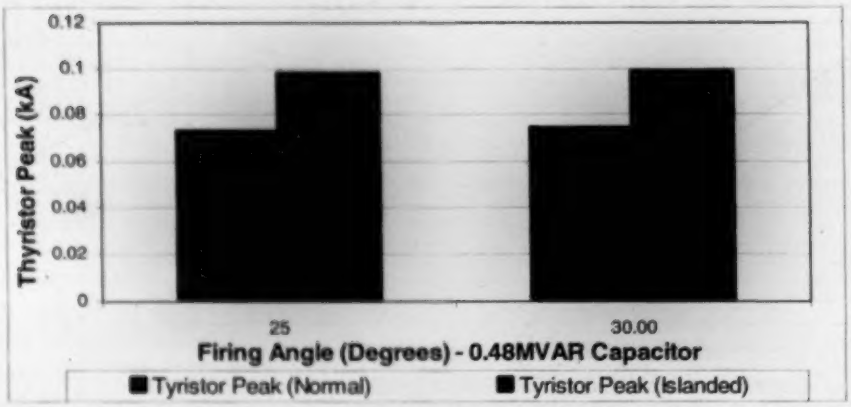

Figure 82: Detection Results with the Firing Angle Varied (Thyristor Peak) – 0.5 MVAR Capacitor Present

4.4 Conclusions on Laboratory Tests

The main objective of the laboratory tests was to confirm the results obtained in Chapter 3 and also evaluate the performance of the anti-islanding method that has been proposed in this thesis in a laboratory setting. In this chapter, laboratory experiments were conducted by scaling a 25kV 3 phase to a 120V 1 phase system and using resistors, capacitors and inductors to model the lines and components of the distribution system. A 7 hp synchronous machine was used to represent a DG and the results of the experiment were run through the algorithm offered in this thesis. There were some limitations with the signal generator due to the large distortions and noise present in the system. However, this did not compromise the results significantly.

The proposed method using the DC component of the extracted upstream current (two consecutive cycles subtracted from each other) for islanding detection is shown to work

extremely well because of a large difference in the DC of this signal between normal and islanded operations. A threshold can easily be set with a large enough margin to eliminate nuisance tripping of the DG while not compromising detection reliability.

Sensitivity studies for the size of capacitor and firing angle were conducted by varying those components of the distribution system and signal generator one by one and analyzing the effects on the detection ability of the proposed method. It has shown that the proposed method using the DC component to detect islanding is very robust and can work reliably under these different system conditions.

To further validate the proposed method, field tests should be completed in an actual distribution system.

Chapter 5

Conclusions and Recommendations

Anti-islanding protection has a very important role in the overall protection scheme for distributed generators in distributed networks. Due to the rising interest in DGs, extensive research has been conducted to solve this major technical barrier and many products are commercially available. While there are advantages and disadvantages to each protective method, a great need has arisen to develop anti-islanding protection which is reliable and cost-effective.

A thorough literature review was conducted to examine current anti-islanding practices and techniques. The advantages and disadvantages of each method have been presented and discussed in Chapter 1. It is clear from these discussions that a reliable new method that would be inexpensive to implement is sought after by the electric industry. The primary goal

of this work was to develop a new method of islanding detection and validate its effectiveness through simulations and laboratory experiments.

This thesis presents the development of a novel method for the detection and prevention of islanding of distributed generators in distribution networks. It is an active local based method which works on the principle of impedance measurement. An SCR based device draws a current pulse by shorting to ground at the terminals of the DG through an impedance every 4 cycles of the fundamental voltage waveform at a specified angle. This current pulse is drawn from the utility and DG and its appearance in the upstream current is drastically different in normal and islanded operations. The upstream current is thus monitored and every two consecutive cycles of the current waveform are subtracted from each other to allow for the detection to be virtually immune from any background waveform distortions. The resulting signal, referred to as the extracted upstream current in this thesis, is analyzed and the DC component is calculated. It is compared to a set threshold that is programmed upon installation, and if it is above, the system is considered to be working normally, with the electric utility supplying power. If the DC component is below the threshold for 4 consecutive signal pattern cycles (16 cycles of the fundamental voltage), the system is considered islanded and the DG is tripped. This feature can possibly be implemented to allow for automatic startup of the DG once the utility service is restored.

To further reduce costs, an alternative method of detection has been proposed for distribution systems without any compensating capacitors present. Instead of measuring the DC component of the upstream current, only the SCR current is analyzed and either the DC component of the current or its peak can be used for islanding detection.

Comprehensive simulation studies were conducted using a realistic distribution system modeled in PSCAD, as shown in Chapter 3. Sensitivity studies were performed, where one variable of the distribution system and the signal generator were varied, and the simulations were conducted, and the results were analyzed. The simulations confirmed the effectiveness of the proposed method. Reliable islanding detection can be achieved using the approach of monitoring the DC component of the extracted upstream current under different system configurations and topologies.

To further validate the proposed method, laboratory experiments were conducted and a distribution system was modeled using resistors, inductors and capacitors and the DG with a 7hp synchronous machine. The signal generator had trouble firing at the correct angle; however, the results still corroborate the simulation findings and did not affect the proposed method's islanding detection ability.

This series of tests corroborated the results obtained during simulation studies and that the proposed method and algorithm are capable of reliable islanding detection if a proper threshold is set.

The advantages of the proposed anti-islanding detection method can be summarized as follows:

- Works reliably and has been determined to detect islanding conditions within the required time. Through extensive simulations and laboratory experiments it was concluded that there is no non-detection zone which means it will function under all operating conditions.
- Will operate in different network topologies

- Easy to implement and relatively inexpensive.
- Local – does not require any upgrades from the distribution system (unlike most transfer trip schemes)
- Very little computational power is needed as the DC component can be calculated by using simple arithmetic and accuracy is not of paramount importance as the difference in the signal is great between normal and islanded operation.
- The disturbance injected into the system has a minimal impact on the voltage, and thus not affect power quality significantly. It should not interfere with existing power line communication schemes and other DGs using same method.
- Will work for both induction and synchronous generators.

This research has established that the proposed method looks very promising for successfully detecting islanding conditions. To further validate the theory, field tests should be conducted. Laboratory tests, as have been shown, can be difficult to implement as the noise is high and signal strength is relatively low. A signal generator/detector should be developed and a suitable location in a distribution system selected, preferably near the end of line so that the DG can be islanded under close supervision without any customers being affected. This will verify the method and also its impact on other power line technologies, such as AMR. Optimization of the proposed method should also be researched in greater detail, such as transformer size for the signal generator and firing angle. Upon successful completion of field tests, this technology can be improved as dictated by its performance in the field and later commercialized.

Bibliography

[1] Distributed Energy Program, U.S. Department of Energy, "Major Potential Benefits of DE", February 2007, http://www.eere.energy.gov/de/major_potential_benefits.html

[2] G. Pepermans, J. Driesen, D. Haeseldonckx, R. Belmans, W. D'haeseleer, "Distributed Generation: Definition, Benefits and Issues," Elsevier Energy Policy 33, 2003. pp. 787 – 789, Oct. 2003

[3] Canadian Wind Energy Association, "Global Wind Energy Markets Continue to Boom – 2006 Another Record Year", February 2007, http://www.canwea.ca/

[4] Lasseter, R. H, "Control of Distributed Resources" in Proceedings: Bulk Power Systems Dynamics and Control IV, Aug. 1998, pp. 323-329.

[5] Annual Energy Outlook 2007 with Projections to 2030, U.S. Department of Energy, "Electricity Supply, Disposition, Prices, and Emissions - Table A8", Feb. 2007, http://www.eia.doe.gov/oiaf/forecasting.html

[6] Cooper Power Systems, Fundamentals of Power Distribution Workshop: Over-Current Protection, Cooper Power, 2001

[7] EPRI on Research Project 1209-1, report EL 3085, May 1983

[8] R. A. Walling, N. W. Miller, "Distributed Generation Islanding – Implications on Power System Dynamic Performance," Power Engineering Society Summer Meeting 2002, IEEE Vol. 1, 21-25 July 2002, pp 92-96.

[9] Sarma S. Mulukutla, Edward M. Gulachenski, "A Critical Survey of Considerations in Maintaining Process Continuity During Voltage Dips While Protecting Motors with Reclosing and Bus-Transfer Practices," Transactions on Power Systems, Vol. 7 No. 3, August 1992, pp 1299-1305.

[10] ANSI/IEEE, *IEEE Guide for Interfacing Dispersed Storage and Generation Facilities with Electric Utility Systems*, IEEE/ANSI Std., 1988.

[11] IEEE, *IEEE Standard for Interconnecting Distributed Resources with Electric Power Systems*, IEEE Std. 1547, 2003.

[12] Electricity Association, G59/1 *Recommendation for the Connection of Embedded Generating Plant to the Regional Electricity Companies Distribution Systems*, Electricity Association Std., 1991.

[13] Wilsun Xu, Konrad Mauch, Sylvain Martel, "An Assessment of Distributed Generation Islanding Detection Methods and Issues for Canada," Aug 2004, http://cetc-varennes.nrcan.gc.ca/en/er_re/pvb/p_p.html?2004-074

[14] Wilsun Xu, "Survey of Power Line Communication Techniques and Assessment of Their Applicability to Islanding Detection," Power Group, University of Alberta, Dec 2002

[15] Wilsun Xu, "A Power Signaling Based Technique for Detecting Islanding Conditions in Electric Power Distribution Systems," Power Group, University of Alberta, July 2003

[16] Philip P. Barker, Robert W. deMello, "Determining the Impact of Distributed Generation on Power Systems: Part 1 – Radial Distribution Systems," Power Engineering Society Summer Meeting, 2000. IEEE Volume 3, pp.1645 – 1656, July 2000

[17] R. A. Walling, N. W. Miller, "Distributed Generation Islanding – Implications on Power System Dynamic Performance," Power Engineering Society Summer Meeting, 2002 IEEE Volume 1, 21-25, pp. 92 - 96, July 2002.

[18] Thomas E. McDermott, Roger C. Dugan, "Measuring Distributed Generation's impact on Reliability and Power Quality," IEEE Industry Applications Magazine, pp. 17–23, Sept. 2003

[19] J. E. Kim, J. S. Hwang, "Islanding Detection Method of Distributed Generation Units Connected To Power Distribution System," International Conference on Power System Technology Proceedings, PowerCon 2000. Volume 2, pp.643 - 647, Dec. 2000

[20] Thomas E. McDermott; Roger C. Dugan; "Measuring Distributed Generation's impact on Reliability and Power Quality," IEEE Industry Applications Magazine, pp. 17–23, Sept. 2003

[21] P. O'Kane; B. Fox; "Loss of Mains Detection for Embedded Generation by System Impedance Monitoring," Development in Power System Protection Conference No. 434, pp. 95-98, March 1997

[22] N. Jenkins, R. Allen, P. Crossley, D. Kirschen, and G. Strbac, *Embedded Generation*, 1st Ed. Institute of Electrical Engineers, 2000.

[23] W. Freitas, Z. Huang, W. Xu, "A Practical Method for Assessing the Effectiveness of Vector Surge Relays for Distributed Generation Applications," IEEE Trans. Power Delivery, vol. 20, No. 1, pp.57-63, Jan. 2005

[24] M. A. Redfern, J. I. Barret, O. Usta, "A New Microprocessor Based Islanding Protecion Algorithm for Dispersed Storage and Generation Units," IEEE Trans. On Power Delivery, Vol. 10, No. 3, July 1995, pp. 1249-1254.

[25] S. K. Salman, D. J. King and G. Weller, "New Loss of Mains Detection Algorithm for Embedded Generation Using Rate of Change of Voltage and Changes in Power Factors," Developments in Power Systems Protection, Conference Publication No. 479, IEE 2001.

[26] M. E. Ropp, M. Begovic, A. Rohatgi, "Prevention of Islanding in grid-connected photovoltaic Systems," in Progress in Photovoltaics: Research and Applications, Vol. 7, No. 1, 1999, pp 39-59.

[27] L. Asiminoaei, R. Teodorescu, F. Blaaberg, U. Borup, "A New Method of On-line Grid Impedance Estimation for PV Inverter," Proceedings of the 19th Annual IEEE Applied Power Electronics Conference, 2004, pp 1527-1533.

[28] J. Motohashi, Y.Imai, T. Ishikawa, T. Kai, H. Kaneda, T. Fujimoto,T. Ishizuka, "Development of Detecting System of Islanding Operation for Dispersed Synchronous Machine Generator Interconnected to Distribution Line," Meiden Review Magazine, Series 110, No.1,2000, pp 1019-1022.

[29] Hung, G-K, C-c Chang, C-L Chen, "Automatic Phase-Shift Method for Islandning Detection of Grid-Connected Photovoltaic Inverters," IEEE Trans. On Energy Conversion, Vol. 18, No. 1, March 2003, pp 169-173.

[30] M. E. Ropp, M. Begovic, A. Rohatgi, G. A. Kern, R. H. Bonn, S. Gonzalez, "Determining the Relative Effectiveness of Islanding Methods Using Phase Criteria and Non-Detection Zones," IEEE Trans. On Energy Conversion, Vol. 15, No. 3, Sept. 2000, pp 290-296.

[31] W. Xu, G. Zhang, Chun Li, W. Wang, G. Wang, J. Kliber, "A Power Line Signaling Based Technique for Anti-Islanding Protection of Distributed Generators: Scheme and Analysis," IEEE Trans on Power Delivery, Submitted and Accepted, 2007.

[32] M. Ropp, D. Larson, S. Meendering, D. McMahon, J. Ginn, J. Stevens, W. Bower, S. Gonzalez, K. Fennell, L. Brusseau, "Discussion of a Power Line Carrier Communications-Based Anti-Islanding Scheme Using a Commercial Automatic

Meter Reading System," Photovoltaic Energy Conversion Conference 2006, Vol. 2, May 2006, pp. 2351-2354.

[33] W. Wang, J. Kliber, G. Zhang, W. Xu, B. Howell, T. Palladino, "A Power Line Signaling Based Technique for Anti-Islanding Protection of Distributed Generators: Field Test Results," IEEE Trans on Power Delivery, Submitted and Accepted, 2007.

[34] Wencong Wang; Jacek Kliber; "Field Test Analysis for Anti-islanding Signal Generator and Signal Detector," Power Group, University of Alberta, May 2005

[35] Wilsun Xu, Emad E. Ahmed, Xiqin Zhang, Xian Liu, "Measurement of Network Harmonic Impedances: Practical Implementation Issues and Their Solutions," *IEEE Trans. Power Delivery* vol. 17, pp. 210-216, Jan 2002

[36] A. Robert and T. Deflandre, "Guide for assessing the network harmonic impedances," CIGRE 36.05, Working Group CC02 Rep., Mar. 1993.

[37] CIGRE Working Group 36-05, "Harmonics, characteristic parameters, methods of study, estimates of existing values in the network," *Electra*, no. 77, pp. 35–54, July 1981.

[38] A. de Oliveira, J. C. de Oliveira, J. W. Resende, and M. S. Miskulin, "Practical approaches for AC system harmonic impedance measurements," *IEEE Trans. Power Delivery*, vol. 6, pp. 1721–1726, Oct. 1991.

[39] M. Nagpal, W. Xu, and J. H. Sawada, "Harmonic impedance measurement using three-phase transients," *IEEE Trans. Power Delivery*, vol. 13, pp. 272–277, Jan. 1998.

[40] W. Wang, J. Kliber, and W. Xu, "An Improved Power-Line-Signaling Scheme for Islanding Detection of Distributed Generators," *IEEE Trans. Power Delivery*, Submitted, August 2007.

Appendix A

Simulation Study: Detailed Results

This section provides detailed results of the simulation studies performed in Chapter 3. Simulations were conducted using PSCAD, an EMTP (Electromagnetic Transients Program) program. Section 3.1 describes the simulation setup (distribution system that was modeled) and the values of the components that were chosen.

Graphs showing voltage, upstream current, and the extracted upstream current signal are presented. A harmonic spectrum graph is also included for all the simulations conducted for the sensitivity study.

Table 6: Branch Length (DG to Load) – 1km to 10km

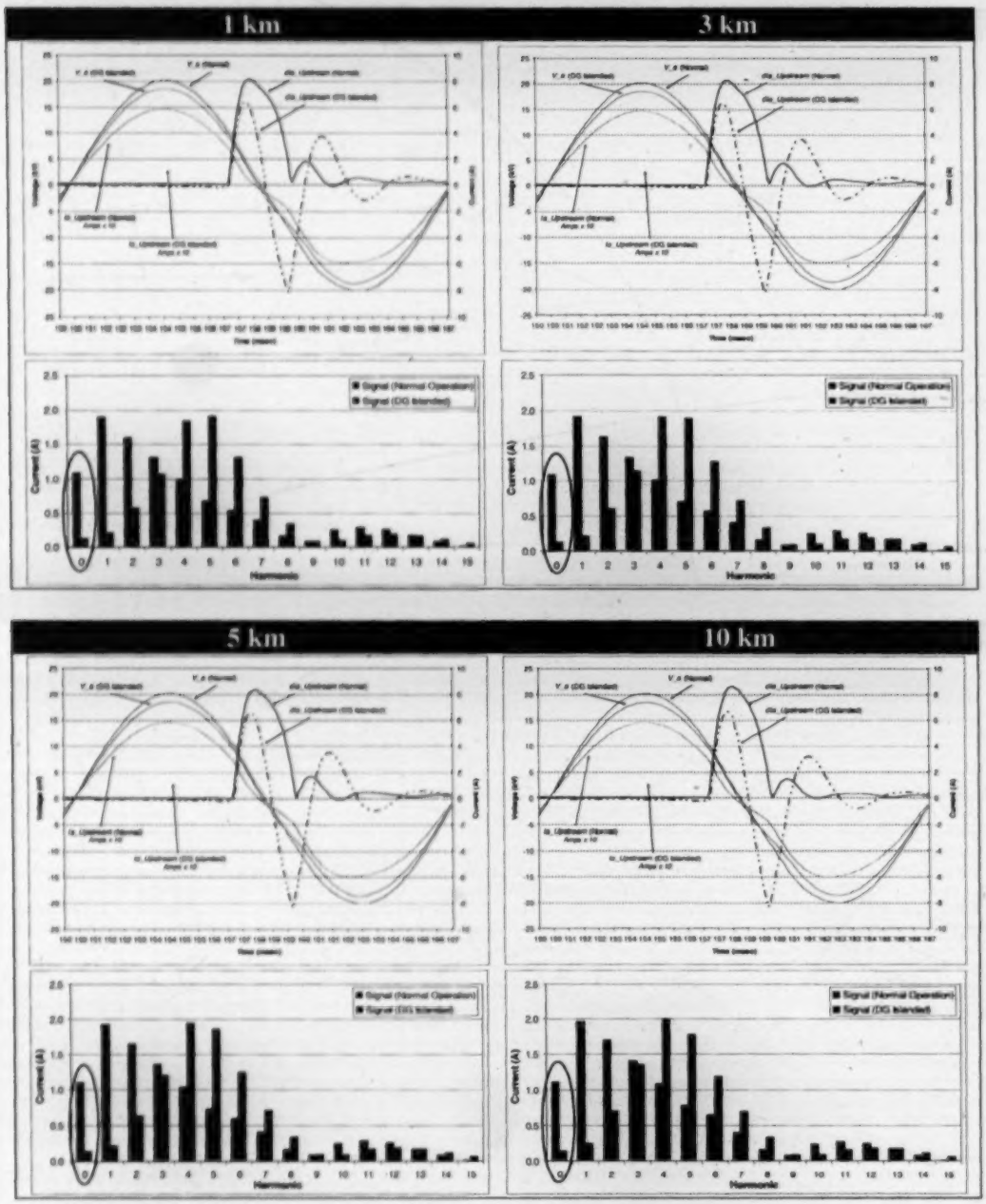

Table 7: Capacitor - 0 MVAR to 2 MVAR

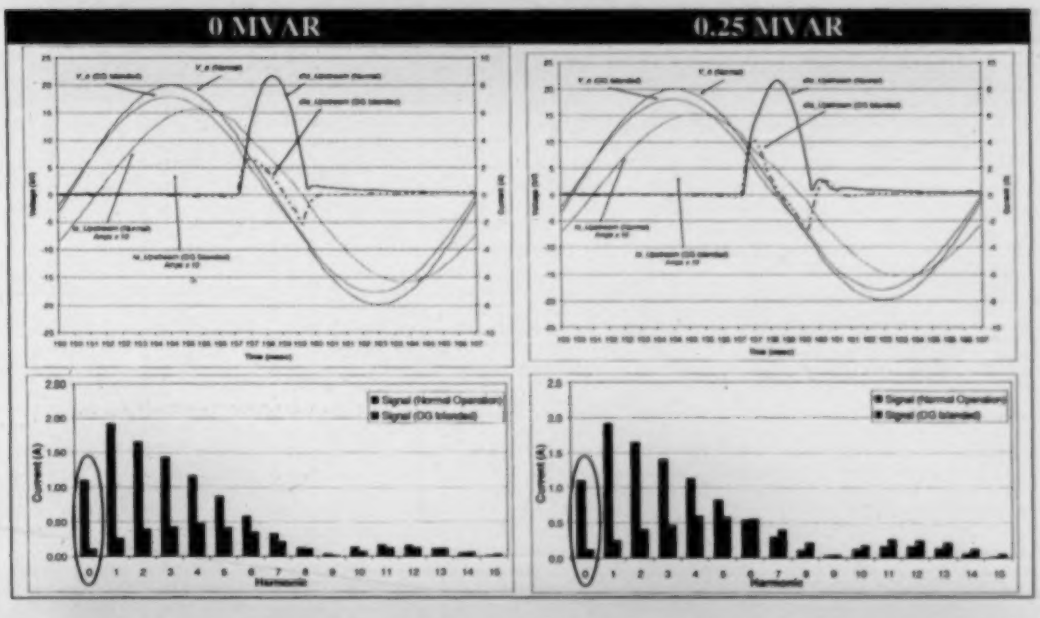

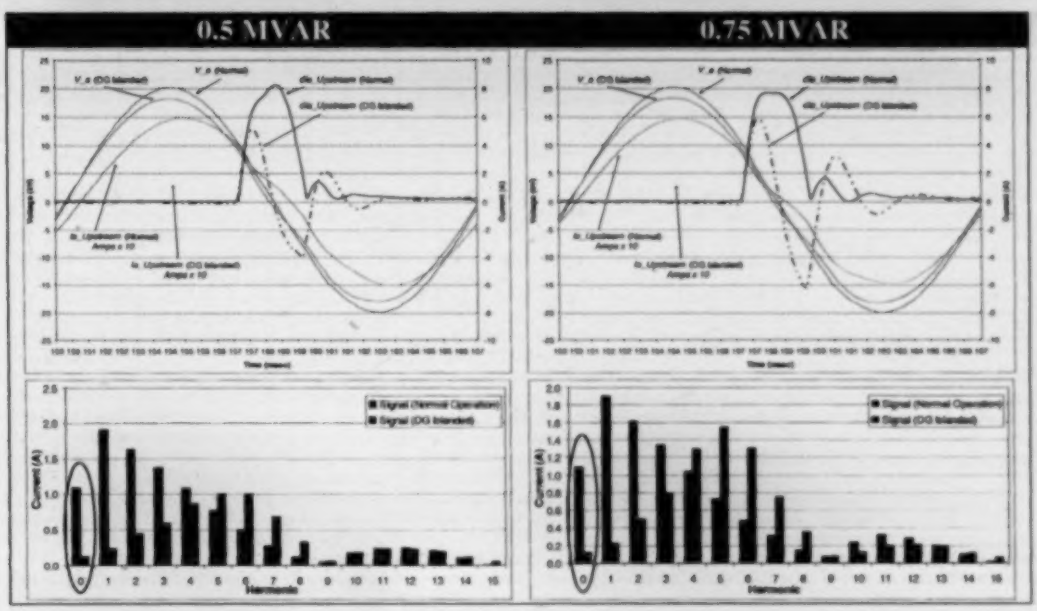

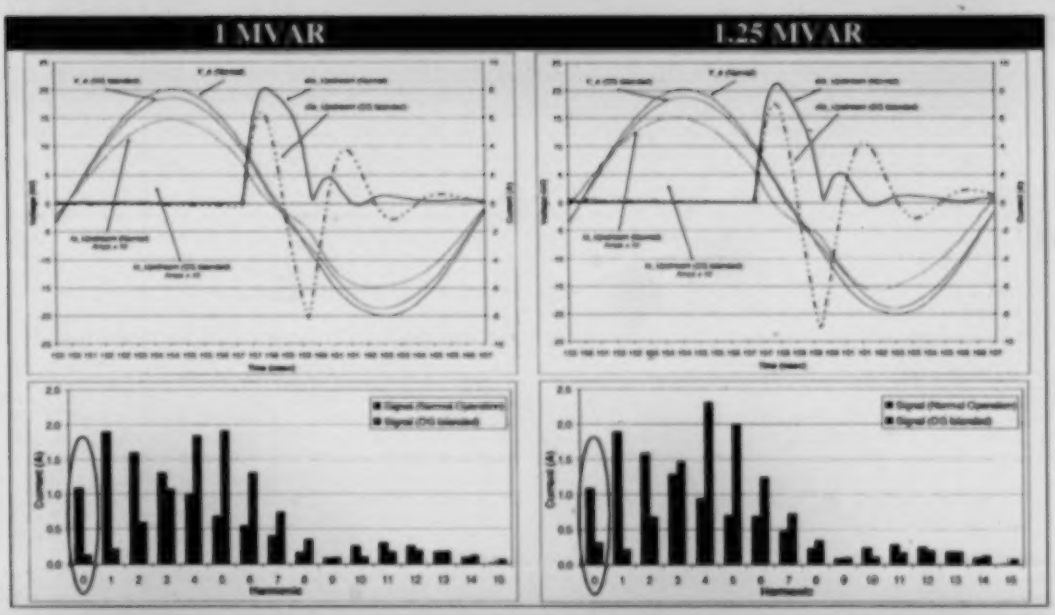
1 MVAR
1.25 MVAR

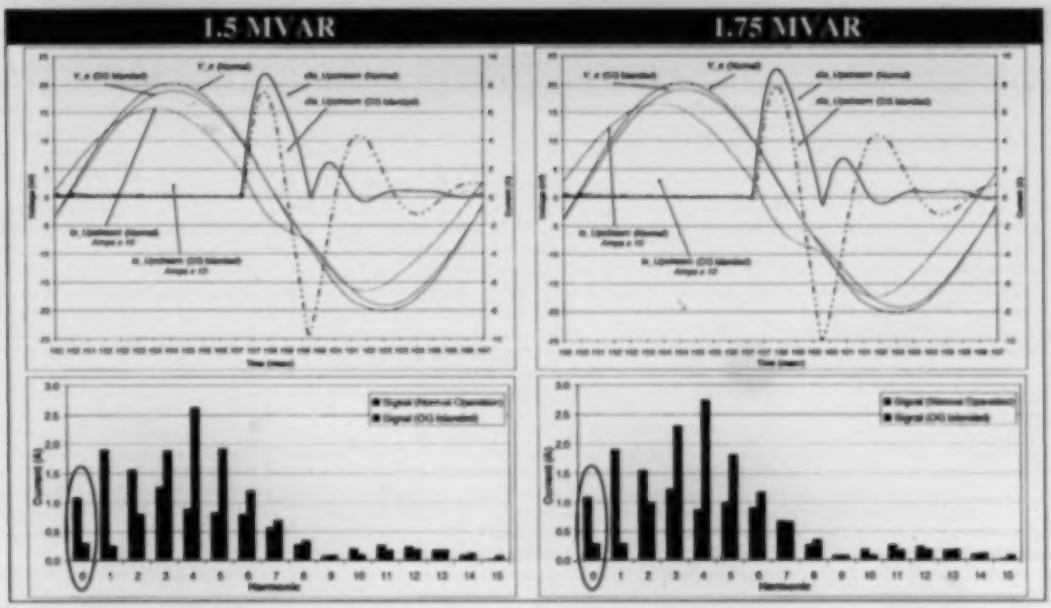
1.5 MVAR
1.75 MVAR

2 MVAR

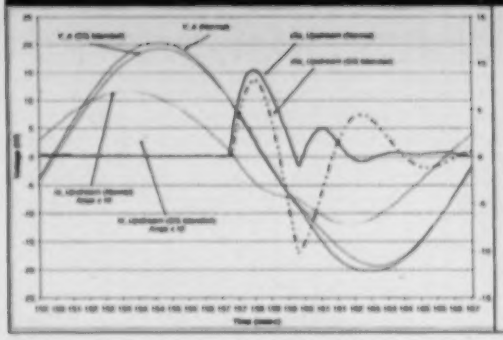

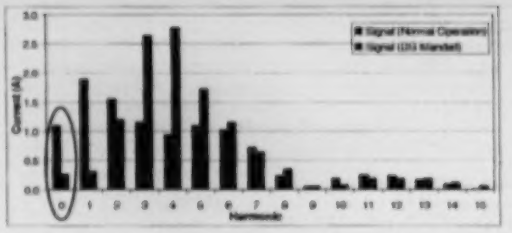
Signal (Normal Operation)
Signal (IDS Islanded)
Current (A)
Harmonic

Table 8: DG Level – 0.5 MVA to 50 MVA

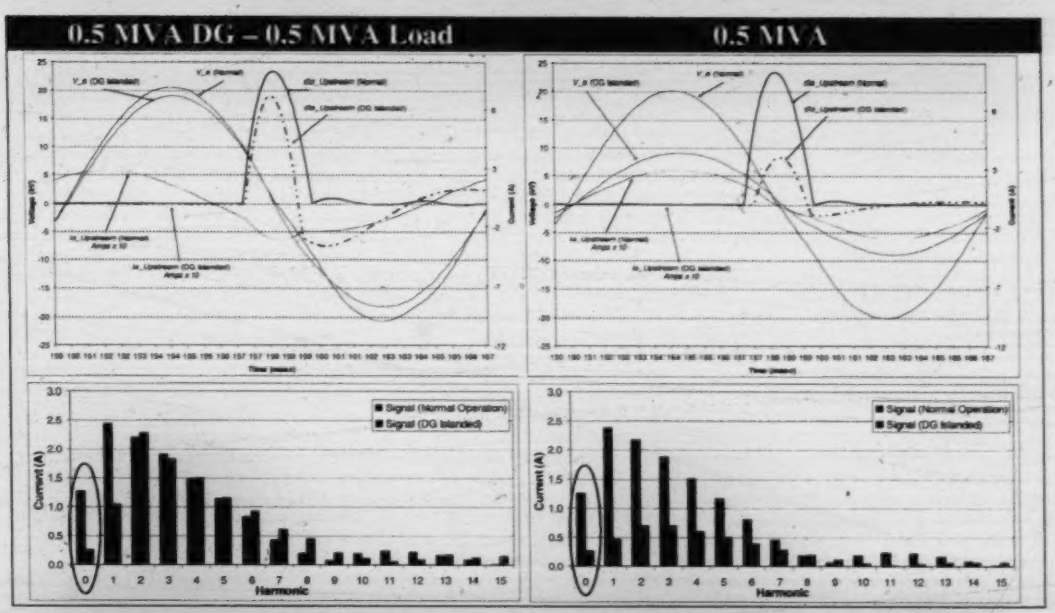

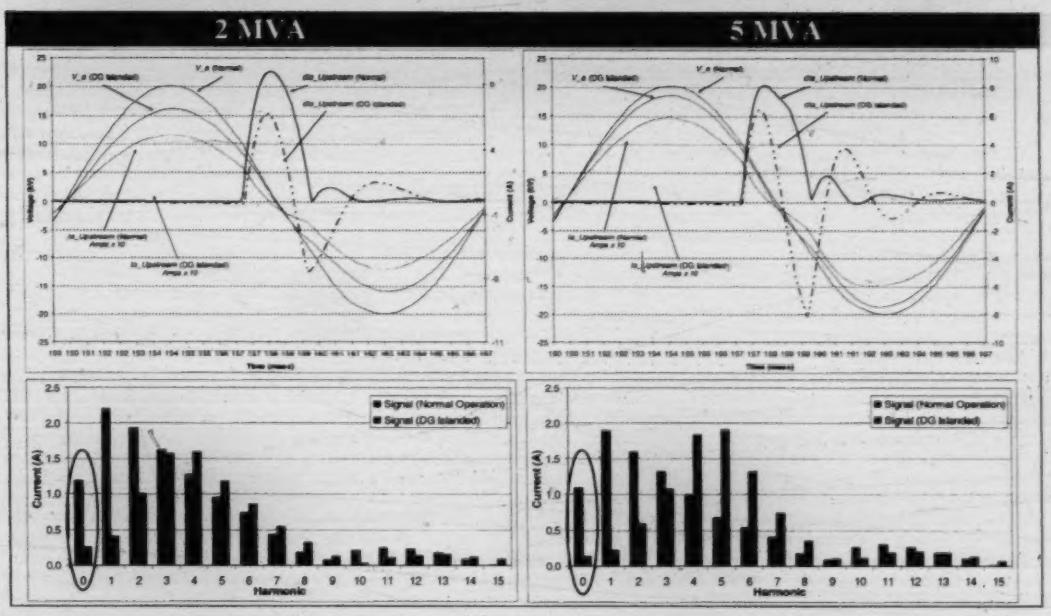

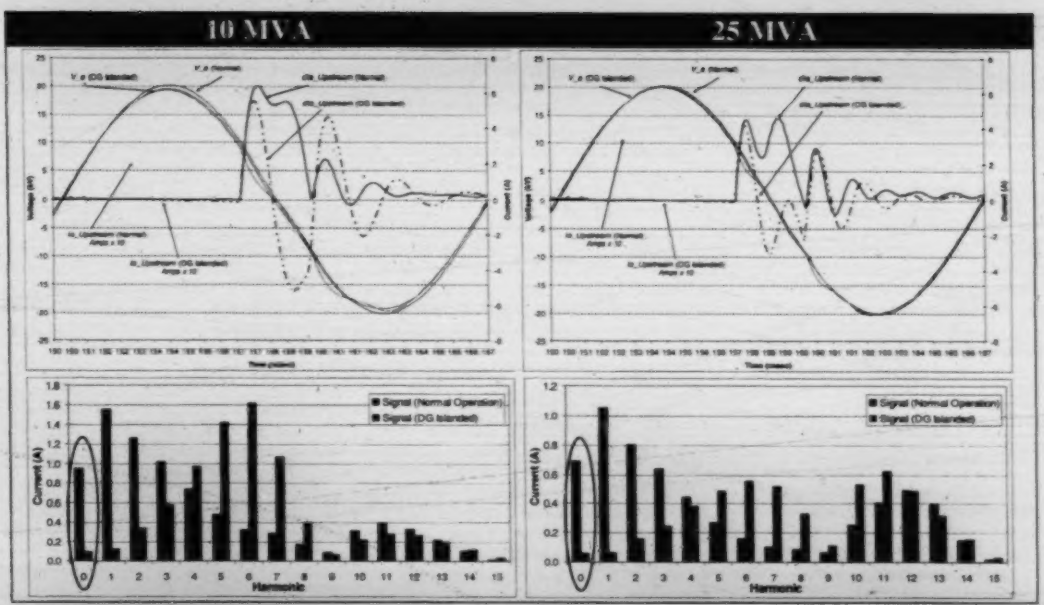
10 MVA
25 MVA
Signal (Normal Operation)
Signal (DG Islanded)
Current (A)
Harmonic

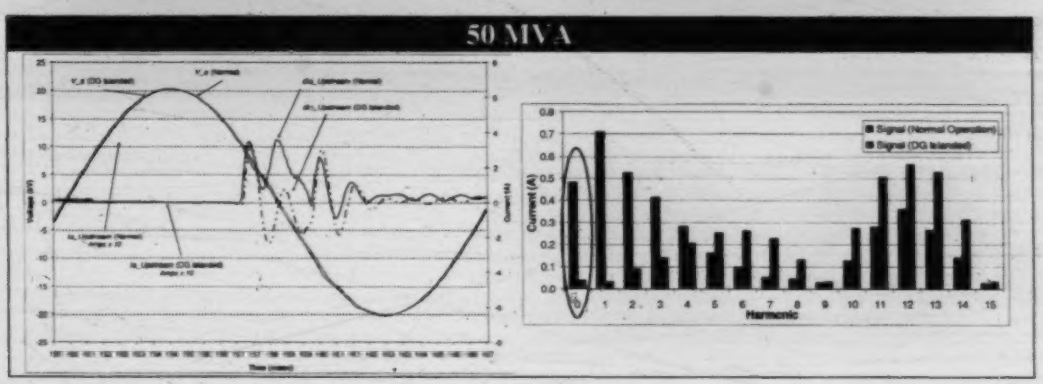
50 MVA
Signal (Normal Operation)
Signal (DG Islanded)
Current (A)
Harmonic

Table 9: Fault Level – 40 MVA to 200 MVA

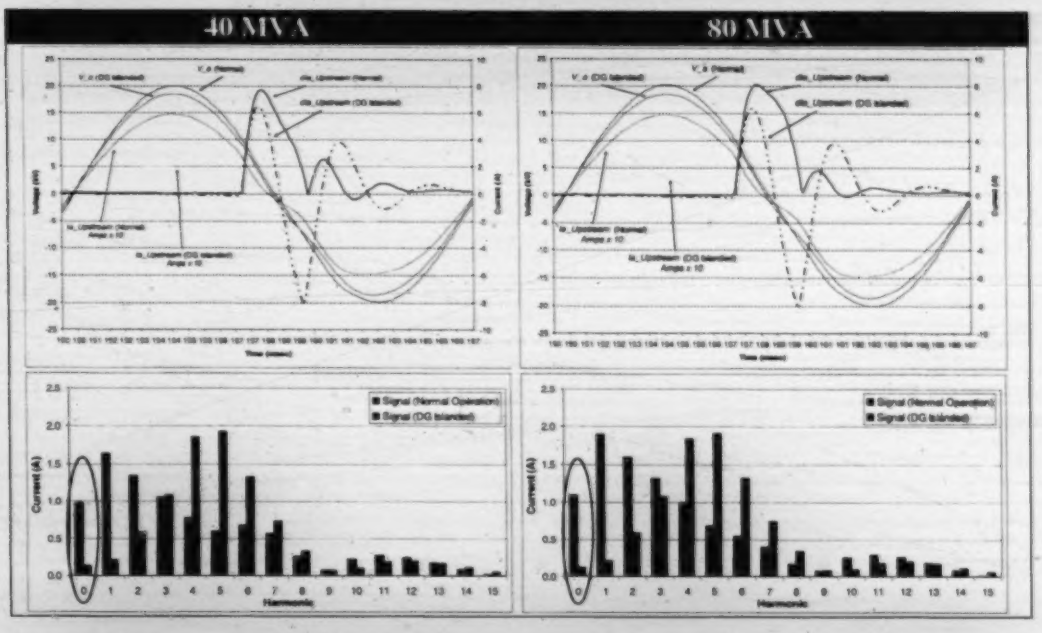

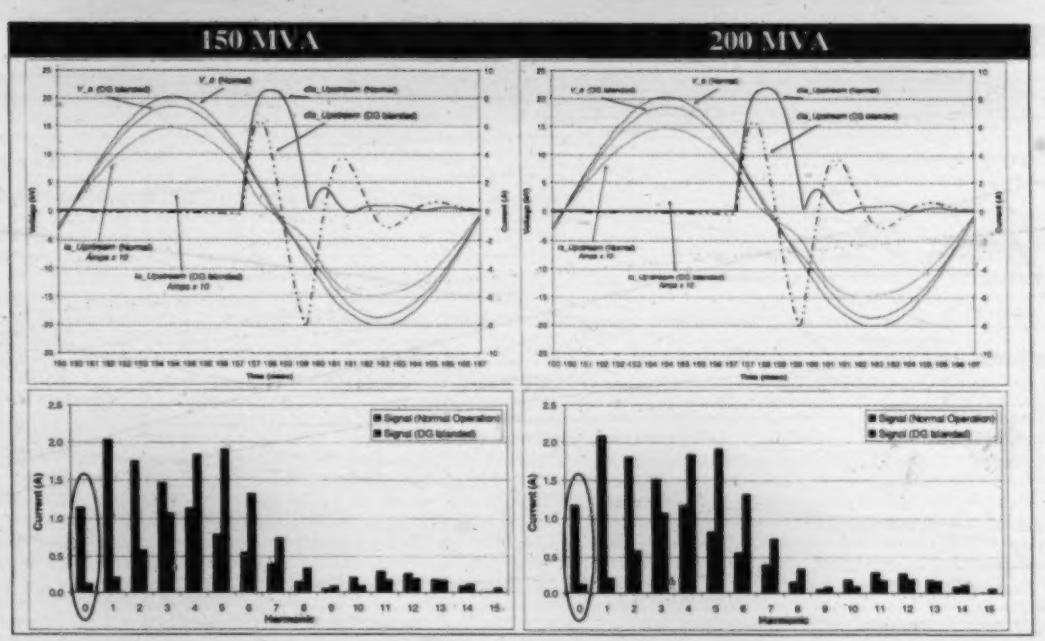

Table 10: Feeder Length – 1 km to 40 km

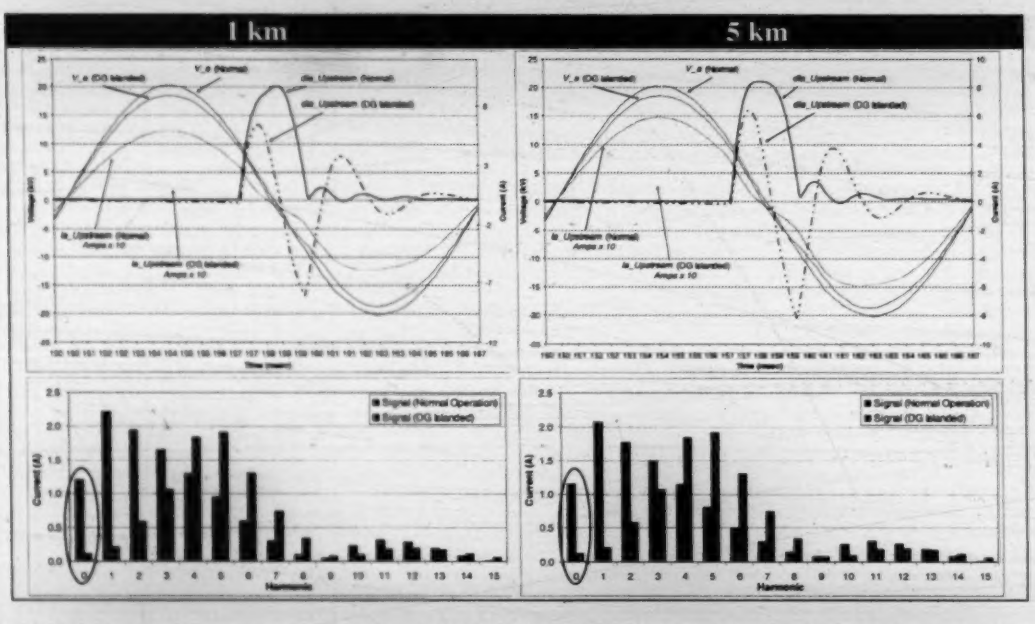

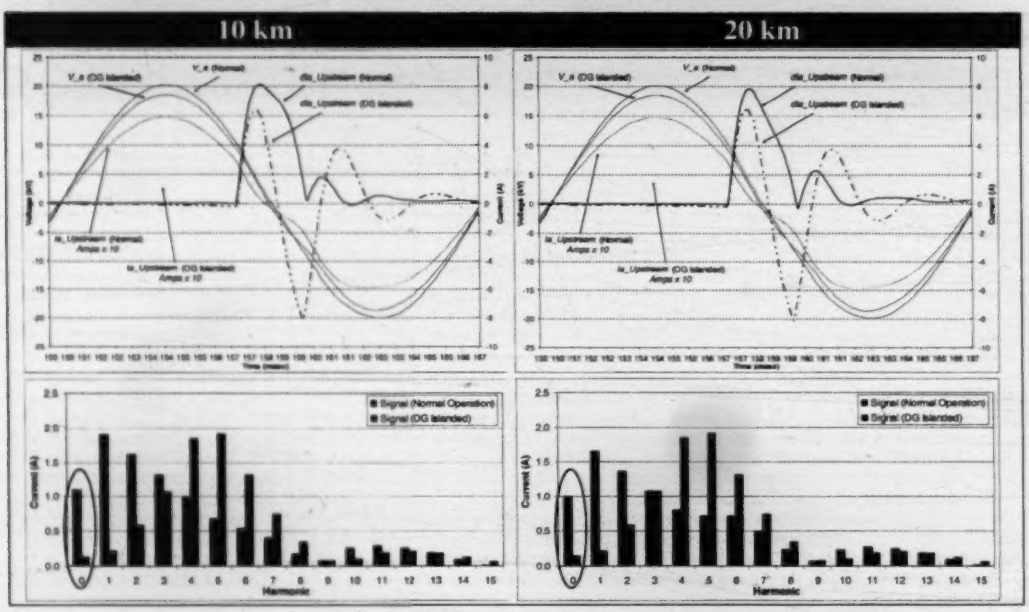

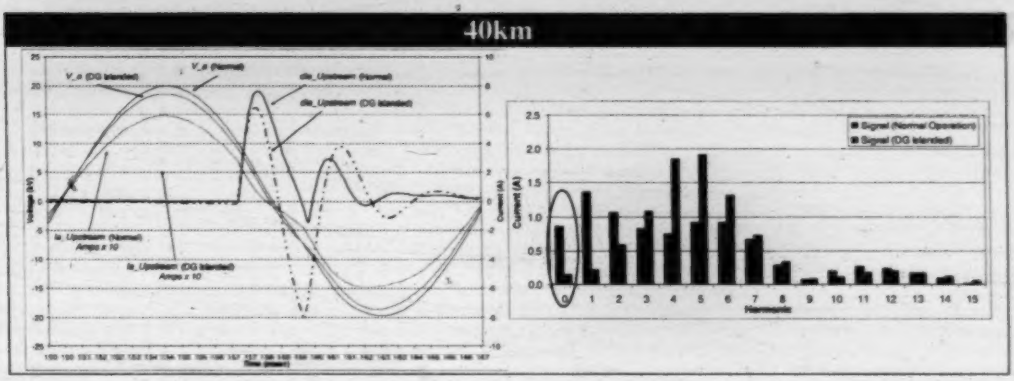
40km
V_a (DG Islanded)
V_a (Normal)
dia_Upstream (Normal)
dia_Upstream (DG Islanded)
Ia_Upstream (Normal)
Amps x 10
Ia_Upstream (DG Islanded)
Amps x 10
Voltage (kV)
Current (A)
Time (msec)
Signal (Normal Operation)
Signal (DG Islanded)
Harmonic

Table 11: Firing Angle – 5 Degrees to 30 Degrees

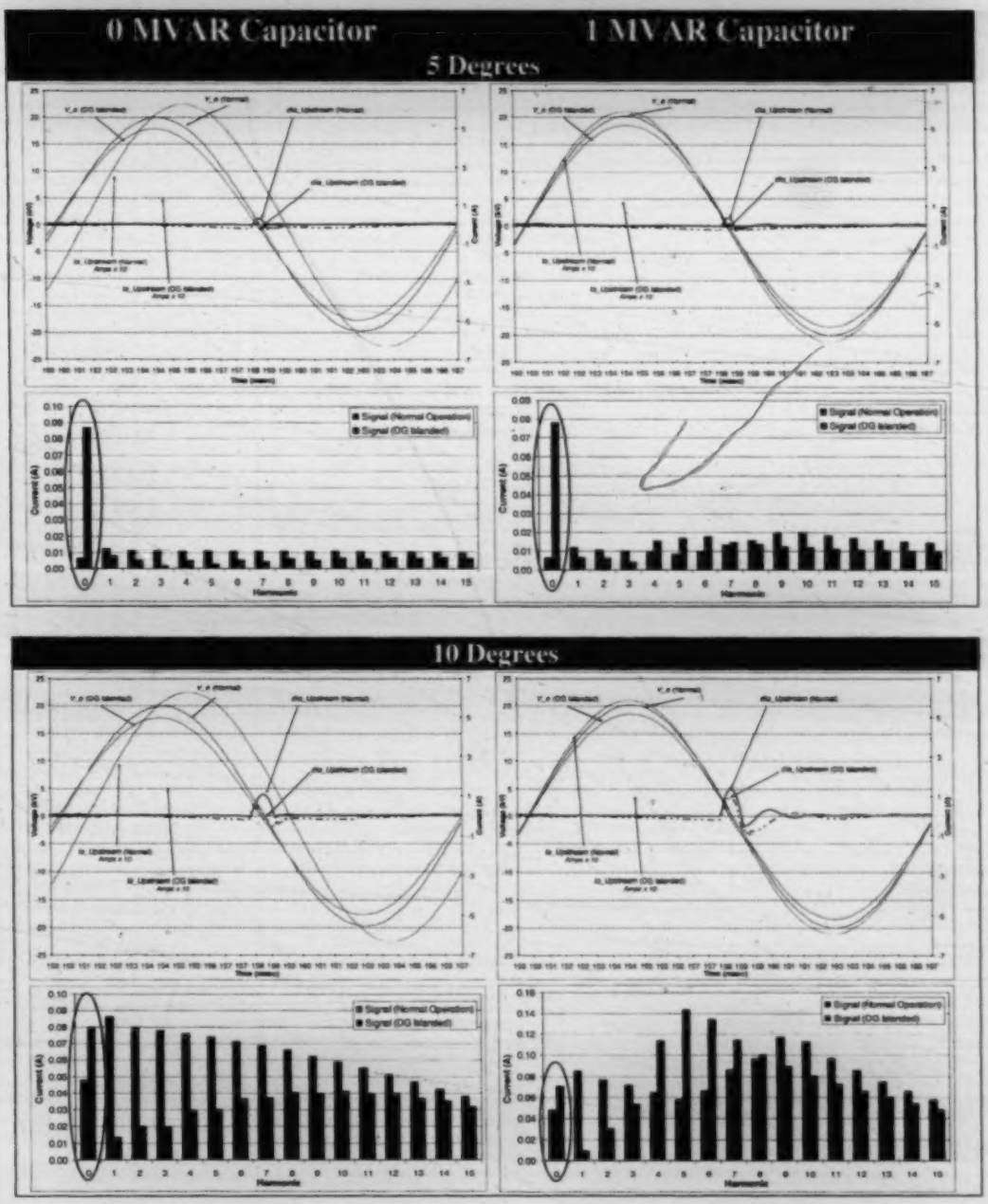

0 MVAR Capacitor	1 MVAR Capacitor

15 Degrees

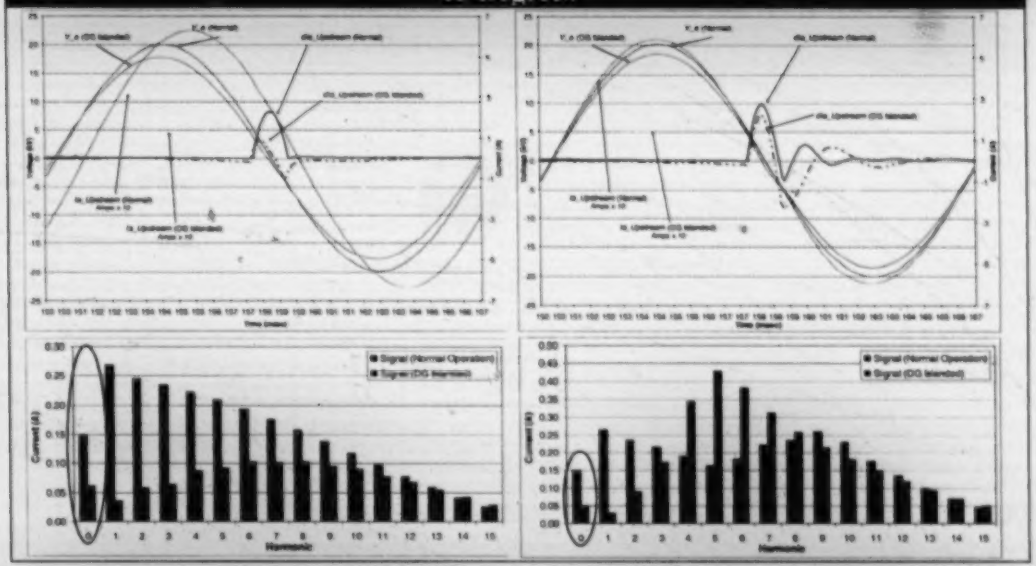

20 Degrees

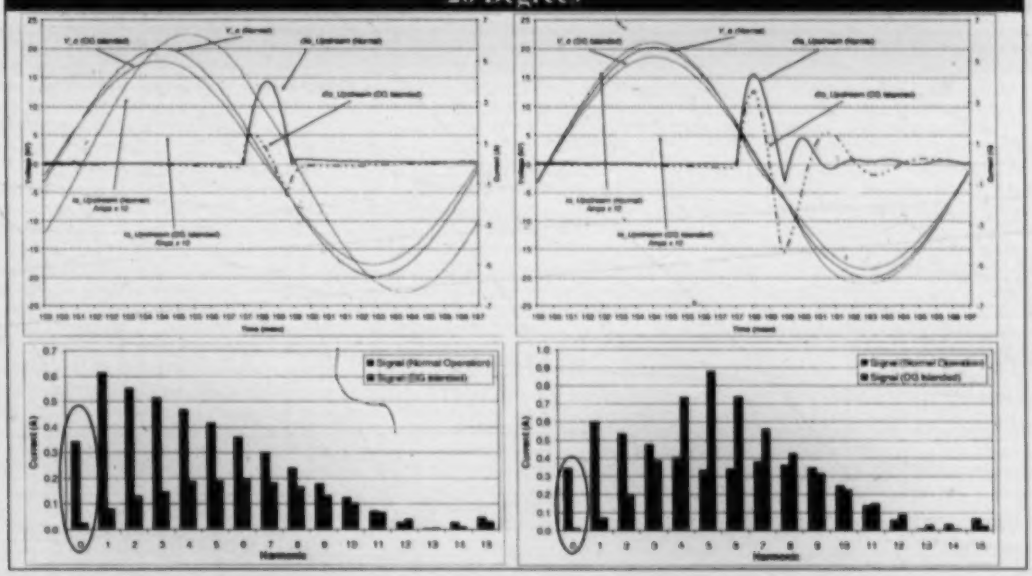

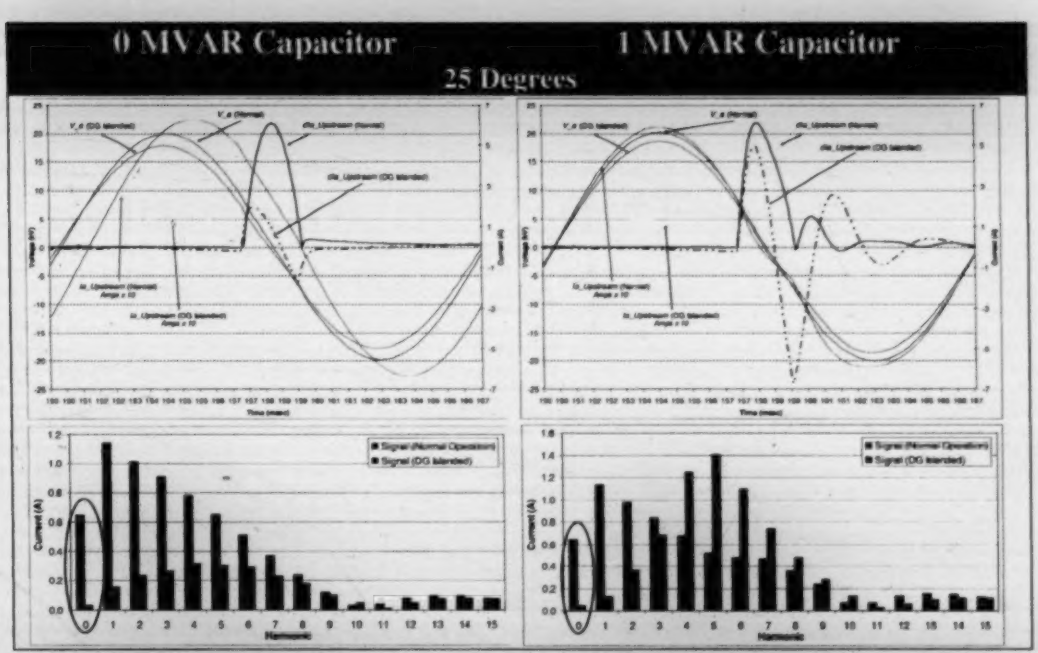
0 MVAR Capacitor
1 MVAR Capacitor
25 Degrees
Signal (Normal Operation)
Signal (DG blended)
Current (A)
Harmonic

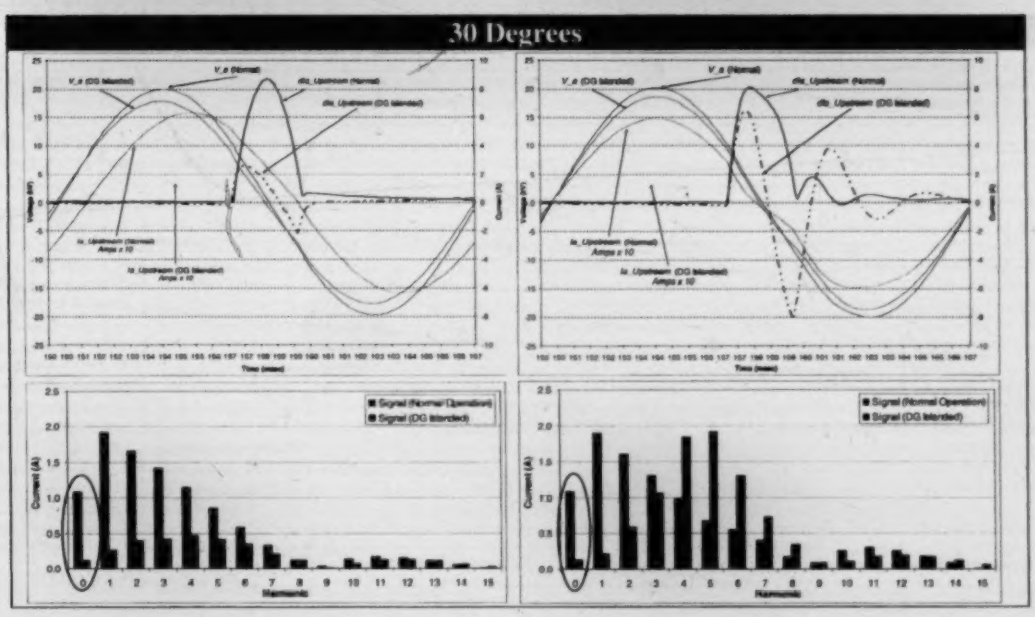
30 Degrees
Signal (Normal Operation)
Signal (DG blended)
Current (A)
Harmonic

Table 12: Load – 0.5 MVA to 5 MVA

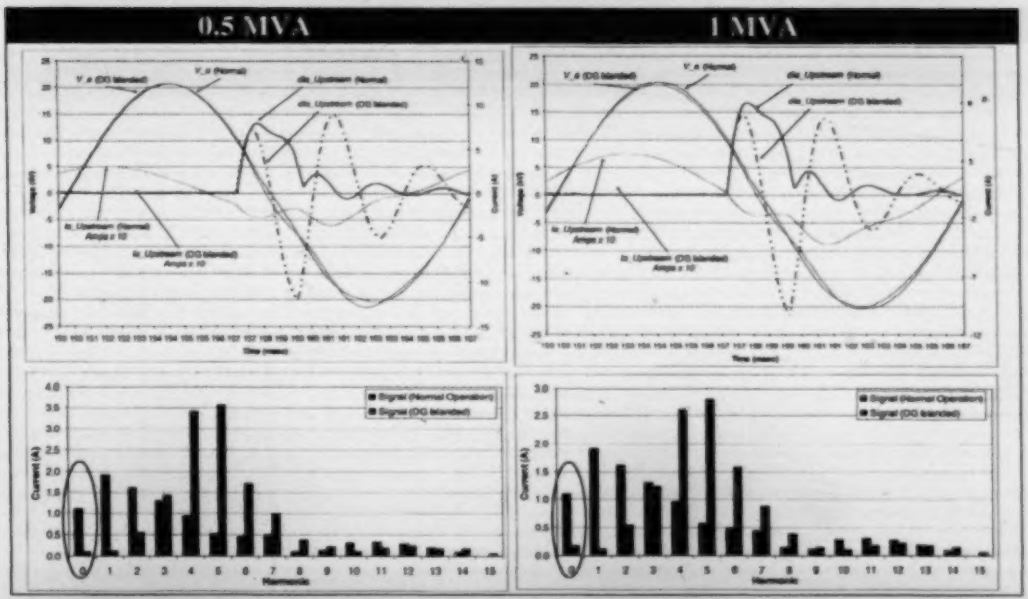

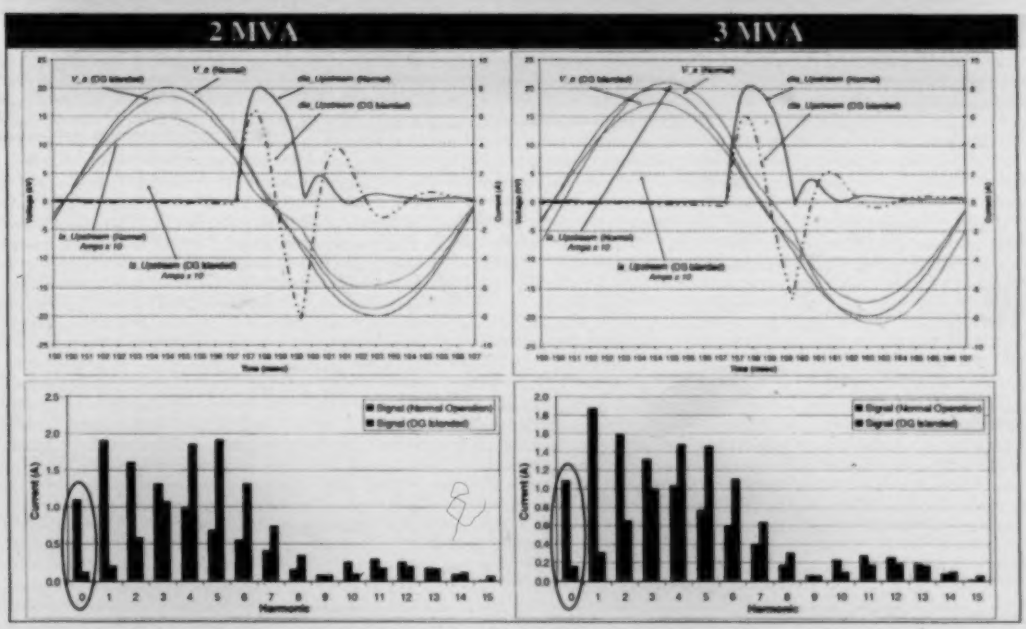

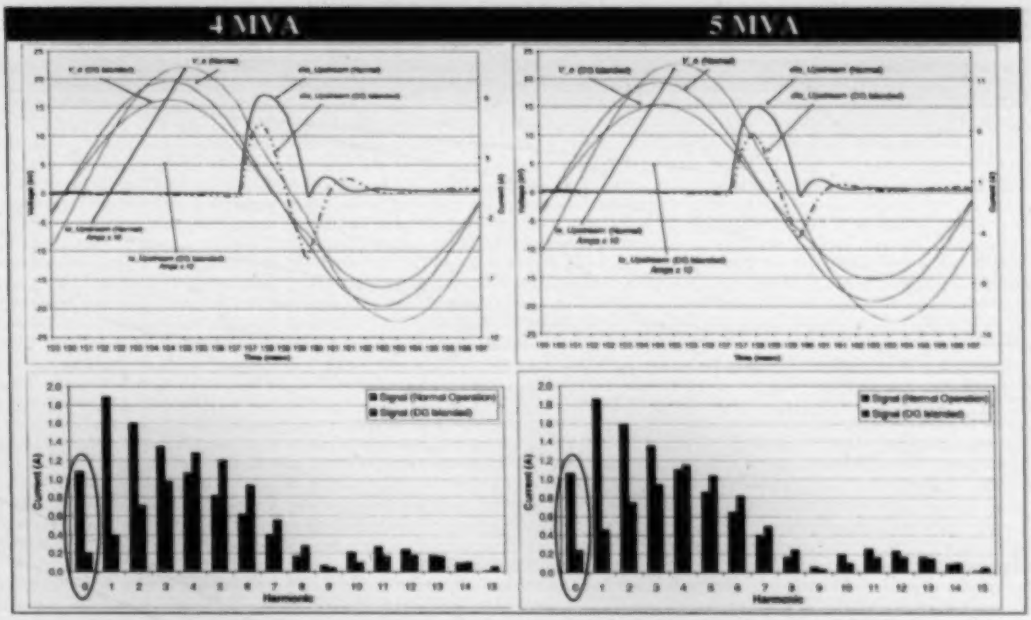
4 MVA
5 MVA
Signal (Normal Operation)
Signal (DC blended)
Current (A)
Harmonic

Appendix B

Laboratory Test Detailed Results

This section provides detailed results of the laboratory experiments performed in Chapter 4. A typical distribution system was scaled to a one phase, 120V system. A 7 hp synchronous machine was used to represent the DG and all components of the distribution system were built using power resisters, capacitors and inductors. Section 4.1 describes the laboratory setup (scaled down distribution system that was built) and the values of the components that were chosen.

Graphs showing voltage, upstream current, and the extracted upstream current signal are presented. A harmonic spectrum graph is also included for all the experiments conducted for the sensitivity study.

Table 13: Capacitor – 0 µF to 160 0 µF (Equivalent to 0 MVAR to 1.93 MVAR at 25kV) – 25 Degree Firing Angle

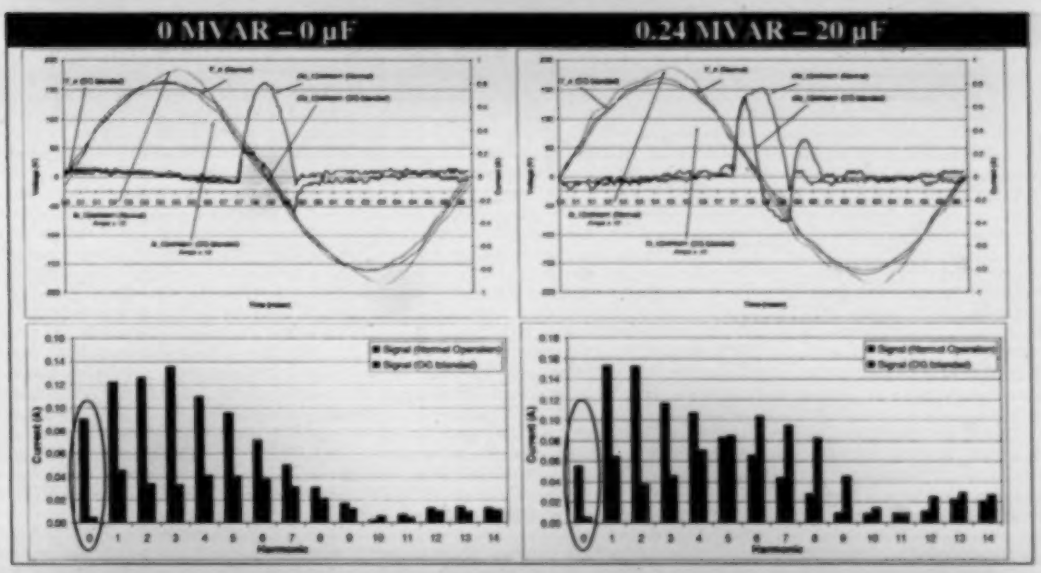

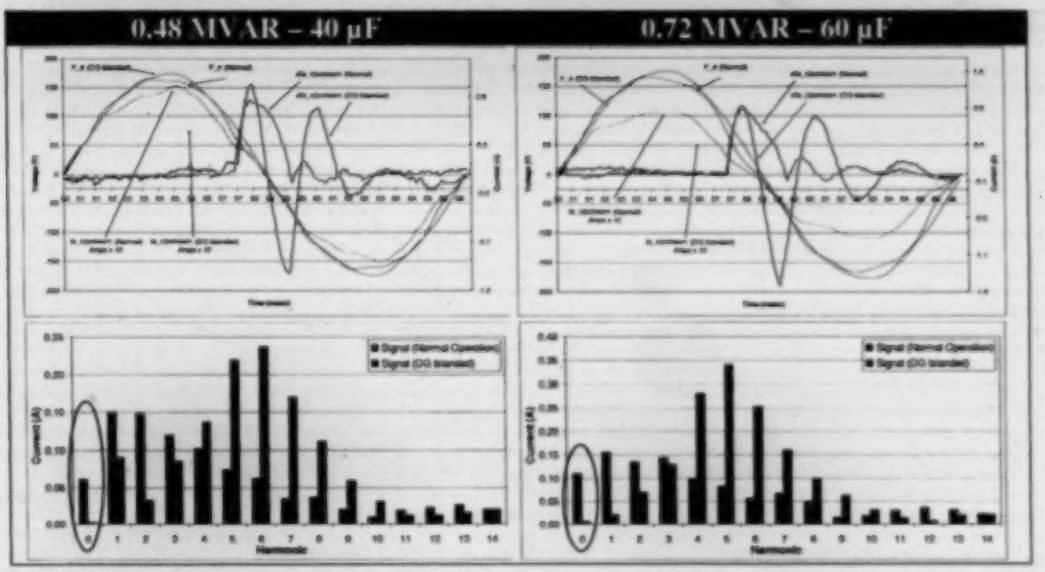

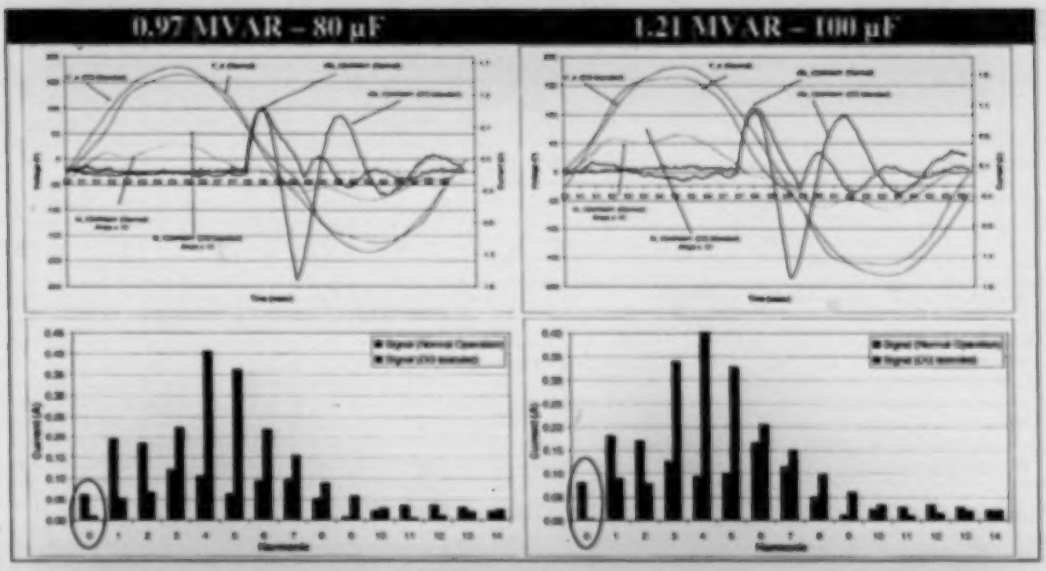
0.97 MVAR – 80 µF
1.21 MVAR – 100 µF

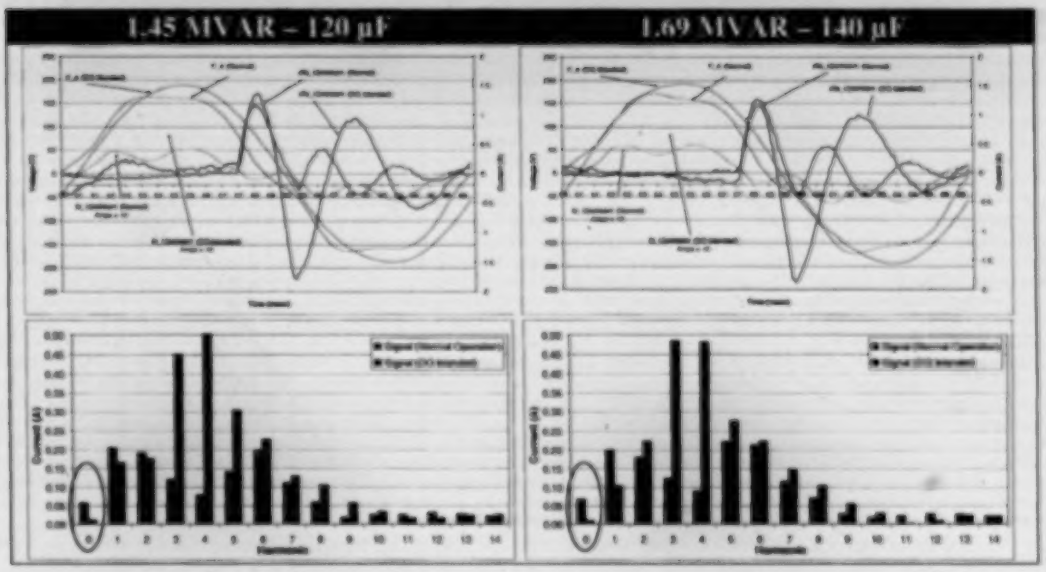
1.45 MVAR – 120 µF
1.69 MVAR – 140 µF

1.93 MVAR – 160 µF

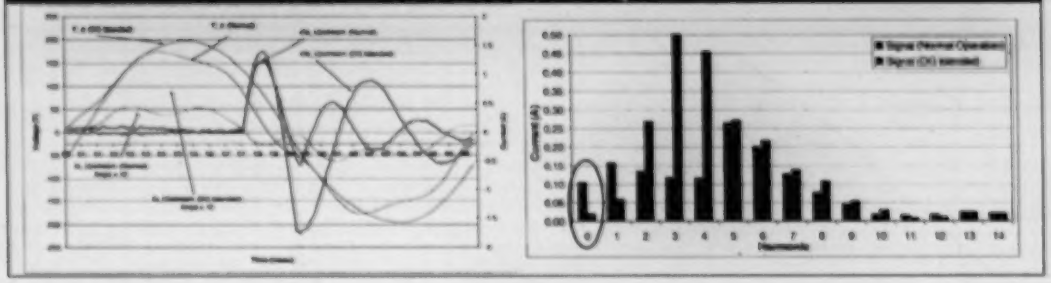

Table 14: Firing Angle – 25 to 30 Degrees (0 and 0.48 MVAR Capacitor)